UC Berkeley
UC Berkeley Electronic Theses and Dissertations

Title

Remote sensing monitoring and ecological modeling of insect outbreak dynamics in the Southern Rocky Mountains Ecoregion

Permalink

https://escholarship.org/uc/item/9w9941jf

Author

Liang, Lu

Publication Date

2015

Peer reviewed|Thesis/dissertation

Remote Sensing Monitoring and Ecological Modeling of Insect Outbreak Dynamics in the Southern Rocky Mountains Ecoregion

By

Lu Liang

A dissertation submitted in partial satisfaction of the

requirements for the degree of

Doctor of Philosophy

in

Environmental Science, Policy and Management

in the

Graduate Division

of the

University of California, Berkeley

Committee in charge:

Professor Peng Gong, Chair

Professor Gregory S. Biging

Professor John D. Radke

Spring 2015

Abstract

Remote Sensing Monitoring and Ecological Modeling of Insect Outbreak Dynamics in the Southern Rocky Mountains Ecoregion

by

Lu Liang

Doctor of Philosophy in Environmental Science, Policy and Management

University of California, Berkeley

Professor Peng Gong, Chair

Mountain pine beetle (*Dendroctonus ponderosae*; MPB) population has existed at endemic levels in the pine forests of western North America for centuries, but in recent decades it grew to epidemic levels and outbroke over extensive areas from British Columba in Canada to New Mexico in the United States. The current MPB outbreaks have impacted large expanses of lodgepole and ponderosa pine forests, reduced their ability to act as carbon sinks, altered wildfire hazards, affected wildlife populations, changed regional climate, modified local surface energy balance and water quality. Those effects are predicted to increase as a consequence of the direct and indirect effects of climate changes. Despite severe impacts of MPB, substantial unknowns and uncertainties still exist about its historical and current spatial-temporal patterns, future potential distributions, disturbance regime characteristics, ways of interaction with other major disturbance events, and impacts on forest resilience mechanisms.

In this dissertation, I first explored the potential of medium resolution satellite imagery in mapping the chronic insect disturbance in the Southern Rocky Mountains Ecoregion. A forest-growth trend analysis method that integrates temporal trajectories in Landsat images and decision tree techniques was introduced to derive annual forest disturbance maps over a period of one decade. This workflow is able to capture the disturbance events as represented by spectral-temporal segments after the removal of observational noises from temporal trajectories in Landsat images, and efficiently recognizes and attributes events based on the characteristics of the segments. Higher overall accuracy (OA) was achieved when compared with the traditional single-date classifications, and a smaller number of training sample units is required compared with maximum likelihood and random forest classifiers.

To test the feasibility of the trajectory-based approach at broader scales, I advanced this method by replacing the decision tree based semi-automatic event labeling procedure with an automatic attribution step via random forest, which was run on a set of segment

features containing information on spatial-temporal neighborhoods. Meanwhile, I developed a new sampling strategy that intensively selects sample units in overlapping areas among images acquired from adjacent rows, and automatically adds spectrally dissimilarity sample units from non-overlapping areas, to improve the efficiency of representative sample selection at the ecoregion scale. The mean OA for all scenes was 82%. The satellite derived multi-temporal landscape quantification results revealed that MPB accounted for 70% of the total area of disturbance. I found that whether fire and MPB are linked disturbances depended on their occurring sequences. Fire severity was largely unrelated to pre-fire MPB outbreak severity, whereas post-fire beetle severity was shown to decrease with fire severity. The recovery rate varied among different disturbance types. Half of the clearcut and fire areas were at various stages of recovery, but the regeneration rate was much slower at MPB disturbed sites. Beetle outbreaks and fire created a positive compound effect on the seedling reestablishment, which suggests that beetle-killed serotinous lodgepole pines might have a new forest resilience mechanism to subsequent wildfire.

Following the depiction of the disturbance pattern in landscapes, I further assessed the effects of a variety of biotic and abiotic factors on the outbreak dynamics in Grand County, Colorado. Thirty-four variables were included to develop a number of general linear models (GLM). Case and control samples were extracted from maps derived from satellite image. I first removed non-significant predictors based on the Bayesian Information Criterion in a multiple backward stepwise selection, and then built the model using the retained variables. A correction factor was added into the traditional GLM to account for model bias introduced by different ratios of case and control observations in the sample and in the population. Finally, I evaluated the model performance with an independent validation dataset, and generated predictive maps of MPB mortality. The final model had an average area under the curve value of 0.72 in predicting the annual area of new mortality. The results showed that neighborhood mortality, winter mean temperature anomaly, and residential housing density were positively associated with MPB mortality, whereas summer precipitation was negatively related. The extent of MPB mortality will expand under both RCP 4.5 and 8.5 climate-change scenarios, which implies that the impacts of MPB outbreaks on vegetation composition and structure, and ecosystem functioning are likely to increase in the future.

Disturbance is the main driver for the heterogeneous landscape mosaic, and the understanding about its pattern, regime characteristics, impacts on forest resilience system and future trend is of great importance to many fields of research, such as carbon cycling, biological conservation, and environmental protection. The overall working approach in this dissertation provides feasible algorithms that can be applied to other regions, and can aid in generating consistent and high temporal frequency data on insect mortality and other disturbances impacting a variety of ecosystem services.

Table of contents

Acknowledgments

I wish to thank, first and foremost, my advisor, Professor Peng Gong, for the patient guidance, mentorship, and mental support that he provided to me, all the way from my undergraduate study in China, through the completion of my master, and doctoral degree. He is not only my academic mentor that impacts me with his knowledge, but also my life model who teaches me to become a better person. I can still remember that eight years ago, I was so nervous about my first presentation in a lab meeting that I could barely talk. He did not critique me but instead encouraged me and provided me lots of opportunities to practice in domestic or international conferences. Gradually, I became more confident to make public speech. Undoubtedly, he is the most influential person in my graduate career.

I thank Professor Greg Biging, my qualifying exam and dissertation committee member, for his support to me as a foreign student, encouragement of my future career, and inspiration towards the sampling design in the third chapter. I also want to thank him for letting me be his teaching assistant for two semesters. His dedicative and creative teaching style has deeply influenced me on my development as a teacher. I also thank Professor John Radke for his advice, and for teaching me to think critically about the true value of geospatial science and meaning of spatio-temporal scale.

My dissertation work has tremendously benefited from my project advisors, Dr. Zhiliang Zhu and Dr. Todd Hawbaker from USGS. I am deeply thankful to them for valuable help with field trips and experimental design, and for teaching me how to apply geospatial science to solve ecological problems. I benefit a lot from the discussions with them, and their insightful comments greatly improve the quality of this dissertation.

My appreciation also goes to all professors in the Ph.D. committee, including Professor Scott Stephens, Professor Steven Beissinger, Professor Rodrigo Almeida, Professor Dennis Baldocchi, Professor Ignacio Chapela, from whom I received various types of support and help during my study in the ecosystem science program.

I am indebted to my friends for their help and accompany during my study in Berkeley, especially Huabing Huang, Xiaoyi Wang, Qi Liu, Qu Cheng, Sao Qu, Qin Ma, Yang Ju, Pengfeng Xiao, Zhishuai Zhang, Cheng Cheng, and Qingkai Kong. When I had a hard time in balancing my study and family responsibility, they shouldered parts of my duty and let me concentrate on my work, such as dissertation writing and job interview. I am fortune to have their friendship and the countless unforgettable happy and touching moments. Thank you from the bottom of my heart. You guys are the best!

I am also grateful for my labmates Iryna Dronova, Yanlei Chen, Liheng Zhong, Joshua Neill, Matheus Nunes in UC Berkeley, and Na Cong, Xuecao Li, Jie Wang in China for their research advice, technical support, comments, and help.

Chapter 1 Introduction

1 Background

This dissertation was motivated by the urgent need for information on current and projected forest disturbance dynamics to enhance and update the understanding of baseline carbon stocks, carbon sequestration, as well as greenhouse gas emissions, and to predict future potential carbon sequestration given climate, policy and land management scenarios in North America (Zhu et al., 2010). Forest ecosystems in North America are generally considered to be a carbon sink in the past decades as a result of a faster forest regrowth rate than harvest rate (CCSP, 2007; Goodale et al., 2002; Potter et al., 2007). Based on estimates in forest inventories, forest ecosystems in the conterminous United States contain approximately 54.6 billion metric tons of organic carbon above and below the ground for the baseline year 1992, with an increase of 11.3 billion metric tons from 1952 (Birdsey & Heath, 1995; Goodale et al., 2002). Though the fluctuation of US carbon storage is generally considered small as reviewed from the historical records, and the majority of the loss is ascribed to human-induced impacts, such as forest clearing for urban development (Birdsey, 1992), the effects of natural disturbances should not be overlooked in future carbon estimation, especially in the face of climate change. Variation in temperature and precipitation can significantly influence the occurrence, timing, frequency, duration, extent and intensity of disturbances (Baker, 1995; Turner et al., 1998), and ultimately alter the composition, structure and function of forest ecosystem (Hicke et al., 2011; Zhou et al., 2013). Within the United States, natural disturbances having the greatest effects on forests include fire, drought, windstorms, floodwater and ice storm, insects and disease (Barnes et al., 1997).

At the current stage, wildland fires receive the most research attention among all natural disturbance types because of their large magnitude, high severity, and their rapid responses to changes in climate (Dale et al., 2001), that consequently have been intensively mapped and well incorporated into the disturbance modeling and emission estimation. While insects are another critical forest disturbance agents, their impacts on vegetation mortality and carbon uptake have not been well understood and considered in a modeling framework to date (Kurz et al., 2008). In recent years, mountain pine beetles (*Dendroctonus ponderosae*; MPB) have caused extensive outbreaks in western North America, from British Columba in Canada to New Mexico in the USA, and affected millions of hectares of forests (Woulder et al., 2006). It was estimated that beetles killed trees contributed almost equivalent carbon to those damaged by fire in the western US from 1984 to 2010 (Hicke et al., 2013), which together represent 9% of the total tree carbon in western forests. Besides carbon, beetle infestation can affect potential fire hazard by altering the arrangement, composition, moisture content of forest fuels, and microclimate over time (Hicke et al., 2012b; Jenkins et al., 2008; Parker et al., 2006; Schoennagel et al., 2012). Beetle outbreaks can cause significant effects on the biodiversity of conifer-dominated forests by changing the nesting, roosting and foraging suitability of species (Martin et al., 2006). A substantial shift in soil and water nutrient chemistry was observed in response to the MPB epidemics, which may degrade the drinking-water quality (Clow et al., 2011; Edburg et al., 2012; Mikkelson et al., 2013).

The associated forest dieback due to beetle infestation could also impact evapotranspiration and albedo, alter the local surface energy balance, and finally affect regional temperature and climate (Boon, 2009; Maness et al., 2012). In terms of economic benefits, a decrease in economic surplus is expected as a result from reduced timber salvage and depressed outdoor recreation industry (Abbott et al., 2008; Prestemon et al., 2013).

Therefore, the delivery of timely and accurate information of bark beetle dynamics is critical in updating knowledge about ecosystem type and structure, as well as fuel conditions so that better model performance on forest disturbance and more adequate assessment of forest carbon stocks and sequestration dynamics can be achieved. These in turn will help support climate change adaptation and mitigation activities. Such information is also helpful in the understanding of the disturbance regimes, their interactions with other disturbance types, and the effects on forest resilience.

Besides the monitoring of contemporary beetle outbreaks, the prediction of future geographical distribution and range shift of this pine killer is also an important component in modeling carbon fluxes under various future climate change scenarios, and this work can hardly be accomplished without a thorough investigation of the various biotic and abiotic factors that govern the outbreak dynamics of bark beetles (Raffa et al., 2008). Although the mechanism of its population dynamics at stand or plot levels has been well understood (e.g., Raffa & Berryman, 1983; Logan et al., 1998), few studies have focused on the investigation of landscape-level drivers that explain the spatial-temporal patterns of MPB mortality due to their complex interactions with fire and the host species as a whole in response to climate change.

2 Review of concepts and literature

In this section, I will first review some important concepts regarding the biology and population development of MPB. I will then summarize the existing knowledge and various techniques in detecting the beetle disturbances. Specifically, the pros and cons of remote sensing in forest infestation monitoring will be discussed in terms of payload selection, and classification methods. Finally, the interactions between insect outbreak and various environmental/anthropogenic factors, especially the effects of climate change on beetle outbreaks will be reviewed.

2.1 Biology and epidemiology of mountain pine beetle

As a native species to North America, MPB is a major regulator of pine forest ecosystems (Haack & Byler, 1993), of which the most common hosts are lodgepole pine (*Pinus contorta*), ponderosa pine (*Pinus ponderosa*) and western white pine (*Pinus monticola*), while lodgepole pines occupy more than 80% of the stem density of the infested stands (Edburg et al., 2012). Its present geographic distribution extends from northern Mexico through the Pacific Northwest to northwestern Alberta in Canada, British Columbia and from the Pacific Coast east to the Black Hills of South Dakota, most frequently occurring at elevations of 1500-2600 m above mean sea level depending on the latitude (Amman, 1973; Sambaraju et al., 2012).

MPB is a univoltine species with a relatively well-defined life cycle from: egg, larva, pupa to adult. Adult beetles emerge and disperse between June and August, though the exact timing is site-specific. For each individual host tree, the infestation process starts from the green stage, when MPBs cut off the nutrition transport from roots by establishing their breeding galleries in the tree phloem, and the associated blue stain fungi accelerate the process by causing water stress. At this stage, the sapwood moisture will gradually drop but the foliage of trees remains visibly unchanged. After the death of the tree, the top of the crown begins to fade from green to greenish-yellow, and later to a uniform yellow, bright red and to brown after twelve months following mass beetle attack. This stage is called red stage. Normally within 3-5 years, most trees will lose all needles and we call that the gray stage (Amman, 1982).

There are also evident symptoms of bark beetle attack at the stand level. In the beginning, the infested trees are sporadically distributed with few red or grey spots in the green stand. As the beetle populations grow, groups centered on the original infested trees are formed, and some groups may even coalesce to large patches. At the peak of outbreaks, basically the whole stand appears to be effected from a landscape view.

In the population cycle of MPB, four phases were recognized in terms of population size relative to the abundance of available hosts: endemic, incipient-epidemic, epidemic and post-epidemic (Safranyik et al., 2007). The beetle density in an endemic population is very low so that only suppressed trees with lower water and nutritional reserves can be attacked (Amman, 1984). Beetles at the incipient-epidemic stage are able to successfully initiate mass attack to a single large-diameter tree within a stand, though the clumps of infested trees are scattered and confined to parts of individual stands (Safranyik et al., 2007). Under favorable conditions, the populations will grow to epidemic level, and the outbreaks start taking place at the landscape scale via long-distance dispersal (Borden 1982). In western Canada, the average duration of epidemics is around 10 years, while the longest recorded one continued for 18 years (Safranyik et al., 1974). Afterwards, the population will decline to a post-epidemic level, as a consequence of local depletion of large-diameter susceptible hosts or lethal low temperatures (Safranyik et al., 1999).

2.2 Beetle monitoring techniques

A variety of beetle outbreak monitoring approaches exist to meet different research scales, extent, resolution needs, as well as management objectives. In this section, I will present three most common and useful streams of techniques, and discuss their benefits and limitations.

2.2.1 Field survey

Ground survey is a widely applied method to confirm disturbance agents, evaluate timber killed, locate trees at green stage, and collect data of the surrounding environment at the individual tree scale. This approach can quickly provide managers and researchers the current knowledge of MPB behavior at sub-outbreak levels, and has been regarded as the most reliable source of information about the agent responsible for forest disturbances (Wulder et al., 2006a). Below, I summarized three conditions when the field surveys behave more powerfully than other monitoring techniques:

1) when precise information on the physiological parameters of host trees (e.g., sapwood moisture, DBH), stand metrics (e.g., number of infested trees), or environmental variables of a particular site (e.g., soil moisture, ground fuel load) is required.

2) when infestations are at the green stage, and the healthy status and beetle loads of individual trees should be determined.

3) when references are needed for coarser resolution datasets, such as for aerial or satellite based maps (Backsen & Brian, 2013).

However, the high economic and labor costs for field surveys restrict their application at a broader scale or on a more routine schedule. Because of the high per-hectare cost, field surveys are typically conducted on a sample basis to derive the population information, which requires additional work on the selection of an optimal sampling strategy to avoid estimation bias. In addition, the long temporal gaps between plot measurements make the monitoring of forest disturbance status and trends challenging (Schroeder et al., 2014). For instance, the revisiting cycle of a full sample of the forested landscape in the western US conducted by the Forest Inventory and Analysis is 10 years, which does not match the forest disturbance and recovery cycle in this region.

2.2.2 Aerial survey

Aerial survey is another method for observing forest insects and disease disturbance from an aircraft, delineating the affected area onto a map, and recording the associated attributes (such as damage type, causal agent, host, symptom). The traditional aerial sketchmapping is conducted using paper maps, and the advent of geospatial techniques enables the compatibility of aerial observations with a GIS database. The Forest Health Monitoring Aerial Detection Surveys (ADS) of U.S. Department of Agriculture were conducted as the major state and federal effort in identifying forest health status since the mid-twentieth century (Man, 2010), while in Canada, the Canadian Forest Service have conducted the Forest Insect and Disease Survey for over fifty years (McConnell et al., 2000).

Generally, the aerial surveys have been praised for its efficiency, low cost, fine resolution, long temporal records and good timing in detecting insect activity. The map scale for an overview survey is generally 1:100,000, 1:126,720, or 1:250,000. Depending on the map availability, desired precision and detail, the typical coverage for an aerial survey is around 480 square miles per hour (McConnell et al., 2000). The long history of archived sketchmapping of forest disturbance in North America promotes studies on the disturbance mechanism over time. Moreover, most aerial surveys are undertaken at an annual cycle from early-July through August, though the exact time may change according to different regions. This coincides with the optimum damage symptom expression of MPB damage as well as its univoltine feature, and thus makes it a perfect data source in beetle activity monitoring.

Despite of all those merits, aerial survey data has been criticized for three main defects. One is the spatial imprecision at fine scales due to reasons, such as misregistration as well as operators' subjectiveness (Meigs et al., 2011), and it is most reliable when used at

coarse scales. A pilot study initiated in the Rocky Mountain Region demonstrated that the overall accuracy, producer's and user's accuracies as estimated from the ground truth points for MPB detection in lodgepole pines exceeded 80% when the spatial tolerance was increased to 500 m (Hohnson & Ross, 2005). The second one is the considerable temporal shift because of the time lag between the attack onset and the spectral signature changes of canopy (Meigs et al., 2011; Kautz, 2014). The third point is the perception on the attribute estimations. Some attributes, such as the mortality area and damage degree are hard to measure even during ground surveys. Thus, the sketchmapping results are not recommended to be extrapolated beyond reasonable expectations without more detailed information (British Columbia Ministry of Forests, Forest Practices Branch & Canadian Forest Service, Forest Health Network for the Resources Inventory Committee, 2000).

2.2.3 Satellite-based remote sensing

Satellite-based remote sensing platforms provide users with a wide range of choices in the spectral, spatial and temporal scales, and thus have been employed to address a variety of monitoring and decision-making issues. As a novel technique, reports on the mapping of bark beetle infestation using remotely sensed data were sporadic before 2000 (e.g., Keane et al., 1994), but the growing momentum is impressive, especially in the most recent decade. In this part, I will focus on the comparison of beetle activity detection performance when different payload selection and classification methods are applied.

2.2.3.1 Payload selection

High spatial resolution imagery with its resolution less than or equal to 5 m × 5m (Franklin & Wulder, 2002), shows great potential for surveying in incipient population conditions, since this resolution of imagery captures characteristics at the stand or tree level (Wulder et al., 2006b). Dennison et al. (2010) used 0.5 m pan-sharpened GeoEye-1 image to classify areas of green, red and gray canopy cover. Coops et al. (2006a) employed the Red-Green Index derived from 2.5 m multi-spectral QuickBird imagery to separate red attack crowns from the non-attack ones. An unsupervised clustering running on 4 m multispectral IKNONS imagery can achieve 71%-92% accuracy in detecting low to medium attack (White et al., 2005). Additionally the level of detail afforded by high spatial resolution imagery provides critical calibration and validation data for lower spatial resolution remotely sensed imagery (Wulder et al., 2006b). However, because most high resolution payloads are operated by commercial companies, the cost per hectare is relatively high and the image availability is limited. Moreover, the trade-off for higher resolution is the smaller overall image extent, which will greatly increase the computational complexity and time if a broad coverage of forest needs is required.

The spatial coverage and temporal continuity provided by coarse spatial resolution payloads make them suitable for monitoring forest dynamics at inter-annual to decadal time scales and from regional to global scales. Images with pixel size larger than 30 m are more frequently used in depicting general forest ecosystem change (eg. Mildrexler et al., 2009; Sulla-Menashe et al., 2013) than type-specific mapping, due to the less representation of each land cover type in a relative big image cell. But there are still some successful cases that take advantage of the time series trajectory. For instance, Moderate Resolution Imaging Spectroradiometer (MODIS) images with an 8 day revisiting cycle

and 500 m spatial resolution were used to map near-real-time beetle infestation in North America (Anees & Aryal, 2014) and gypsy moth outbreaks (Spruces et al., 2011) through the use of time series.

Because of the low availability and computational complexity of fine spatial resolution data, and the relative low landscape representation in coarse resolution images, moderate spatial resolution image is a good choice in balancing the tradeoff between accuracy and landscape detail. Consequently, a rising amount of studies are devoted in insect disturbance mapping using moderate resolution image, among which, Landsat Thematic Mapper (TM) data is especially popular because of its free availability, multispectral properties, broad spatial extent and temporal continuity. Single date Landsat image analysis has been successfully applied to map MPB infestations (Franklin et al., 2003), but higher accuracy can be achieved when time series stacks were used (e.g. Goodwin et al., 2010; Liang et al., 2014a; Meigs et al., 2011; Meddens et al., 2013; Neigh et al., 2014; Skakun et al., 2003; Walter & Platt, 2013). The details about the effects of different classification methods will be discussed later.

Other new generation satellite platforms, such as hyperspectral, multi-angular, light detection and ranging (Lidar), and radio detection and ranging (Radar) systems offer potential for better detection of beetle outbreaks. For example, EO-1 high resolution hyperspectral Hyperion moisture indices incorporating both the shortwave infrared and near infrared bands were significantly correlated with levels of beetle damage (White et al., 2007). Canopy directional reflectance obtained from the automated multi-angular spectroradiometer platform (AMSPEC) data was highly related with field measured disturbance levels (Hilker et al., 2009).

Radar is less widely used in monitoring infestation severity or coverage, but it has shown promising results in studying the mass aerial migration pattern of insects through the boundary layer clear-air returns (Chapman et al., 2005; Nieminen et al., 2000). For instance, the Prince George Doppler Weather Radar was applied to estimate the aerial movement distance and the vertical distribution of MPB in British Columbia (Ainslie et al., 2011; Jackson et al., 2008).

Lidar utilizes the round-trip times of laser pulses from signal emission to return from objects to measure the range between the sensor and the object surface. In forest ecosystem, it is mostly widely used in deriving information about canopy height, density, and forest attributes such as biomass with higher accuracy than multispectral imagery, due to its greater sensitivity to forest structure variability (Hudak, 2006; Latifi et al., 2010). The typical function of lidar in beetle-related research is to relate lidar metrics with field observations (Bright et al., 2013), or with disturbance history metrics derived from multi-spectral images (Bright et al., 2012; Pflugmacher et al., 2014), or with high resolution digital camera imagery (Bater et al., 2010; Coops et al., 2009) to map percent dead basal area, aboveground biomass or carbon stocks. Moreover, fine-scale lidar data can be used as a reference to validate the results of coarser resolution image classifications (Bright et al., 2014).

In summary, factors to be considered in the selection of payloads when planning to map MPB infestations include the spatial resolution, timing, frequency, extent, cost, computational complexity, thematic detail and accuracy. It is virtually impossible for any single remote sensing platform to fulfill all these requirements. Users need to rank the factor importance and well understand the payload characteristics in order to match the information needs of forest managers, decision makers or research in other scientific domains.

2.2.3.2 Classification methods

A variety of classification methods have been proposed to map tree mortality. According to the classification units, the methods can be grouped into pixel-based and object-oriented approach (eg. Bunting & Lucas, 2006; Coggins et al., 2008). Depending on the density of available images, they can be categorized into single-date and multi-temporal classification.

Single-date classification is the most applied technique, because of its easy operation and shorter preparation time needed to conduct normalization and image registration. This approach is suitable for urgent updates on the current infestation condition. Nonetheless, two major gaps exist in terms of long-term tree mortality detection. First, most current single-date classifications are developed using high resolution images, such as 30 cm resolution aerial imagery (Meddens et al., 2011), 0.5 m resolution GeoEye-1 (Dennison et al., 2010), 2.5 m resolution Quickbird (Coops et al., 2006a), and 4 m IKONOS (White et al., 2004). Although technically feasible, it is not feasible to obtain fine resolution images consistently over time. Second, traditional single-date machine learning algorithms require large training sample size to represent all the variability present in a category. However, the acquisition of adequate time-series ground truth survey data is usually impossible considering the high economic cost and time efficiency. Some studies would gather training and test samples based on the images to be classified, but this way has been criticized for introducing substantial uncertainties (Powell et al., 2004).

Multi-temporal classification has been demonstrated to be more effective in separating multiple post-outbreak attack stages from other classes than single-date classification (Byrne et al., 1980; Meddens et al., 2011). An integrated approach using multi-temporal remotely sensed data has begun to emerge (Woulder et al., 2006; Hilker et al., 2009; Coops et al., 2010; Meigs et al., 2011). In general, the multi-temporal classification methods can be categorized into three main types: threshold-based, trajectory-based, and post-classification change detection.

    1) Threshold-based change detection employs certain thresholds that represent different degrees of crown foliage changes to separate the mortality from no change in either manual or machine learning algorithms (eg. Wulder et al., 2006b). Under most conditions, indices transformed from the image digital number or spectral reflectance were used for general surveys of beetle damage. Some typical indices include: Red-green index - the ratio of red to green reflectance (Coops et al., 2006a; Hicke & Logan, 2009); Enhanced wetness difference index - subtraction of the wetness component in the Tasseled Cap Transformation (Cohen et al., 2003; Franklin et al., 2003; Skakun et al., 2003). Threshold-based change detection can be

easily operated and interpreted when displaying the difference in wetness in colors. However, the cut-off values are site-specific since they highly depend on the landscape characteristics, such as the infestation status, heterogeneity, tree cover and topography. A uniform value could lead to potential bias if it has been applied across a relative large extent. In addition, while stand-replacing events are featured by prominent changes in vegetation structure and function that can be easily detected with a large cut-off value (Skole & Tucker, 1993), relatively subtle changes arising from insect attacks might be harder to separate from background changes using a small threshold.

2) Trajectory-based mapping detects changes using the temporal trajectory of spectral values through simultaneous analysis of all available images in the dense image stack. Before the public open access to the Landsat archives, most studies employed the high temporal frequency but coarse resolution satellite data such as AVHRR and MODIS (Myneni et al., 1997; Coppin et al., 2004; Lunetta et al., 2006). Now, a rising number of studies are working on the algorithm development of Landsat time-series stack in monitoring forest disturbance history. Two successful examples include the Landsat-based detection of trends in disturbance and recovery (LandTrendr; Kennedy et al., 2010) and the Vegetation Change Tracker (Huang et al., 2010). The core idea of LandTrendr is temporal segmentation, that decomposes often noisy time series into a sequence of straight-line segments with distinct features designed to capture the event that happened for the duration of each segment. VCT works similar to LandTrendr with differences in that each individual image is first analyzed to create a mask for water, cloud and cloud shadows, as well as forest samples, and the time-series of derived indices and masks is then used to characterize changes (Huang et al., 2010). Both methods recognize disturbance events by the rate of changes in time series of spectral properties. This makes the head and tail years of the trajectory more difficult to judge, because the attribution for a particular year is entirely determined with regard to its spectral deviation from the two adjacent years (Kennedy et al., 2010). In addition, the event labeling depends on pre-implemented modules in the package, and thus is not flexible in adjusting to user-defined functions. Furthermore, both algorithms are able to find most of the abrupt disturbances, but neither was fully optimized to capture the chronic and low severity insect damage (Schroeder et al., 2014). Nonetheless, this type of method is promising because of the free availability of more satellite images at fine to medium spatial resolution in the future, and temporally dense observations are necessary to distinguish between type and frequency in heterogeneous landscapes (Neigh et al., 2014).

3) Post-classification change detection: Unlike the former two types of methods that focus on the relative differences in spectral response between images covering the same extent or the changing trend of the spectral curve over time, post-classification mapping runs classifiers on each individual image first, and then compares the results to detect changes in land cover types. This type of method has been widely applied in various land cover change or forest disturbance studies (eg. Kuemerle et al., 2009; Griffiths et al., 2013). Besides the final change products, it also generates the land cover map for each image, which could be attractive to managers or

decision makers if they need consistently updated land cover synthesis. However, because the accuracy of change detection highly depends on the classification results at each date (Coppin et al., 2004), the errors could propagate and lead to poor accuracy, especially under the circumstance when longer time series is involved. Some methods were proposed to alleviate this issue and the common principle lies in the development of a land cover transition matrix, since the consequence of error propagation is the occurrence of illogical land cover transitions. Liang et al. (2010) identified the uncertainties in the MODIS Collection 5 global land cover products using a land cover type conversion lookup table. Liu and Cai (2012) employed the spatial-temporal contextual information modeled by Markov random field theory to reconstruct the change trajectories. Wang et al. (2014) applied the similar approach to carry out the global land cover mapping at 250 m resolution with multiple year time series MODIS data. Those efforts greatly improved the accuracy of post-classification accuracy, but the design of the land cover transition matrix is mostly arbitrary and the intricacies of the algorithm as well as the computational complexity might limit its application outside of the remote sensing community.

2.3 Climate change and mountain pine beetle

Bark beetles are cold blooded. They can respond quickly to changing climate by shifting their geographical distribution to maintain their climatic niche (Carroll et al., 2003), which makes climate warming the biggest concern in affecting the extent and severity of beetle disturbance (Bale et al., 2002). Some direct effects of climate change on bark beetle include developmental timing and cold tolerance, and indirect effects include community associates, host-tree physiology, and host-tree distribution (Bentz 2010). Evidences of range expansion into new habitats as a result of increasing temperature have been documented in many cases (eg. Battistia et al., 2006; Nealis & Peter, 2009), and they are attacking hosts farther north and at higher elevations than historic norms (Tran et al., 2007; Safranyik & Carroll, 2006).

The bark beetle's life cycle is temperature dependent (Figure 1). Their daily emergence rates are proportional to cumulative degree-days above 14.4 °C, and captures of released MPB were directly related to heat accumulation above 16 °C (Safranyik et al., 1989). Most beetles fly between the temperature from 22 °C to 32 °C (Safranyik, 1978), and the flight propensity increases with ascending light intensity and relative humidity if temperature is within the optimal range. Once the temperature exceeds 35 °C, the flight propensity begins to decline and will disappear above 38 °C (McCambridge, 1971). Cold temperature is the most threating factor of beetle mortality (Safranyik, 1978; Cole, 1981): eggs can not survive below -18 °C (Reid & Gates, 1970), and the lethal temperature for pupae is between -18 °C and -34 °C, and for adults is between -23 °C and -34 °C (Logan et al., 1995). The degree of cold tolerance is determined by the amount of glycerol (Bentz & Mullins, 1999), which gets accumulated with the mature of larvae, and usually reaches its peak during the winter period from December to February. Thus, if an extreme cold weather that lasts for several days strikes before the sufficient accumulation of glycerol or after the beetles have already metabolized it, massive mortality can occur (Safranyik et al., 1974).

Although some studies suggest that there may be sufficient genetic variability in MPB populations to match changes in the climatic environment (Bentz et al., 2001), the rate of climatic niche evolution is not predicted to be faster than that of climate change (Quintero & Wiens, 2013). This is the basis for many studies in estimating the potential distribution of bark beetle under current and projected future climate conditions. Both process-based and statistical models have been applied in exploring the responses of beetles to changing climate and estimating the future potential habitats. Process-based models are focused on linking population dynamics with climate in a physiologically explicit way, whereas statistical models build the association of outbreaks with climate events from the perspective of data correlation.

Bentz et al. (2010) used BioSIM that was driven by hourly temperature to identify regions with a high potential for MPB outbreaks across North America. Using a process-based model, Hicke et al. (2006) found that projected warming in the western United States will result in substantial reductions in the overall area of adaptive seasonality. Aided by an ecological niche model, Evangelista et al. (2011) predicted that new areas of forest susceptible to MPB mortality would emerge over time but the existing distribution would also shrink under future climate condition, leading to an overall decrease in suitable habitats. Based on the results of logistic regression models, Sambaraju et al. (2012) indicated that increases in mean temperature by 1 to 4 would profoundly increase the outbreak risk at higher elevations first then at higher latitudes, whereas variance in mean temperature would not change the overall trend in outbreak potential. Carroll et al. (2004) modeled the climatic suitability using historical weather in British Columbia, Canada, and a substantial shift in climatically suitable habitats was found towards northern and higher elevations. Noticeably, the MPB outbreaks from historical survey data followed this shifting pattern. In Oregon and Washington, USA, the odds of outbreak at locations with highly suitable weather was 2.5 times higher than those with low suitability, as calculated from a weather suitability index (Preisler et al., 2012). Although a large body of studies have confirmed the importance of climatic variables in shaping the outbreak dynamic patterns at the macro-scale (eg. Chapman et al., 2012; Jewett et al., 2011; Lester & Irwin, 2012; Mitton & Ferrenberg, 2012), many of them only consider a limited number of explanatory variables because of model complexity, especially for the process-based approaches, which might eventually introduce errors into the simulated model results.
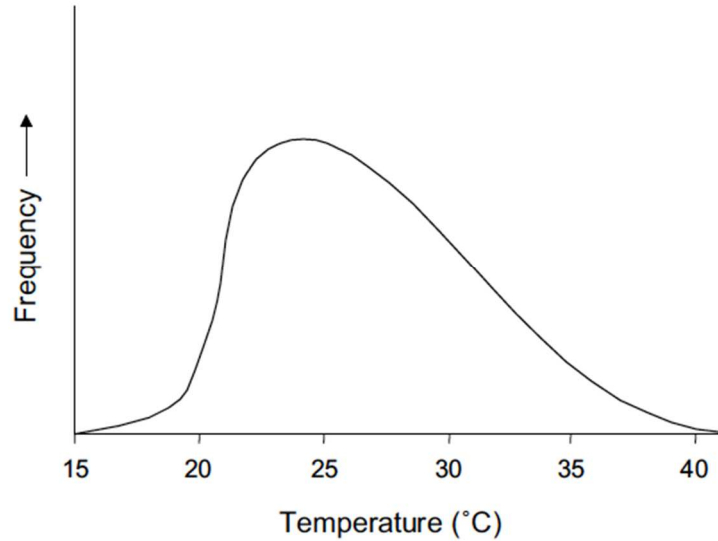
Figure 1. The relationship between emergence frequency of mature MPB and temperature (adapted from McCambridge 1971).

3 Objectives and thesis structure

As revealed from the literature review in Section 2, although great improvements have been achieved in terms of MPB monitoring, detection and modeling, caveats and knowledge gaps still exist. The overarching goal of my dissertation is to enhance the time-series mapping ability of medium resolution remotely sensed data in areas characterized by heterogeneous disturbance-derived mosaic and rapid landscape pattern changes. This will allow for a better and more seamless integration with ecological modeling as well as landscape analysis, to improve our understanding about the resilience mechanisms of forest ecosystem and facilitate the forest management and decision making. Each chapter addresses one specific objective, and the structure is organized as follows:

Chapter 2 developed a practical workflow to derive the progressive MPB outbreaks in a time sequence using medium resolution remotely sensed data over a decadal long period. I proposed a forest growth trend analysis to conduct the mapping by eliminating the observational noise in the time-series, capturing the disturbance events as represented by spectral segments, and quantitatively attributing events based on their distinct features, with an integrated Landsat temporal trajectories and decision tree techniques. The accuracy was compared with two single-date classifiers, i.e., the Maximum Likelihood classifier and Random Forest with varying number of training samples, to assess the sensitivity of classification outcomes to the sample size.

Chapter 3 advances the procedure in Chapter 2 and conducts the long-term mapping in the Southern Rocky Mountains ecoregion, with the aim of depicting the disturbance and recovery patterns, characterizing their regimes, and describing the disturbance-succession pathways. I first developed a sampling strategy that took advantage of the Landsat scene-overlapping area between images to promote sampling efficiency at a

large scale, and then automatically added representative samples based on the spectral similarity rule to improve the mapping accuracy. The analysis method proposed in Chapter 2 was improved via an automatic event attribution step using random forest and a set of ecological meaningful features that contain the spatio-temporal information of the focal segment. Based on the generated annual time-series of disturbance/recovery, I derived their key regime parameters, such as onset year, magnitude, duration, and disturbance-recovery pathways, to investigate the complex interactions among various disturbance types in this region, and the effects on the forest resilience mechanism.

In chapter 4, I quantify the anthropogenic and environmental drivers that explain the dynamic patterns of MPB mortality at the landscape level, and simulate areas with future potential MPB mortality under projected climate-change scenarios. I applied the general linear models (GLM) to rank the importance and significance of various biotic and abiotic factors. The response variables were defined as the new MPB mortality, and the case and control samples were extracted from the remote sensing derived current distribution of pine beetle outbreaks in a stratified random sampling manner, of which the sample sizes were determined via Moran's I to avoid spatial autocorrelation effects. I then complied a set of comprehensive landscape-level explanatory variables, including anthropogenic, topographic, vegetation, climate and dispersal-related parameters from various geospatial sources. The GLM with the best performance, which was evaluated in both qualitative and quantitative ways, was applied to predict potential new areas of MPB mortality using the outputs of downscaled global climate models from the Coupled Model Intercomparison Project 5.

Finally, in chapter 5, I provide conclusions from this research and point out some future research directions that can be carried out based upon the outcomes of this dissertation.

Chapter 2 Trajectory-based classification for beetle outbreak detection with time-series Landsat stack

This article has been published previously and is reproduced here with permission from the publisher, Elsevier

Abstract

Disturbances are key processes in the carbon cycle of forests and other ecosystems. In recent decades, mountain pine beetle (MPB; *Dendroctonus ponderosae*) outbreaks have become more frequent and extensive in western North America. Remote sensing has the ability to fill the data gaps of long-term infestation monitoring, but the elimination of observational noise and attributing changes quantitatively are two main challenges in its effective application. Here, we present a forest growth trend analysis method that integrates Landsat temporal trajectories and decision tree techniques to derive annual forest disturbance maps over an 11-year period. The temporal trajectory component successfully captures the disturbance events as represented by spectral segments, whereas decision tree modeling efficiently recognizes and attributes events based upon the characteristics of the segments. Validated against a point set sampled across a gradient of MPB mortality, 86.74% to 94.00% overall accuracy was achieved with small variability in accuracy among years. In contrast, the overall accuracies of single-date classifications ranged from 37.20% to 75.20% and only become comparable with our approach when the training sample size was increased at least four-fold. This demonstrates that the advantages of this time series work flow exist in its small training sample size requirement. The easily understandable, interpretable and modifiable characteristics of our approach suggest that it could be applicable to other ecoregions.

1 Introduction

Understanding patterns of forest disturbances is important for assessing past and future ecosystem structure, function, productivity and diversity (Turner, 2010; Wang et al., 2012). In recent years, mountain pine beetle (MPB) outbreaks have occurred over extensive areas, from British Columba in Canada to New Mexico in the United States. MPB is endemic to North America; however, the recent outbreaks have reached epidemic levels that have affected millions of hectares of forests (Hicke et al., 2013). The effects of MPB infestation range from altered surface fuel and wildfire hazards (Hicke et al., 2012b; Jenkins et al., 2008; Parker et al., 2006; Schoennagel et al., 2012), changed vegetative composition (Collins et al., 2011), converted live carbon sinks to dead and slowly decaying carbon sources (Caldwell et al., 2013; Kurz et al., 2008; Running, 2008), impacted nutrient cycling and water quality (Edburg et al., 2012; Mikkelson et al., 2013), shifted evapotranspiration and albedo, modified local surface energy balance (Boon,

2009) and changed regional climate (Maness et al., 2013). Those effects are predicted to increase as a consequence of the direct and indirect effects of climatic changes (Bentz et al., 2010; Raffa et al., 2008; Williams et al., 2010). However, unlike wildfires that have received intensive mapping efforts at different scales, characterizations of the extent and severity of MPB using multi-temporal data have only begun to emerge (Coops et al., 2006b; Goodwin et al., 2010; Meddens et al., 2011; Meigs et al., 2011; Wulder et al., 2006a).

Remote sensing, both with aerial photography and satellite imagery, has been widely acknowledged as a useful way to map tree mortality over large areas (Hansen & Loveland, 2012). Landsat time series stacks (LTSS) are well suited to this type of analysis, because they are freely available, cover a long time period, have a broad spatial extent, are multispectral and have temporal continuity (Franklin et al., 2003; Wulder et al., 2006a). Two frequently used disturbance mapping approaches are (1) trajectory-reconstruction and (2) decision trees (DTs). Trajectory-based change detection examples include the Landsat-based detection of trends in disturbance and recovery algorithm (LandTrendr) (Kennedy et al., 2010) and the Vegetation Change Tracker (Huang et al., 2010; Masek et al., 2013; Vogelmann et al., 2011). Both methods recognize disturbance events by the rate of changes in time series of spectral properties. This makes the first and last years of the trajectory more difficult to judge, because the attribution for a particular year is entirely determined with regard to its spectral deviation from the two adjacent years (Kennedy et al., 2010). In addition, the event labeling procedure depends on pre-implemented modules in the software and, thus, is not flexible in adjusting to user-defined functions. DT approaches include work by Goodwin *et al.* (Goodwin et al., 2008) who utilized the annual changes in normalized difference moisture index and a set of thresholds to classify the presence of MPB infestation over 14 years, resulting in overall accuracies ranging from 71% to 86%. DT-based approaches have the capacity to integrate expert knowledge and flexible classification schemes. However, poor image quality from sensor drift, geometric misregistration and topographic and cloud shadows will introduce distortions to images and affect the accuracy of change detection.

In this study, we describe a forest growth trend analysis method that integrates the robust change detection strengths of the trajectory reconstruction approach and the flexible user-defined advantages of DT approaches to characterize MPB mortality with an 11-year LTSS. We were interested in determining whether or not this proposed method could reach an accuracy target of 85% or greater. Additionally, we compared its accuracy with single-date image classifications, which are still important and commonly used in disturbance mapping, especially in two-date post-classification change detection. We are aware that the accuracy of single-date image classification is not only determined by the input variables and classifiers, but is also heavily dependent on the quality and quantity of training samples (Gong et al., 2013), which may have larger impacts than the implemented techniques (Campbell, 2002). Thus, we also assessed the effect of different sample sizes on the accuracy of single-date image classifications, and we tested how much our proposed method can improve sampling efficiency as compared with the single-date classifiers.

2 Study area and data

2.1 Study area

Our study area was located in Grand County, in north-central Colorado (Figure 1), with a total land area of 4783 km^2. This landscape is dominated by evergreen forests mainly composed of lodgepole pine (*Pinus contorta*), along with other tree species, as well as shrub and grass cover types. Summer in Grand County is typically hot and dry, which is suitable for MPB development. The average precipitation per year is approximately 400 mm, whereas the U.S. average is 930 mm. This county has one of the highest concentrations of lodgepole pines and has been heavily affected by the MPB outbreak that started around 2002 and reached the peak of tree mortality between 2005 and 2008 (Klutsch et al., 2009).
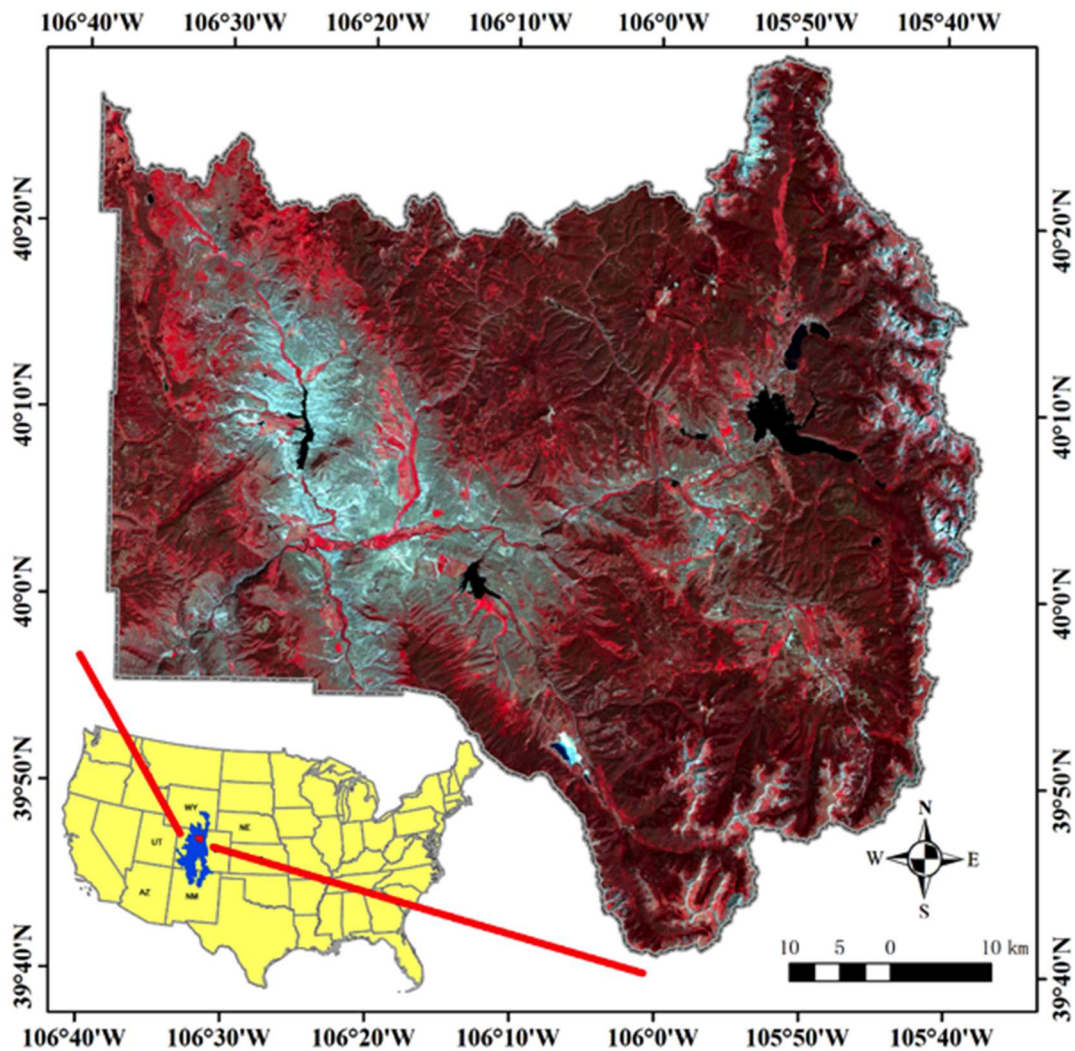
Figure 1. The study area used for our analyses. The Southern Rocky Mountain ecoregion is shown in blue, and Grand County, Colorado, USA, is shown in red. The imagery is a false-color composite of one Landsat image acquired on 21 August 2009.

2.2 Landsat time series stack

Grand County lies entirely within Landsat path 34 row 32. We restricted the image acquisition season from June to September, because this snow-free period is the recommended time window to detect MPB mortality (Wulder et al., 2006a). For each year, one cloud-free or mildly contaminated image was selected to build the LTSS, and if no such image existed, several partly cloudy images with a similar phenology were used as replacements (Table 1). All data were processed to Level 1T (terrain corrected). Radiometric calibration and atmospheric correction for cloud and aerosol effects were performed using the Landsat Ecosystem Disturbance Adaptive Processing System [34]. Clouds and their shadows were automatically screened using the Function of mask (FMASK) algorithm (Zhu & Woodcock, 2012). Cloud removal effects were judged satisfactory via visual checking, though the extent of cloud cover was slightly overestimated. We accepted this false positive error, because commission errors were more desirable than omission errors in cloud filling. The number of clear observations in the LTSS over the period of 2000 to 2011 is shown in Figure 2, and 98% of the study region contained more than 10 cloud-free observations.

Table 1. Characteristics of the Landsat images used in this analysis.

	Year	Month and Day	Julian Day	Cloud Cover (%)	Cloud Cover over MPB Host Area (%) *
1	2000	Jul 13	193	42.35	1.09
2	2000	Jul 21	201	4.74	
3	2001	Jun 28	179	18.87	4.24
4	2001	Jul 22	203	17.05	
5	2002	Jul 1	182	1.92	0.15
6	2003	Jul 4	185	5.48	0.49
7	2004	Jul 8	188	10.49	7.94
8	2005	Sep 11	254	2.08	0.25
9	2006	Jul 28	209	2.30	1.26
10	2007	Jul 31	212	20.39	4.22
11	2007	Aug 16	228	13.19	
12	2008	Aug 20	231	28.91	9.79
13	2008	Sep 5	247	36.83	
14	2009	Aug 21	233	2.04	0.00
15	2010	Sep 25	268	3.37	0.89
16	2011	Aug 11	223	22.13	2.67
17	2011	Aug 27	239	16.45	

Notes: MPB, mountain pine beetle; * the final cloud cover in a particular year in MPB host forest areas is after using clean pixels in one image to fill cloudy areas in another image that is in the same phenological state.

Since MPBs attack a limited number of tree species, we confined our analysis to the extent of their host species in the LANDFIRE Refresh 2001 Existing Vegetation Type data layer (EVT), which was developed using *circa* 2001 (1999–2003) Landsat imagery (Nelson et al., 2013). The spatial resolution of the LANDFIRE data matches the LTSS, and the time period of the imagery from which the EVT data were derived depicts the

pre-disturbance distribution of vegetation in Grand County. Currently, MPB mortality is concentrated in lodgepole and ponderosa pine (*Pinus ponderosa*) forests, but other pine species, like limber pine (*Pinus flexilis*) and bristlecone pine (*Pinus aristata*), have also been found to be suitable hosts (Gibson et al., 2008). We included all EVT pixels that contain any of those species (Table S1), and smoothed the image with a 3 × 3 majority filter, which was designed to reduce observed salt-and-pepper effects and to minimize omission errors that are much higher than commission errors for the selected classes (National c2001 Assessment, 2001).
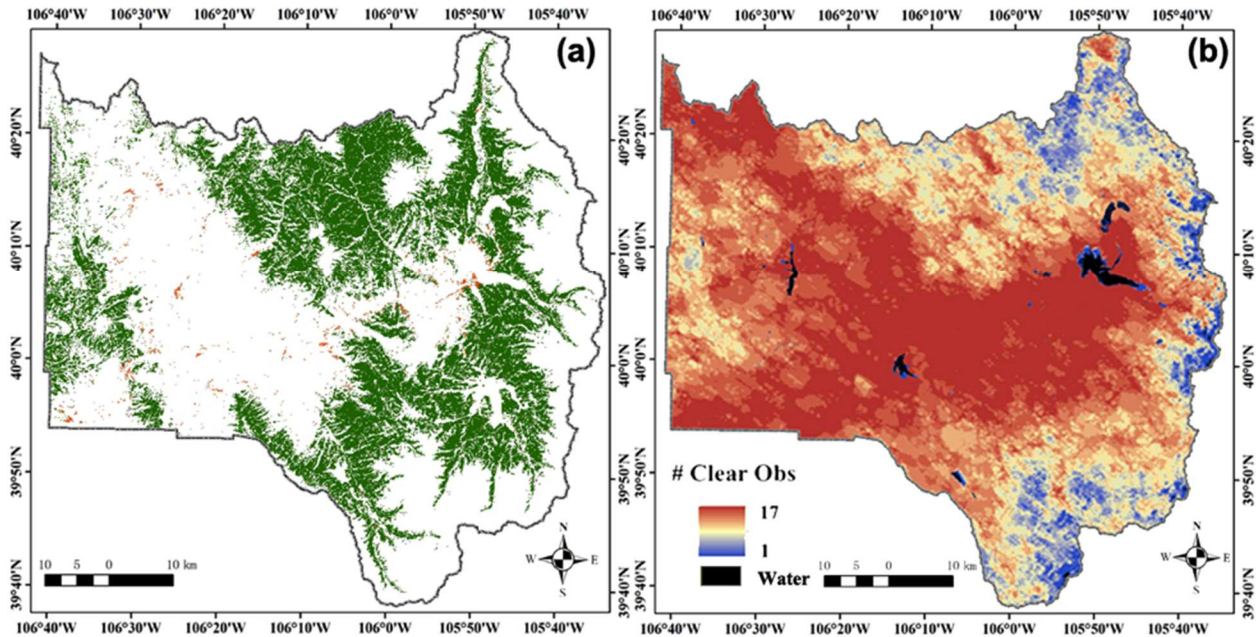
Legend

- ⬛ (magenta) Rocky Mountain Foothill Limber Pine-Juniper Woodland
- ⬛ (green) Rocky Mountain Lodgepole Pine Forest
- ⬛ (orange) Southern Rocky Mountain Dry-Mesic Montane Mixed Conifer Forest and Woodland
- ⬛ (dark) Rocky Mountain Subalpine-Montane Limber-Bristlecone Pine Woodland
- ⬛ (light green) Southern Rocky Mountain Ponderosa Pine Savanna

Figure 2. Forest type map for Grand County, from (**a**) the LANDFIRE existing vegetation type data and (**b**) the number of clear Landsat observations over the period of 2000 to 2011.

2.3 Reference sample selection

We randomly placed training samples over forested areas and reconstructed their disturbance history with the aid of normalized burn ratio (NBR) time series from the LTSS and the 1-m resolution U.S. Department of Agriculture (USDA) National Agricultural Imagery Program (NAIP) imagery (obtained from the USDA Geospatial Data Gateway), which were available for years 2005, 2009 and 2011 in Grand County. The NBR time series were calculated using bands 4 and 7 from the Landsat imagery (Key & Benson, 2006) and then multiplied by 100, so they could be represented as integer values instead of floating point values. For each training location, we identified the disturbance event type, duration and onset time (Table 2). Disturbance event types included: healthy, MPB mortality or clearcuts. Fire was not included, because large fires

17

did not occur in our study area during the time period of this study (2000 to 2011), as indicated by the U.S. Geological Survey Monitoring Trends in Burn Severity database (Eidenshink et al., 2007). In total, we collected 106 training samples, among which, 53 were sites with MPB mortality, 37 were clearcuts and 16 were healthy. We selected the relatively small number of training samples, because many studies suggested that trajectory-based methods perform well when trained with a relatively small sample size (Kennedy et al., 2010; Meigs et al., 2011; Sulla-Menashe et al., 2013). Statistical classifiers require more training data to fully represent each class in the feature space (Mathur & Foody, 2008). Thus, we expanded the original training sample size by 10 times to a total of 1,060 training samples. For those newly added samples, we only identified their disturbance types in the three years for which NAIP imagery were available instead of the whole NBR trajectory from the LTSS.

For validation purposes, we randomly sampled points in strata that were formed in the complete temporal-spectral space as a representation of the gradient of MPB mortality. In this manner, our test samples were able to cover a complete spectrum of disturbance events and a range of mortality. Considering the large data volume of the 11-year LTSS, for which the dimension was 2964 (rows) × 2901 (columns) × 102 (bands), we employed an efficient unsupervised classification tool, Clustering Based on Eigenspace Transformation, to improve the speed of clustering over conventional K-means without losing accuracy (Chen & Gong, 2013). Fifty strata were developed, and we proportionately allocated a total of 100 points to each stratum. In the absence of sufficient ground and ancillary information, we visually interpreted the status for each point at each individual year. By checking the proportion of points in the three classes, we found that they are almost equally distributed without severe over- or under-representation; the mean number of validation samples in each disturbance type each year was 39 (healthy), 38 (MPB mortality) and 23 (clearcuts; Table S2).

Table 2. Examples of normalized burn ratio (NBR) trajectories, National Agricultural Imagery Program (NAIP) data and *in situ* photos for healthy forest, MPB mortality and clearcut classes.

Class	Landsat	NAIP	Photo
Healthy conifer forest			
MPB mortality			

Clearcut
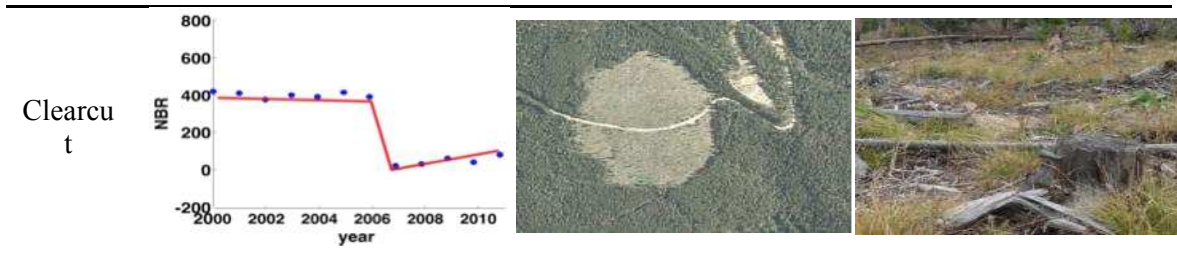
3 Method

3.1 Temporal segmentation

We developed time series of disturbance maps by combining the temporal trajectory analysis approach of LandTrendr (Kennedy et al., 2010) with a decision tree labeling procedure. Temporal trajectory analysis was used to decompose often noisy time series into a sequence of straight-line segments with distinct features designed to capture the event that happened for the duration of each segment. NBR (Key & Benson, 2006) was chosen to represent the vegetation condition, because of its sensitivity to disturbance (Kennedy et al., 2010) and its capacity to minimize radiometric differences among images. The general procedure was to use a set of parameters to enhance the signal-to-noise ratio of the NBR time series in order to capture the salient events happening in each period or segment. Details can be found in Kennedy et al. (2010), and the final effect of temporal segmentation, whether it was under-segmentation (split up into too few parts) or over-segmentation (subdivided into too many parts), was determined by the parameters listed in Table 3. Optimal LandTrendr parameter settings have been tested in the forests of the Northwest Pacific Region at both Landsat and MODIS scales (Kennedy et al., 2010; Sulla-Menashe et al., 2013). However, because we are not aware of reported parameter results in the literature specific to the Southern Rocky Mountain ecoregion, we tested a range of candidate parameter values (Table 3).

Table 3. LandTrendr parameters, descriptions, suggested values from Kennedy et al. (2010) and the values tested for this study and ultimately selected for this study to reduce the raw normalized burn ratio (NBR) time series values to a number of linear segments.

Parameter	Description and Units	Kennedy et al. (2010)	Values Tested	Value Selected
Despike	An outlier will be removed if the proportional difference in NBR values between two adjacent points is less than this parameter.	0.90	0.75; 0.9; 1	0.90
Max_seg	The maximum number of segments allowed in fitting.	4	3; 4; 5	4
VertexOvershoot	The first round regression detected vertices can overshoot (max_seg + 1) vertices by this value.	3	0; 3	0
pval	A pixel will be considered as no change if its *p*-value of the F-statistic for the entire trajectory is above this	0.05	0.05; 0.1	0.1

	threshold.			
Recovery_threshold	If the slope of a segment positively spans the whole spectral range within 1/recovery_threshold years, it will be rejected.	0.25	0.25; 1	0.25
BestModelProportion	A simpler model will be chosen if its F-statistic exceeds this proportion of the best fitting model.	0.75	0.75; 1	0.75

We ran LandTrendr on all combinations of the candidate parameter values, which resulted in 144 unique combinations in total, and then visually compared their temporal segmentation results with the original NBR time series for the 106 training samples. Thus, the calibration involved 15,264 comparisons. Each individual comparison for a sample was coded in a binary state using two criteria: the overall match in the shape and the timing of vertices. A good match occurred if the disturbance event that happened at that pixel was successfully captured, and the slope and magnitude for each segment deviated little from the central trend. The vertex timing was judged by how well the algorithm captured the onset and ending time of each disturbance event. If both criteria were satisfied, that comparison would be scored as 1, and otherwise, it would be 0. The optimal parameter set was decided based upon the pooled rankings across all training samples. The processing time took about 200 minutes (on 5,376,538 unmasked pixels) for this step, which was run on a workstation with an Intel i7-2600 3.4 GHz quad core CPU and 8 gigabytes of physical memory.

3.2 Decision tree-based spectral segment labeling

The outputs of the temporal segmentation included the fitted segments, and a set of vertices connecting individual segments. We employed a DT to attribute disturbance events associated with those vertices and segments, with leaf nodes representing class labels and branches representing decision scenarios. The DT was built with predictors characterizing each segment: the disturbance occurrence onset time, duration and the magnitude of NBR change. We defined the onset time as the starting year of a segment. Magnitude was the absolute change in NBR between the ending year and the onset year, whereas duration was the time elapsed over the length of one segment. Different types of disturbance events were characterized by distinct features. For instance, clearcuts could be recognized by segments with a short duration and large, negative change in NBR, whereas MPB mortality segments tended to have a gradual, but long-duration decline in NBR values.

Decision rules were used to identify forest conditions in a top-down sequence (Figure 3), and the definition of key parameters are explained in Table 4. These parameters were manually calibrated with the same training samples described in Section 3.1. Specifically:

(1) Segments were separated into regrowth, stable or disturbed status according to their magnitude (mag) at the first level of the DT. If the absolute magnitude of one segment was less than the pre-set threshold (<thre_mag1), it was treated as disturbed. If the magnitude was within a threshold range (±thre_mag1), then it was considered to be stable. Otherwise, it was considered to be in a regrowth stage (>thre_mag1).

(2) To label a segment as regrowth or stable, healthy vertices were identified based on an NBR threshold (thre_vertex1). Thus, a vertex in either a regrowth or stable period with its NBR value greater than the thre_vertex1 parameter was labeled as healthy.

(3) Segments classified as disturbed in Step 2, were labeled as clearcuts if their rate of change in NBR was greater than a second threshold (thre_mag2); otherwise, segments were labeled as MPB mortality. The rate of change was defined as the average NBR change per year, which is a reflection of both magnitude and duration. The thre_mag2 parameter was designed based on the assumption that clearcuts always have more abrupt and rapid decreases in NBR than MPB mortality.

(4) In the third level of the DT hierarchy, the label from the previous year (pre_label) was critical in determining the label for the current vertex. This was based on the assumption that events are temporally dependent and forests can only logically transition from certain states to another. For instance, clearcuts often result in abrupt declines in NBR followed by persistent, but slow increases in NBR. Although the magnitude of change in the post-clearcut period is not as sharp as that of the pre-clearcut period, the vertices in the subsequent years will still be assigned as clearcut to ensure that the disturbance class labels have temporal consistency.

(5) The final step involved attributing the vertices for the first year of the time series. We separated this step, because there was no vertex information prior to the first year. After MPB mortality, standing tree trunks and branch residuals remain on site, whereas clearcuts usually have a significant amount of bare ground. Thus, NBR values in areas with MPB mortality should generally be higher than they are in clearcut areas. The thre_vertex2 parameter defined the cutoff value for separating clearcuts and MPB mortality in these cases.
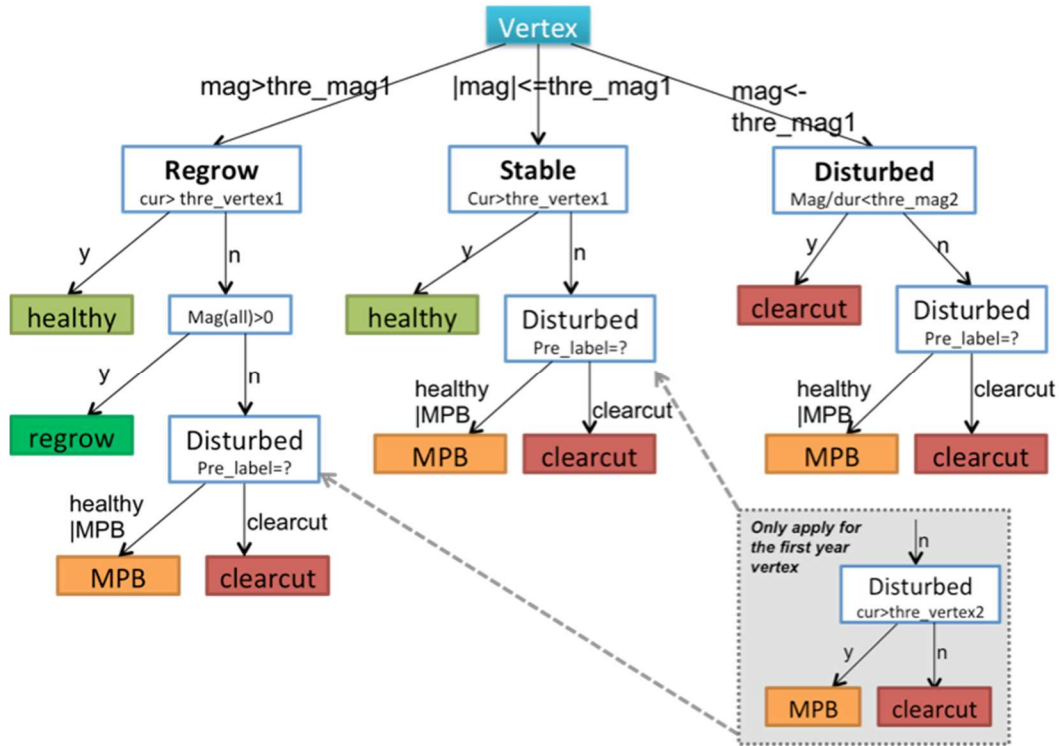
Figure 3. The decision tree used to attribute temporal segments into the different disturbance classes.

Table 4. Abbreviations and control parameters used in the decision tree.

Parameter	Description
mag	Magnitude of change in NBR between the current vertex and the following vertex: $NBR_{next\ year}-NBR_{current\ year}$.
cur	The NBR value for current vertex.
pre_label	The vertex label in the previous year.
thre_mag1	The magnitude threshold that distinguished stable from either disturbance or recovery.
thre_mag2	The magnitude threshold that separated MPB mortality from clearcut.
thre_vertex1	If the current vertex NBR value was above this threshold, it was treated as healthy, otherwise, it was further analyzed into disturbance types.
thre_vertex2	If first year's vertex value was below this threshold, it was treated as a clearcut pixel and MPB mortality otherwise.

Notes: MPB - mountain pine beetle; NBR - normalized burn ratio.

3.3 Post-labeling process

Both the temporal segmentation and DT were run at the pixel level. Thus, it was possible that two adjacent pixels could simultaneously experience the same event, but were labeled differently due to errors. Since most disturbance events were patchy, the behavior of spatially adjacent pixels could be used to enhance the robustness of the classification. Based on this logic, we filled small holes in a large patch that were undetected or mislabeled. To do this, we first applied a 3×3 majority filter to reduce the salt-and-

pepper effect and merged pixels into more complete patches, and then, we used a 3-year temporal filter to remove illogical transitions over time. For example, this step would change a pixel classified as MPB mortality in Year 1, healthy in Year 2 and MPB mortality in Year 3, to MPB mortality for all 3 years.

3.4 Single-date classification

Single-date mapping strategies were assessed using a traditional maximum likelihood classifier (MLC) and a random forest (RF) algorithm. MLC is a parametric method widely used in forest remote sensing (Breiman, 2001). In contrast, RF is a machine-learning technique that combines the results of many (thousands) of weak classifiers, such as classification and regression trees (Dietterich, 2000). RF is often praised for its good overall performance, as well as robustness to noise (Tucker, 1979). We implemented the classifiers on both the raw spectral bands and a combination of raw spectral bands and spectral indices that were sensitive to forest defoliation and canopy water content (Table 5, Crist & Cicone, 1984; Gao, 1996; Key & Benson, 2006; Johnson & Ross, 2005; Rock et al., 1986; Wilson & Sader, 2002).

Table 5. Spectral indices used in the single-date classifications, including formulas and references.

Spectral Indices	Formula	Reference
Normalized Difference Vegetation Index	$(b4 - b3)/(b4 + b3)$	Wilson & Sader, 2002
Normalized Difference Moisture Index	$(b4 - b5)/(b4 + b5)$	Rock et al., 1986
Moisture Stress Index	$b5/b4$	Gao, 1996
Normalized Difference Wetness Index	$(b2 - b4)/(b2 + b4)$	Crist & Cicone, 1984
Normalized Burn Ratio	$(b4 - b7)/(b4 + b7)$	Key & Benson, 2006
Tasseled Cap Brightness	$0.3037{\times}b1 + 0.2793{\times}b2 + 0.4743{\times}b3 + 0.5585{\times}b4 + 0.5082{\times}b5 + 0.1863{\times}b7$	Johnson & Ross, 2005
Tasseled Cap Greenness	$-0.2848{\times}b1 - 0.2435{\times}b2 - 0.5436{\times}b3 + 0.7243{\times}b4 + 0.084{\times}b5 - 0.18{\times}b7$	Johnson & Ross, 2005
Tasseled Cap Wetness	$0.1509{\times}b1 + 0.1973{\times}b2 + 0.3279{\times}b3 + 0.3406{\times}b4 - 0.7112{\times}b5 - 0.4572{\times}b7$	Johnson & Ross, 2005

Note: band numbers in the formulas refer to the Landsat 5 band order.

3.5 Accuracy assessment and the sample size effect

We conducted both qualitative and quantitative accuracy assessments. First, a confusion matrix was created for each individual year, and associated accuracy measures were generated, including the overall accuracy, kappa, producer's accuracy and user's accuracy. Second, we also visually evaluated the results by comparing the mapped spatio-temporal pattern of mortality with those observed by the Forest Health Monitoring Aerial Detection Survey (ADS) data (Friedl & Brodley, 1997). The ADS data are generated by aerial sketchmapping, a technique for observing and mapping forest damage from an aircraft. Although ADS had been criticized for its imprecision at fine scales due to reasons, such as misregistration and the subjectiveness of the operators (Meigs et al.,

2011), it is reliable when used at coarse scales (Friedl & Brodley, 1997). A pilot study initiated in the Rocky Mountain Region demonstrated that all three types of accuracies for the MPB detection in lodgepole pines exceeded 80% when the spatial tolerance was increased to 500 m (Friedl & Brodley, 1997). We thus had confidence that the epicenters and patterns of spread derived from ADS polygons could be used as a reference dataset to compare against our results. We also altered the size of the training sample dataset from 106 to 1060 in increments of 10% and tested the effects of sample size on accuracy. This produced 10 corresponding sets of results to test the effect of sample size on accuracy metrics for both the MLC and RF classifications.

4 Results

4.1 Parameter calibration for temporal segmentation and decision tree labeling

Parameter calibration in the forest growth trend analysis involved two parts. At the temporal segmentation stage, the set of parameters producing the highest score from all 144 combinations was chosen (Table 3). By using the same set of training samples, we also determined the four threshold values in the DT. We set the allowed variability in NBR for stable segments (thre_mag1) to be 20 (the unit for all thresholds was NBR × 100) as reflected from Figure 4. The cut-off NBR value of vertices (thre_vertex1) to distinguish healthy forest from disturbances was 350. Threshold Thre_mag2, used to separate clearcuts from MPB mortality, was set at −150. A higher degree of overlap was observed between the post-clearcut and MPB mortality NBR values, and thus, we set thre_vertex2 to the third quantile of NBR values in clearcuts, which was 50.
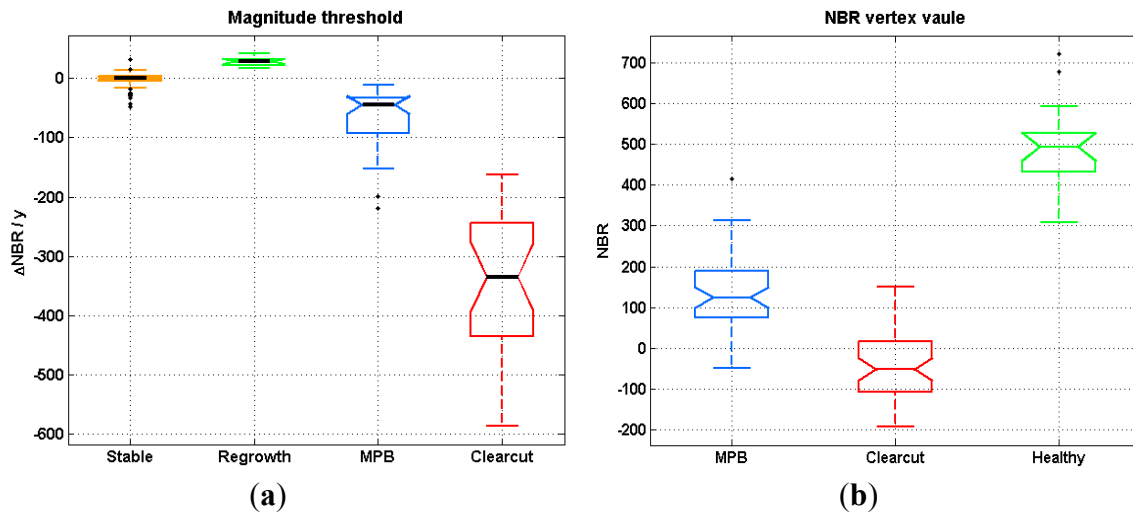
Figure 4. Tukey boxplot for (a) the averaged annual normalized burn ratio (NBR, multiplied by 100) changes of stable, regrowth, MPB mortality and clearcut plots; (b) current vertex values of post-MPB mortality, post-clearcut events and healthy plots. The bottom and top of the box are the first and third quartiles, and the band inside the box is the median. The whiskers represent the 1.5 interquartile range of the lower and upper quartile.

4.2 The performance of forest growth trend analysis

The forest growth trend analysis achieved an overall annual accuracy ranging from 86.74% to 94.00%, and the average was 90.31% (Table 6). Except for the user's accuracy for MPB mortality (84.81%) and the producer's accuracy for clearcuts (77.30%), the mean value for all types of accuracies was above 85%. Larger standard deviations of accuracies among different years were found in the producer's accuracy for healthy forest and the producer's accuracy for clearcuts. As indicated from the confusion matrix (Table S2) and Figure 5, healthy pixels were well distinguished from the two disturbance types in the first few years and became less separable from MPB mortality after 2005. Pixels with MPB mortality were confused with either healthy or clearcut classes, but the proportion was not high. Confusion between clearcuts and healthy classes occurred in the first few years of our study and then between clearcuts and MPB mortality in later years. Visual examination showed that the shifting of MPB outbreak epicenters and the expansion of the outbreak boundaries was congruent between the two independent datasets (ADS and validation points). Maps of the onset year of MPB mortality revealed that the MPB outbreak in Grand County was initiated at multiple locations and spread outward from those locations over time to affect nearly all habitats with suitable hosts (Figure 6).
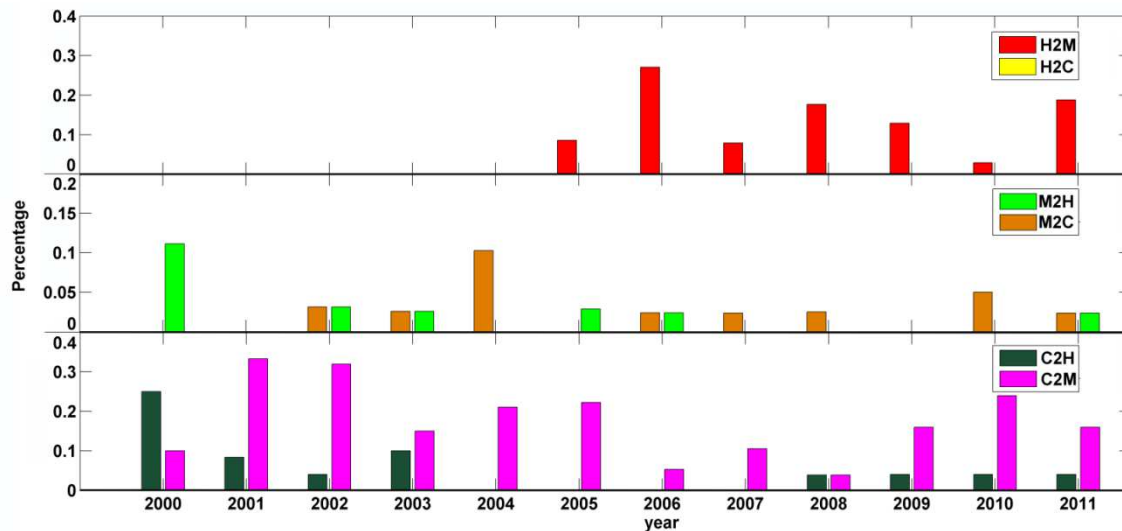
Figure 5. The proportion of validation samples that were erroneously labeled in other classes. Notes: H, healthy; M, MPB mortality; C, clearcut; H2M is explained as "healthy samples classified to MPB mortality."

4.3 Comparison with single-date classification and sample size effects

The accuracy achieved by the single-date classification ranged between 37.20% and 75.20% and was lower than the time series classification, running on either the raw or combined spectral bands trained by the same set of samples (Table 7). We also observed that the time-series classification accuracies were relatively stable over time. In contrast, the single-date image classifications had high year-to-year variability in accuracy, which was shown by a distinct, increasing trend of the producer's accuracy for MPB mortality from 2005 to 2011. The producer's accuracy for healthy forest decreased substantially

over the same time period. Table 7 also listed the accuracies generated from RF and MLC with only the raw spectral bands and the combined use of raw spectral bands and spectral indices. The accuracy of the RF classification improved when the spectral indices were included as predictors, and this effect was not evident with the MLC. Between the two single-date classification methods, RF had better overall performance than MLC.

(a)   (b)

27
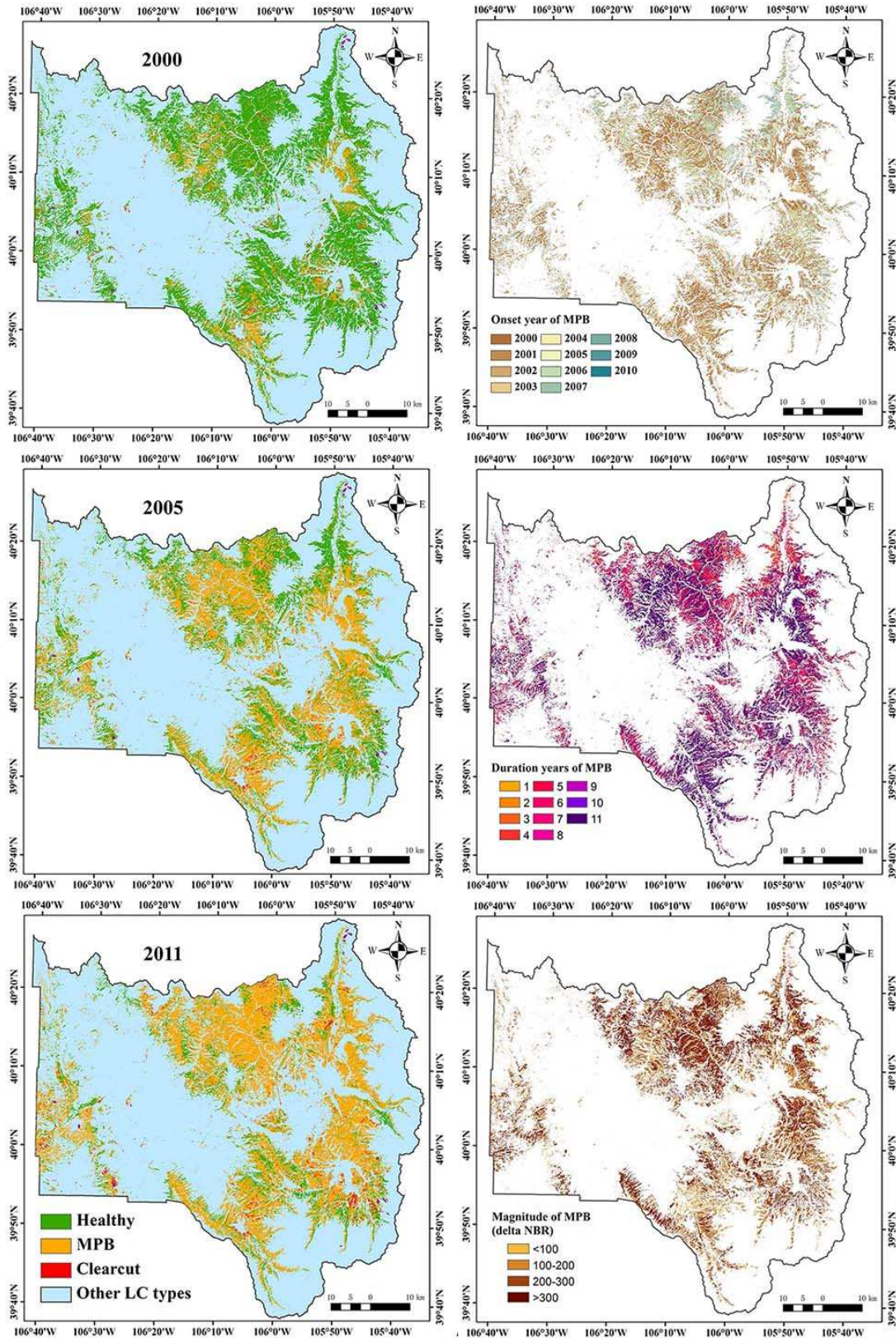
Figure 6. (a) Classification results of the forest growth trend analysis in the years 2000, 2005 and 2011; (b) maps of the onset year, duration and magnitude of mountain pine beetle (MPB) mortality.

By varying the number of training samples used to train the MLC and RF classifiers in 10% increments to a maximum of 1060 training samples, we obtained 10 sets of results for the single-date classifications. Figure 7 shows the relationships between accuracy and sample size, for overall accuracy generated from the MLC and RF classifiers, as well as the producer's accuracy and the user's accuracy for the MPB mortality class. Despite some small fluctuations, all accuracies increased with the training sample size, and the changes were especially pronounced for the initial increases in sample size. The highest overall accuracies were achieved when 100%, 100% and 90% of the training samples were used by RF (89.43%, 90.48%, 88.66%) and 100% of the training samples were used by MLC (88.41%, 82.93%, 85.90%). This improvement was substantial compared to the results based on the original set of 106 training samples. The overall accuracy for RF increased by 30% on average from the smallest to the highest training sample size, 8% for the producer's accuracy and 33% for the user's accuracy. For MLC, the average increase was 40% in overall accuracy, 31% in the producer's accuracy and 43% in the user's accuracy between the smallest and largest training sample sizes. We also noticed that after a certain training sample size, the accuracy stopped increasing or even slightly decreased, and the saturation position was around the 40% sample size (or 424 points) for all accuracy metrics and both classifiers. Accuracies after the saturation point were comparable to the time series classification results.

Table 6. Accuracy assessment results for individual years of the time series classification.

Year	OA	Kappa	Healthy		MPB Mortality		Clearcut	
			PA	UA	PA	UA	PA	UA
2000	89.00	82.21	100.00	83.02	88.89	94.12	65.00	100.00
2001	90.00	84.23	100.00	95.74	100.00	79.49	58.33	100.00
2002	89.00	82.88	100.00	95.56	93.75	78.95	64.00	94.12
2003	93.00	88.92	100.00	93.18	94.87	92.50	75.00	93.75
2004	92.00	87.41	100.00	100.00	89.74	89.74	78.95	78.95
2005	91.00	85.51	91.49	97.73	97.14	80.95	77.78	100.00
2006	86.74	78.99	72.97	96.43	95.24	78.43	94.74	94.74
2007	94.00	90.49	92.11	100.00	97.67	89.36	89.47	94.44
2008	91.00	86.20	82.35	96.55	97.50	84.78	92.31	96.00
2009	91.00	85.81	87.10	96.43	100.00	84.62	80.00	100.00
2010	90.00	84.56	97.14	97.14	95.00	84.44	72.00	90.00
2011	87.00	79.64	81.25	92.86	95.35	80.39	80.00	95.24
mean	90.31	84.74	92.03	95.39	95.43	84.81	77.30	94.77
SD	2.18	3.45	9.25	4.46	3.47	5.47	11.35	5.92

Notes: OA, overall accuracy; PA, producer's accuracy; UA, user's accuracy; SD, standard deviation.

Table 7. Accuracy comparison among the time series classification, random forests (RF) and maximum likelihood classifier (MLC) with the same set of 2005, 2009 and 2011 validation samples. Only the mountain pine beetle (MPB) mortality class is included here.

Year		Time-Series Trend Analysis	RF		MLC	
			raw *	combined	raw	combined
	UA	80.95	68.00	67.30	71.96	88.00
2005	PA	97.14	18.78	62.40	85.08	65.90
	OA	91.00	63.82	74.40	75.20	73.50
	UA	84.62	46.15	100.00	39.63	0.00
2009	PA	100.00	35.43	48.70	100.00	100.00
	OA	91.00	53.47	72.90	40.94	38.70
	UA	80.39	78.47	77.80	37.92	22.20
2011	PA	95.35	83.06	10.80	100.00	100.00
	OA	87.00	66.62	40.40	38.15	37.20

Notes: "raw" denotes classification with solely spectral data, and "combined" denotes classification with the combined use of spectral and index data; PA, producer's accuracy; UA, user's accuracy; OA, overall accuracy.
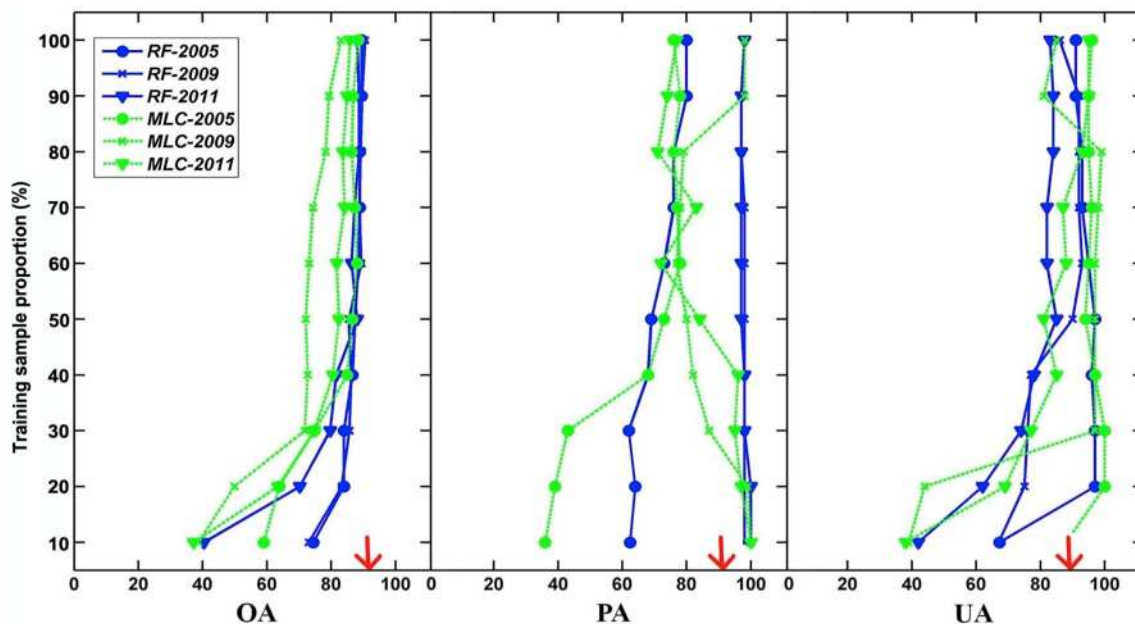
Figure 7. Relationships between accuracy and sample size for the maximum likelihood classifier (MLC) and random forests (RF) using multiple training sets. Graphs arranged from left to right display the trends of overall accuracy, the producer's accuracy and the user's accuracy for the mountain pine beetle (MPB) mortality class as the training sample proportion increases from 0.1 to one. Blue and solid lines represent RF results, whereas green and dashed lines represent MLC results. Red arrows indicate the mean accuracies produced by the forest growth trend analysis in the years 2005, 2009 and 2011.

5 Discussions

For the single-date classification, we found the following: (1) The RF achieved better overall accuracy than MLC in detecting forest disturbances. MLC relies on assumptions about the data distribution (e.g., normally distributed), whereas the ensemble learning techniques used by RF do not (Ghimire et al., 2010). Meanwhile, by grouping many individual classifiers, RF combined the strengths and minimized the weaknesses of each (Pal & Mather, 2003). (2) MLC is less affected by the selection of input layers than RF. RF relies on all outputs produced by each individual tree that is built upon the random selection of input layers, and thus, a larger amount of features could create a higher probability of "irrelevant" features being selected; but, when this occurs, it is usually negated by using the ensemble of results from individual trees. (3) The accuracies of single-date image classifications showed prominent year-to-year variability. The omission error for MPB mortality declined consistently from 2005 to 2011, whereas the omission error for healthy forest increased significantly. During this period, Grand County was in a steady transition from a landscape dominated by healthy forests to a landscape dominated by "grey-stage" forests. Not coincidently, the declining trend in the proportion of healthy forest matches the declining tendency of its omission errors over the years.

From the experiment on the sample size effect, on the one hand, we could determine the optimal sample size in the single-date MPB mortality mapping, which, to our knowledge, has not been discussed before. Both MLC and RF were sensitive to sample size, and several studies are in accordance with our conclusion (Foody, 2009; Li et al., 2013; Pal, 2005). Parametric algorithms are well known for their requirement of representative samples, and this requirement is usually satisfied by having a sufficiently large sample size (Rodriguez-Galiano et al., 2012a). Studies on sample-size effects for non-parametric classifiers are relatively rare. Rodriguez-Galiano et al. (2012b) observed a significant reduction in overall accuracy and the kappa values when the sample size reduced more than 50% of a non-parametric RF applied to Landsat images.

In our case, if we take both accuracy and labor/economic/time costs into consideration, the most optimum sample size for single-date classification is four to five times the original training sample size, which included 106 samples. On the other hand, we could compare the efficiency of single- and multi-date classifications. By using the same 106 training samples, our time series approach substantially outperformed the single-date classification, and their accuracies were similar only after expanding the training sample size to a large number (e.g., 10 times), which matches the finding from another study concluding that either single- or multi-date methods in Landsat-based forest disturbance mapping could result in high classification accuracy (Meddens et al., 2013), but our results confirm their findings only for large training sample sizes.

Although the forest growth trend analysis method is promising in many ways, several shortcomings exist: (1) Regardless of the high overall accuracy, the commission error for clearcuts and the omission error for beetle mortality were relatively high. The commission errors in clearcuts could be caused by the spectral similarity between post-clearcut pixels dominated by successional vegetation and healthy forest pixels. Errors of commission for MPB mortality usually happened in areas hosting a mixture of grey stage

trees and bare land, which could lead to a misclassification to clearcuts. (2) Parameter calibration was the most time-consuming part in the whole procedure and requires the expertise of image analysts. In some sense, the identification of various disturbance types using temporal trajectories is more challenging than the visual interpretation of false-color or true color image composites. Several potential solutions include the use of a tool called TimeSync, which was developed to aid with the temporal segmentation calibration and to verify the output from Landtrendr (Cohen et al., 2010). In addition, the Forest Inventory and Analysis (FIA) Program of the U.S. Forest Service consistently collects information on status and trends in forest species, health status, in total tree growth, mortality and removals by harvest. If FIA plots, or similar types of data, and their exact locations are available to users, they could aid the identification of the plots' disturbance history. In terms of the labeling, although the manmade decision tree, as shown in Figure 3, can be easily interpreted, a machine learning-based decision tree could be employed to make this step fully automatic.

6 Conclusions

Reconstructed forest disturbance histories are needed for a range of applications, and our paper tested an effective and efficient approach to generating disturbance histories using the Landsat time series stack. Our algorithm was designed to take advantage of differences in the magnitude and direction of changes in spectral indices, which are proxies for the physiological processes following different types of forest disturbances. The site-specific accuracy assessment in the three validation years indicated that the overall accuracy ranged from 86.74% to 94.00%, and the mean value of all types of accuracies was above 85%. Especially, our method outperformed standard classification approaches (maximum likelihood classification and random forest) by 15.8% to 52.3% when small training sample sizes (106 samples per study area) were used, which is a cost-saving advantage. Another strength of our strategy is that most parameters, especially at the attributing stage, are easily interpreted and modified, which will especially benefit users tackling similar problems of labeling change detection results.

In conclusion, our results demonstrate the potential for a forest growth trend analysis to characterize forest disturbance events with an optimal sampling scheme, both in economic and time terms, at a satisfying mapping accuracy level. Some short-term goals for our further studies will include improving the labeling step by replacing it with an automated machine learning technique, linking the magnitude of change with more ecologically meaningful properties, such as vegetation cover, extending the algorithm to the ecoregion scale, building spatio-temporal dynamic outbreak models on the time series maps with projections into the future. In addition to those applications, the spatially explicit information produced by our approach could also serve as raw material to facilitate other research to uncover new patterns of disturbances occurring on the landscape and to investigate the drivers generating the patterns of disturbances.

Table S1. MPB host species in LF Refresh 2001. Their vegetation type code, vegetation type, system group name, canopy cover, area of occupancy in Grand County, associated omission error and commission error are listed.

Code	Vegetation type	System group name	Canopy cover	Area (km^2)	Omission error (%)	Commission error(%)
2049	Rocky Mountain Foothill Limber Pine-Juniper Woodland	Limber Pine Woodland	Open	0.73	NA	NA
2050	Rocky Mountain Lodgepole Pine Forest	Lodgepole Pine Forest and Woodland	Closed	140.01	54.50	18.60
2051	Southern Rocky Mountain Dry-MesicMontane Mixed Conifer Forest and Woodland	Douglas-fir-Ponderosa Pine-Lodgepole Pine Forest and Woodland	Closed	43.58	53.30	46.20
2057	Rocky Mountain Subalpine-Montane Limber-Bristlecone Pine Woodland	Limber Pine Woodland	Open	2.25	NA	NA
2117	Southern Rocky Mountain Ponderosa Pine Savanna	Ponderosa Pine Forest, Woodland and Savanna	Sparse	0.004	NA	NA

Note: NA – No data in the LANDFIRE national quality assessment report.

Table S2. Confusion Matrix of the forest growth trend analysis for each year from 2000 to 2011.

	Reference data			
2000	H	A	C	UA(%)
H	44	4	5	83.02
Classification A	0	32	2	94.12
C	0	0	13	100.00
PA(%)	100.00	88.89	65.00	
2001	H	A	C	UA(%)
H	45	0	2	95.74
A	0	31	8	79.49
C	0	0	14	100.00
PA(%)	100.00	100.00	58.33	
2002	H	A	C	UA(%)
H	43	1	1	95.56
A	0	30	8	78.95
C	0	1	16	94.12
PA(%)	100.00	93.75	64.00	
2003	H	A	C	UA(%)
H	41	1	2	93.18
A	0	37	3	92.50
C	0	1	15	93.75
PA(%)	100.00	94.87	75.00	
2004	H	A	C	UA(%)
H	42	0	0	100.00
A	0	35	4	89.74
C	0	4	15	78.95
PA(%)	100.00	89.74	78.95	
2005	H	A	C	UA(%)

	H	A	C	
H	43	1	0	97.73
A	4	34	4	80.95
C	0	0	14	100.00
PA(%)	91.49	97.14	77.78	

2006	H	A	C	UA(%)
H	27	1	0	96.43
A	10	40	1	78.43
C	0	1	18	94.74
PA(%)	72.97	95.23	94.74	

2007	H	A	C	UA(%)
H	35	0	0	100.00
A	3	42	2	89.36
C	0	1	17	94.44
PA(%)	92.11	97.67	89.47	

2008	H	A	C	UA(%)
H	28	0	1	96.55
A	6	39	1	84.78
C	0	1	24	96.00
PA(%)	82.35	97.50	92.31	

2009	H	A	C	UA(%)
H	27	0	1	96.43
A	4	44	4	84.62
C	0	0	20	100.00
PA(%)	87.10	100.00	80.00	

2010	H	A	C	UA(%)
H	34	0	1	97.14
A	1	38	6	84.44
C	0	2	18	90.00

PA(%)	97.14	95.00	72.00	
2011	H	A	C	UA(%)
H	26	1	1	92.86
A	6	41	4	80.39
C	0	1	20	95.24
PA(%)	81.25	95.35	80.00	

Chapter 3 Forest disturbance regimes, interactions, and successional pathways in a mountain pine beetle infected ecoregion

Abstract

The pine forests in the southern portion of the Rocky Mountains are a heterogeneous mosaic with some areas receiving extensive and intensive stress from human activity, fire, and mountain pine beetles (MPB; *Dendroctonus ponderosae*), and other areas in various stages of recovery from disturbances. Understanding the underlying disturbance regimes, their interactions, and disturbance-succession pathways are crucial for adapting management strategies to mitigate their impacts. With this purpose, we depicted the forest disturbance and recovery history over a 13-year time series in the Southern Rocky Mountains Ecoregion with Landsat image stacks, aided by a novel sampling strategy that takes advantage of the scene-overlap among adjacent Landsat images, and an automated workflow integrating a temporal segmentation technique developed from Landsat-based Detection of Trends in Disturbance and Recovery algorithm, a set of spatio-temporal segment features and Random Forest classifier. The mean overall accuracy for all scenes was 82%. Analysis of the disturbance trends revealed that MPB contributed to 70% of the total disturbed area. We found that burn severity was largely unrelated to the severity of pre-fire beetle outbreaks in this region, where the severity of post-fire beetle outbreaks has been shown to decrease with burn severity. Approximately half the clearcut and burned areas were in various stages of recovery, but the regeneration rate was much slower for MPB-disturbed sites. Pre-fire beetle outbreaks and subsequent fire produced positive compound effects on seedling re-establishment in SRME, which suggests that serotinous lodgepole pine is resilient to wildfires occurring after beetle mortality.

1 Introduction

The vegetation of the Southern Rocky Mountains Ecoregion (SRME) is a heterogeneous disturbance-derived mosaic, where fire, blow-down, insect outbreaks and clearcut are regarded as the primary disturbance types (Barbour & Billings, 2000; Veblen et al., 1994). Under the pressure from warming climate and human interventions, the disturbance and recovery regimes, which refer to the spatial and temporal DR dynamics over a long time period (Turner, 2010), are undergoing rapid changes in the subalpine zones of Rocky Mountains. Fire is perhaps the most commonly studied disturbance agent (eg. Justice et al., 2002; Simon et al., 2004; Stroppiana et al., 2000) and the total area burned and the number of large fires have risen dramatically across much of the western United States over the past 25 years (Calkin et al., 2005; Stephens, 2005). Meanwhile, massive conifer mortality since the mid-1990s in this ecoregion has been related to outbreaks of bark beetles: primarily mountain pine beetle (MPB), spruce beetles, and western balsam bark (Smith et al., 2015). Among them, MPB mortality has intensively expanded in high elevation conifers in the Rocky Mountains reaching epidemic levels not previously recorded (Gibson et al., 2008). The amount of carbon in trees killed by fires and by MPB outbreaks has been quite similar over the past decade (Hicke et al., 2013).

The subsequent recovery of forest vegetation is also highly spatially and temporally variable, since disturbances couple with environmental factors to determine the rates and pathways of succession (Pfulgmacher et al., 2013). Both disturbance and recovery (DR) fundamentally shape the trajectory of forest carbon storage, influence forest structure, composition, biomass, land surface water and radiation dynamics, and affect feedbacks between forest ecosystems and climate (Baldocchi, 2008; Bonan, 2008; Franklin et al., 2002; Gough et al., 2007; Kurz et al., 2008). Thus, understanding DR patterns, as well as their interactions are critical for assessing their impacts on the forest resilience mechanisms, and benefit relevant studies, such as habitat forecasting, general circulation modeling, international carbon pricing negotiation, and biodiversity conservation (Gibbs et al., 2007; Liang et al., 2014a; Running, 2008). Under this context, the first goal of this paper is to update the knowledge on the historical and current patterns of DR regimes in SRME, with our focus on the changes of MPB disturbance over the past decade.

The occurrences of multiple disturbances in this ecoregion provide us a good opportunity to investigate their interactions - a raising concern in ecology because they may cause ecosystems to be pushed beyond thresholds (White & Pickett, 1985; Groffman et al., 2006; Turner, 2010), yet a challenging question due to the scarcity of quantitative data. A disturbance may be linked with another by changing its extent, severity, or probability of occurrence. For SRME, there is substantial interest in how the extensive outbreaks of bark beetles may affect future wildfire (Turner, 2010). While spruce beetle outbreaks were detected to have no overlap with stand-replacing fires in the Colorado Rocky Mountains (Veblen et al., 1994), conclusions regarding MPB and fire interactions are more controversial. Increased (Hopkins, 1909; Schoennagel et al., 2012), decreased (Simard et al., 2011), and unrelated (Bond et al., 2009; Veblen et al., 1994) active crown fire potentials were found following MPB outbreaks, depending on the outbreak stage and burning conditions (Harvey et al., 2014). Additionally, there is no consensus whether MPB outbreaks following fires affect forest vegetation. Although it is presumed that fire-injured forests are more susceptible to beetles (Geiszler et al., 1984), some have pointed out that wildfire is an unlikely driver of outbreaks by MPB (Powell et al., 2012). Till now, no study has been conducted to investigate their interactions across the whole South Rockies. Accordingly, the second goal we attempted to address was to determine whether MPB outbreaks and wildfire are linked disturbances in this ecoregion.

If such linkages exist between disturbances, they may produce compound effects on ecosystems, which could be reflected in amplified severity beyond that of any singular disturbance, or the creation of novel characteristics that would not normally happen in isolation (Buma & Wessman, 2011), such as the shifting of dominant forest cover types (Johnstone et al., 2010), and reduced regeneration rates (Buma & Wessman, 2011). Understanding the consequences of those interactions is critical for conservation and management purposes. Our third goal is thus focused on revealing the effects of various compounded disturbances on lodgepole pine forest regeneration in SRME as compared with singular disturbances.

Long-term data of historical and current disturbances that has same spatial and temporal extent are lacking, but required to address our 3 research goals. Dendrochronology is the

most applicable and prevalent technique, but can be limited in geographical scope and may not detect all disturbance types. Forest Health Monitoring Aerial Detection Surveys is the major state and federal forest health monitoring effort since the mid-twentieth century (Man, 2010), but it has been criticized for spatial imprecision caused by misregistration as well as operators' subjectiveness, and the temporal shift between the attack onset and the spectral signature changes of canopy (Meigs et al., 2011; Kautz, 2014). Satellite spectral indices have been proven to be useful in accurately delineating forest disturbances over long time spans at broad spatial scales (Wulder et al., 2006), but if done with single date imagery, relative subtle changes arising from insect attacks are more difficult to monitor than prominent changes associated with stand replacing events (Skole & Tucker, 1993). We recently completed a twelve-year forest disturbance mapping in Grand County, Colorado with good success using Landsat time-series stack (Liang et al., 2014b). But so far, this approach has not been applied over large scales due to its dependency on human interpretation in attributing disturbance events. Here, we will advance this approach by developing an efficient and effective sampling strategy and automating the event attribution step, to serve the purpose of decadal forest DR mapping at the ecoregion scale.

2 Study area

Our study area in the SRME extends south from southern Wyoming through Colorado to the northern New Mexico (lower left: ~35°N, 109°W; upper right: ~43°N, 103°W) (Figure 1). To avoid confounding different types of insect mortality (e.g. spruce vs. pine beetles), we confined our analysis to the extent of MPB host species in the LANDFIRE Refresh 2001 Existing Vegetation Type data layer that was developed with *circa* 2001 Landsat imagery (Nelson et al., 2013), and was smoothed with a 3×3 majority filter to reduce noise and minimize the reported high omission errors (National c2001 Assessment; Figure 1). Pine forest selected as MPB host species included lodgepole pine (*P. contorta*; 95.4%), limber pine (*P. flexilis*; 2.9%) and ponderosa pine (*P. ponderosae*; 1.7%). Their total coverage was approximately 60,675 km^2. Hereafter, these forest types are referred to as 'forest'.
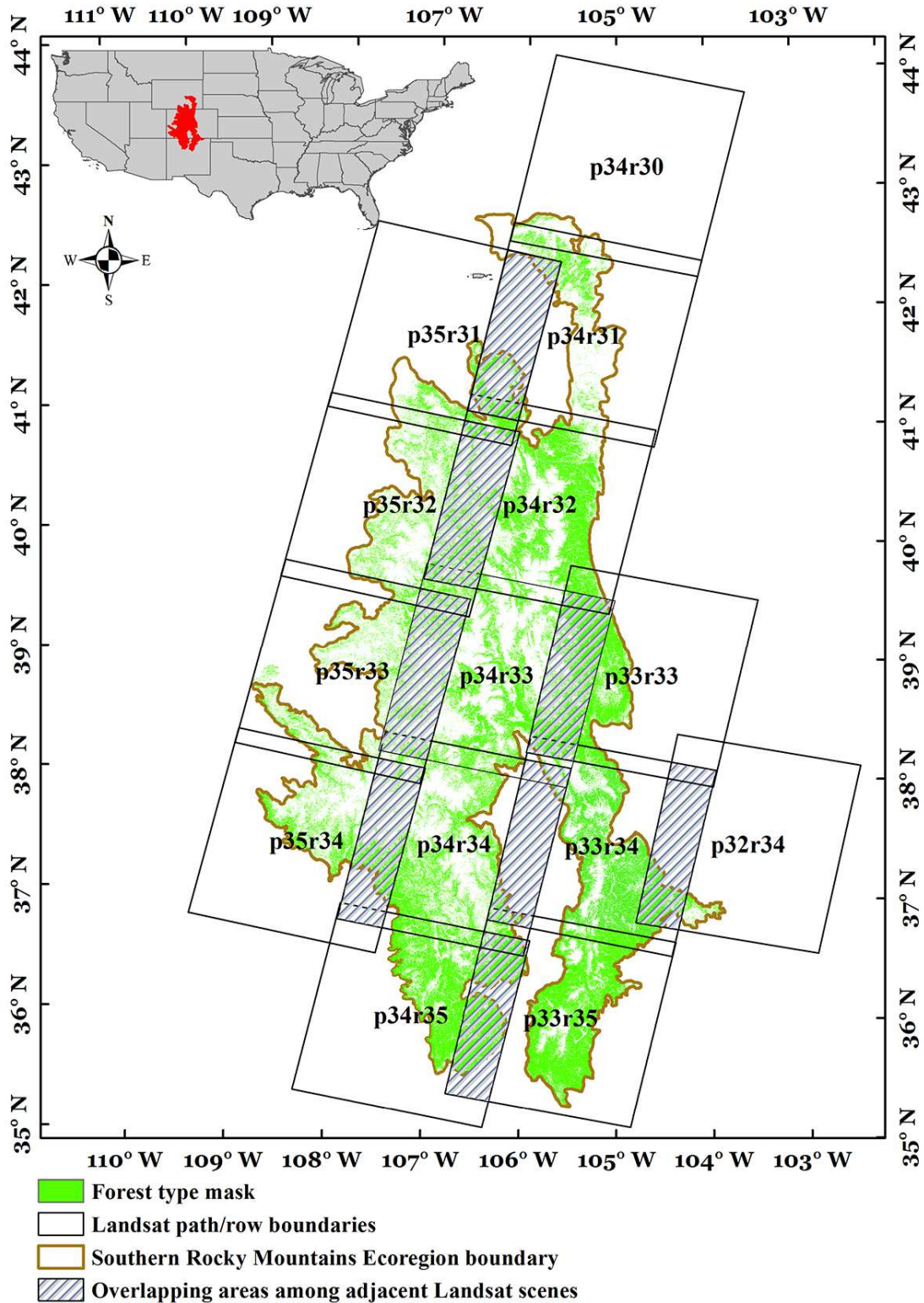
Figure 1. The coverage of Southern Rocky Mountains Ecoregion (U.S. Environmental Protection Agency, 2013), and the frame of 14 intersected Landsat scenes with trimmed edges.

3 Methods

3.1 Remote sensing image pre-processing

Landsat time series stacks (LTSS) are well suited to this study, because of their free availability, long time period coverage, broad spatial extent, multispectral characteristics, and temporal continuity. All Landsat images were acquired from the Landsat Surface Reflectance Climate Data Record generated by the Landsat Ecosystem Disturbance Adaptive Processing System (URL: http://earthexplorer.usgs.gov; accessed: 22 August 2014). We restricted our analysis to images acquired June through October, during which, June to September is the most active growing season for vegetation and thus provides the strongest spectral contrast between the healthy and beetle mortality forest. Images in October usually have better quality than summer in this mountainous region and were used as substitutions when clouds heavily contaminated all images in the ideal time window. We tried to find images containing less than 20% cloud cover, and if no such data existed, two or more cloudy images with similar phenology characteristics were used as replacements to guarantee one clear observation of a MPB infected area for most regions. Fourteen Landsat scenes intersected the boundary of SRME, and 247 images were collected from 1999 to 2011 in total with approximately 18 images per scene (Figure 2). We used the Normalized Burn Ratio (NBR; Key & Benson, 2005) to reconstruct the spectral trajectory, because of its sensitivity to disturbance and its capacity to minimize radiometric differences among images (Kennedy et al., 2010).
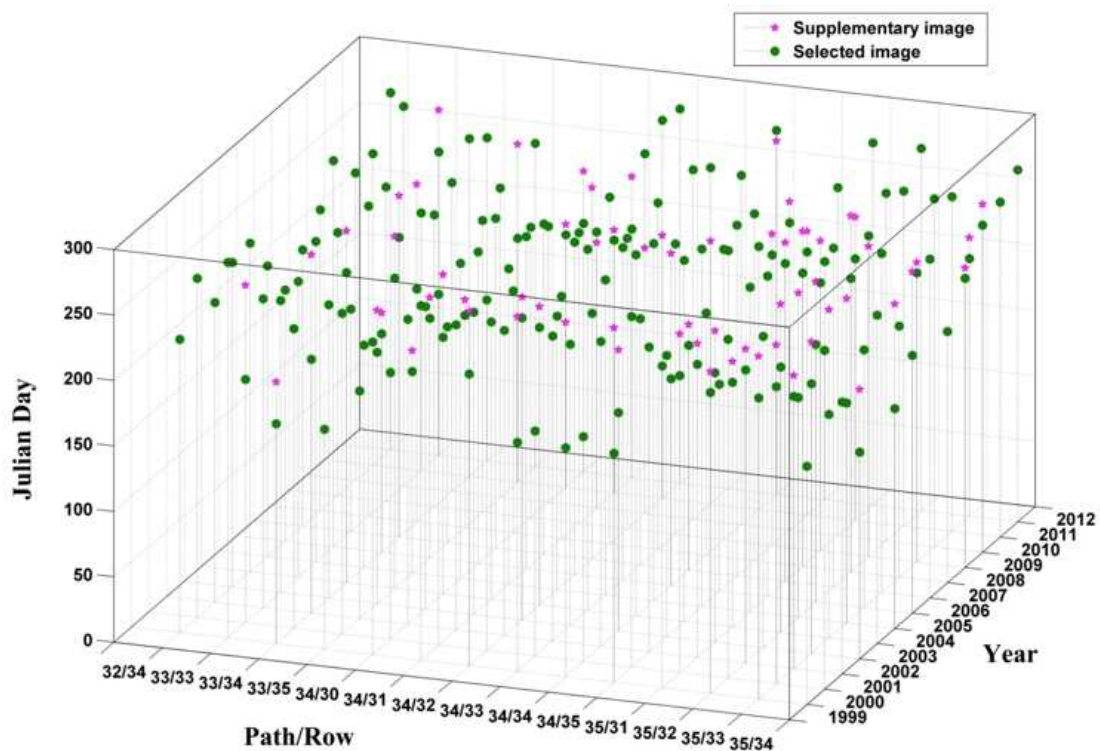

Figure 2. Scene acquisition dates of the fourteen Landsat scenes by year. Supplementary images used to fill the cloud gaps of the image in the same year were marked as magenta stars.

3.2 Reference sample selection

To improve the sampling efficiency at the ecoregion scale, we developed a new strategy by intensively selecting samples in the Landsat scene-overlapping area (SOA) between images along the same row, which occupies 20% to 40% coverage of the entire scene. The intention is to save efforts in image interpretation or on-site data collection. Meanwhile, although 20%-40% of the full scene coverage is a good representation of the landscape, to make the final sample set an unbiased indication of what the population is like, we then automatically add spectrally dissimilar samples from the non-overlapping area (NOA). Specifically, our sampling strategy involved the following steps (Figure 3):

1) *Clustering*. The LTSS was divided into SOA and NOA, and K-Means clustering was applied on them separately, in order to group pixels sharing similar trajectories together.
2) *Calculate spectral distances between cluster centers*. The spectral distance between the center of each SOA and NOA cluster was calculated.
3) *Remove spectrally similar NOA clusters*. NOA clusters that shared similar spectral signature with any SOA cluster would be treated as duplicated samples and removed. That is, only NOA clusters with their centers to all SOA cluster centers larger than one distance standard deviation of the distance set are retained. The combination of all SOA clusters and non-duplicated NOA clusters was thus able to represent the majority spectral space of the overlapped images.
4) *Stratified random sampling and event labeling*. Finally, we conducted stratified ransom sampling on the combined cluster set. For each sample, we interpreted their DR history with the aid of NBR trajectories, false-color composite Landsat layers, and high resolution Google Earth images.
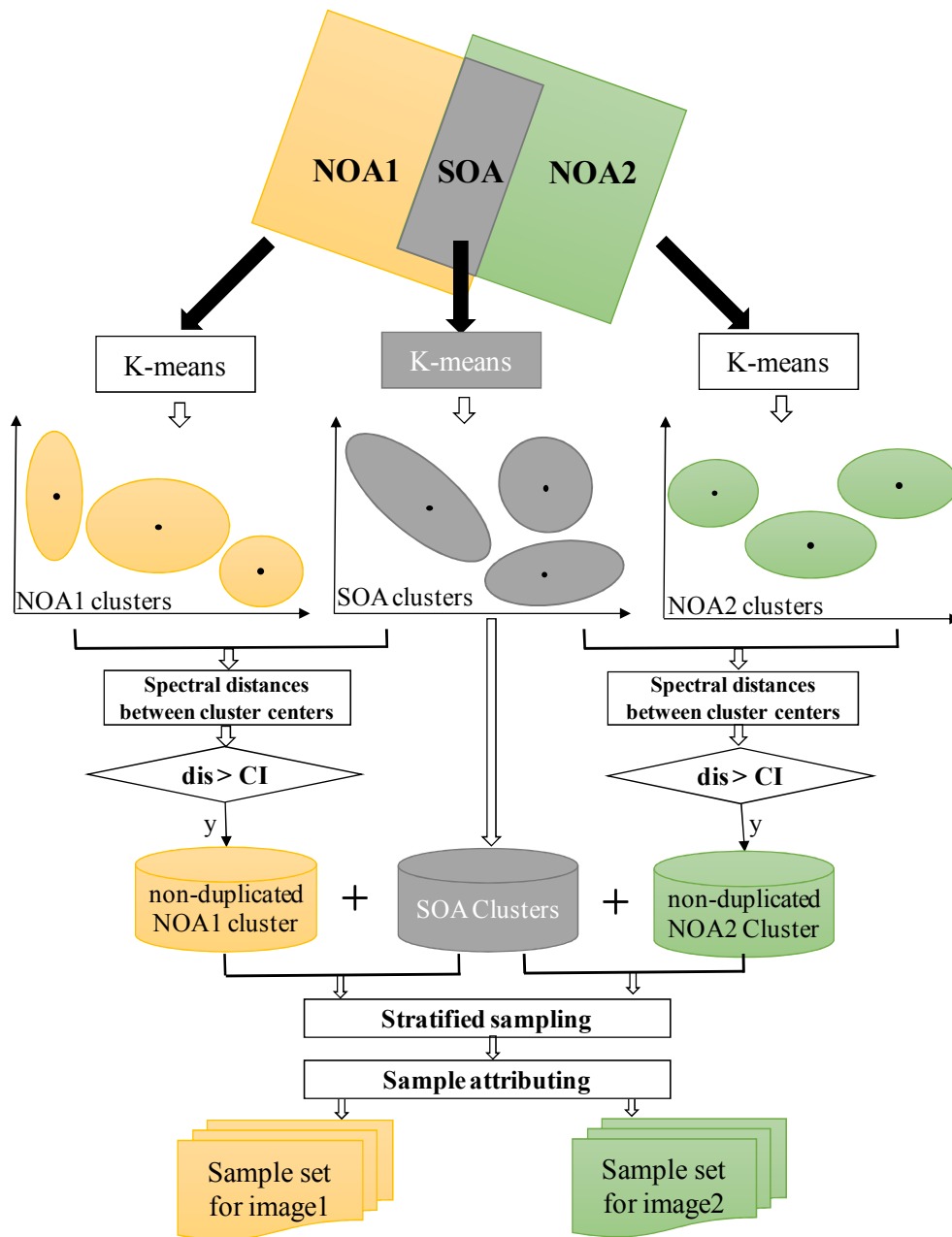
Figure 3. Sampling work flow. SOA: Landsat scene-overlapping area; NOA: non-overlapping area; dis - spectral distance; CI: one distance standard deviation of the spectral distance set.

3.3 Temporal segmentation

Temporal segmentation is one approach used to extract useful information from spectral trajectories, and has been successfully implemented with Landsat time-series in Landsat-based detection of Trends in Disturbance and Recovery tool (Landtrendr; Kennedy et al., 2010). The idea is to decompose the often-noisy time series into a sequence of straight-line segments that can represent distinct vegetation states. The general procedure is to first remove noise-induced spikes, then identify potential vertices that can separate

distinct periods before and after them, apply a set of trajectory-fitting algorithms to best capture the salient events happening in the trajectory, and finally choose the best model using an F-statistic (Kennedy et al., 2010). The quality of temporal segmentation is controlled by a group of parameters, and the calibration method was outlined in Liang et al. (2014a). For each pixel, the outputs include several fitted segments with a set of features describing the trajectory.

3.4 Segment-based random forest classification

We used temporal segments as the basic unit in the Random Forest (RF) classification instead of pixels. Because different DR events have distinct segment features, such as duration, severity, and onset, the combination of which can thus result in better differentiation. For instance, clearcuts could be recognized as segments with rapid and severe spectral value changes, whereas the changes of MPB mortality segments tend to be long, but slow. Besides the features of the focal segment, we also constructed a set of spatial neighborhood features and temporal neighborhood features to feed the RF classifier, which were designed based on the assumption that events that happened within a proximal zone at the same time or to a fixed location at different times are highly correlated with each other. The technical details of feature construction are explained as following:

Segment features: Vertex year is the starting year of the event occurrence. The fitted vertex value is the NBR value that comes out of Landtrendr segmentation. Magnitude is defined as the absolute NBR change between the head and tail vertex of the focal segment ($\Delta NBR = NBR_{head} - NBR_{tail}$). Duration denotes the time span from the head to the tail vertex, and slope is the ratio of magnitude to duration (Figure 4).
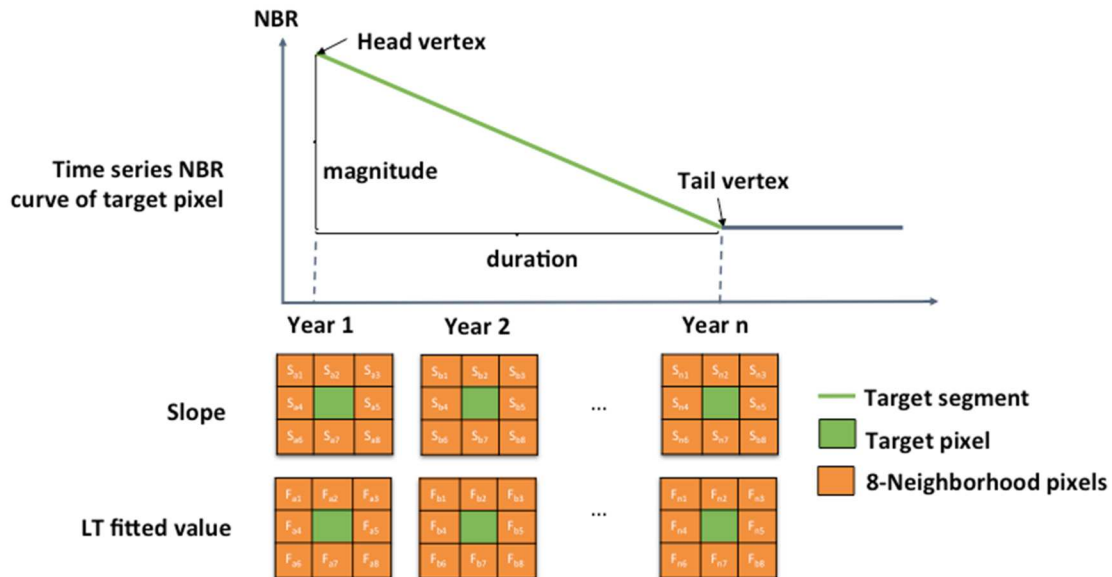
Figure 4. An illustration of the segment features and the neighborhood features listed in Table 1.

Temporal neighborhood features included the duration, magnitude, and slope of the prior and posterior segments of the focal one.

Spatial neighborhood features were calculated based on the slopes and vertex values of the eight spatially adjacent pixels over the duration of the focal segment. The slope set is denoted as N_s and the vertex value set is defined as N_f:

$$N_s = \{(S_{a1}, S_{b1}, \ldots, S_{n1}), (S_{a2}, S_{b2}, \ldots, S_{n2}), \ldots, (S_{a8}, S_{b8}, \ldots, S_{n8})\}$$

$$N_f = \{(F_{a1}, F_{b1}, \ldots, F_{n1}), (F_{a2}, F_{b2}, \ldots, F_{n2}), \ldots, (F_{a8}, F_{b8}, \ldots, F_{n8})\}$$

Where, S is slope and F is the fitted vertex value. The first subscript a to n indicates the first year a of the time span to the last year n, and the second subscript 1 to 8 represents the first to the eighth neighbor pixel. For example, S_{a1} is the slope of the first neighbor pixel in the first year of the focal segment duration.

Following that, we calculated the maximum value for each subset in N_s, to highlight the event with the most significant change (max8slope), and computed the mean and standard deviation of max8slope to represent the overall condition in the neighborhood system (avg_max8slope; std_max8slope). The same processing routine was applied to the N_f, with an additional minimum value calculation.

In total, forty-two segment features falling into fifteen categories were created. Five broad classes that represent major forest DR status in SRME were classified: healthy, MPB mortality, fire, clearcut, and regrowth. For sudden canopy removal events, we separated fires from clearcuts using the U.S. Geological Survey Monitoring Trends in Burn Severity database (Eidenshink et al., 2007). We then applied a plurality vote to the ten RF outcomes generated from different training partitions, and produced the annual time-series DR maps by applying the segment label to their corresponding years. Finally, the classification performance was evaluated via 10-fold cross validation. The overall accuracy (OA) was calculated by summarizing the percentage of segments that were labeled the same by the RF classifier and our samples, with the assumption that the temporal segmentation step is flawless. This assumption is made because it is difficult to obtain historical, temporally-explicit ground truth data covering the whole ecoregion.

3.5 Disturbance regime, interactions and disturbance-recovery pathways

We derived size, onset year, magnitude, and duration as the key disturbance regime parameters for MPB mortality, fires and clearcuts. Onset represents when events are initiated over time. Magnitude is an indicator of the percent vegetative cover change (Kennedy et al., 2010), and duration suggests the most dominant event over the last decade for a particular location.

Two types of interactions exist between MPB outbreaks and fire in terms of their occurring order: MPB+fire (fire happens after beetle outbreaks), and fire+MPB (beetle outbreaks happen following fire). We attempt to determine their linkages by investigating how recent bark beetle outbreaks influenced subsequent burn severity, and whether burn severity affects the severity of pre-fire beetle outbreaks. To answer the question, we first

allocate pixels into four groups based on their disturbance history. MPB+fire and fire+MPB target groups refer to the assemblage of pixels containing the process of the two interaction modes. MPB / fire population group is the collection of pixels not showing the interaction patterns but possessing beetle outbreaks / fire events. The inclusion of the population groups was designed to control for the interaction groups to be compared with a spectrum of outbreak or burn severity occurring over the study region.

We then assessed the magnitude values for MPB events of the two target groups against those of the MPB population group separately using analysis of varianace (ANOVA), and the same procedure was applied to fire. The significance test on the means of the target and population groups provided a way of examining the effects of one disturbance event on the severity of the other. For instance, if no significant difference was found between the MPB outbreak magnitude in the fire+MPB target group and the MPB population group, the fire probably did not play a role in changing the severity of beetle outbreaks.

Finally, we depicted the disturbance-recovery pathway by summarizing the area size and proportion of each disturbance event that transitioned to either another disturbance type or to the recovery stage.

4 Results

4.1 Sampling and mapping

To demonstrate how the new sampling strategy functions, we displayed the centers of SOA and NOA clusters from one scene as an example in the Tasseled Cap space for visualization purpose, so that the concentrations of data within the total data volume can be most readily observed (Figure 5). It was intuitively evident that the centers of the duplicated NOA clusters were highly overlapped with the SOA clusters, whereas those of the few non-duplicated NOA clusters were much further away from them. This demonstrated that our sampling strategy could promote both the efficiency and accuracy in choosing representative samples when compared with random sampling over the entire scene.

The inclusion of spatio-temporal features has been proven to be effective as revealed from our accuracy evaluation results. The segment based OA for individual scenes varied from 74% to 92.5%, with the mean value at 85.9%, and if no such input is considered, the classification will yield uniformly lower accuracies for all scenes, with the mean value at 82%.
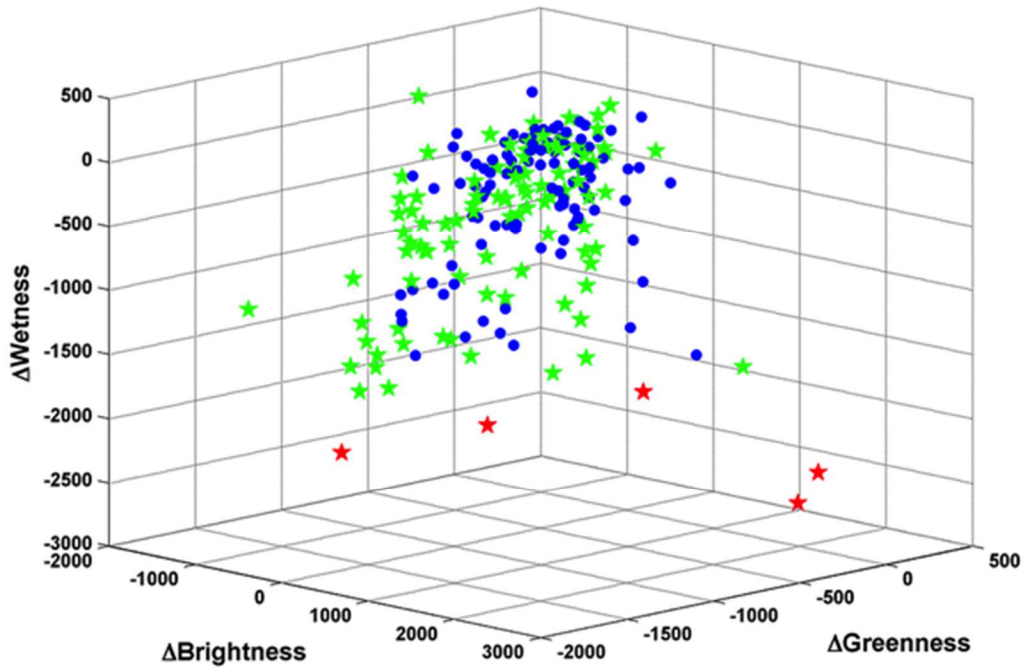
Figure 5. Centers of SOA, NOA and duplicated NOA clusters in the Tasseled Cap space of one Landsat scene (path: 32; row: 34). Each axis represented the absolute changes in brightness, greenness, and wetness over the study period.

4.2 Disturbance regime descriptors

Spatial distribution dynamics: Mountain pine beetle outbreaks had a clustered pattern (Figure 6). Early in the time span of this study, MPB outbreaks were scattered across the SRME and lasted for a limited number of years. However, by the early 2000's, the MPB epidemic in northern Colorado and southern Wyoming along the continental divide appeared and persisted over several years (Figure 6).

a)

c)
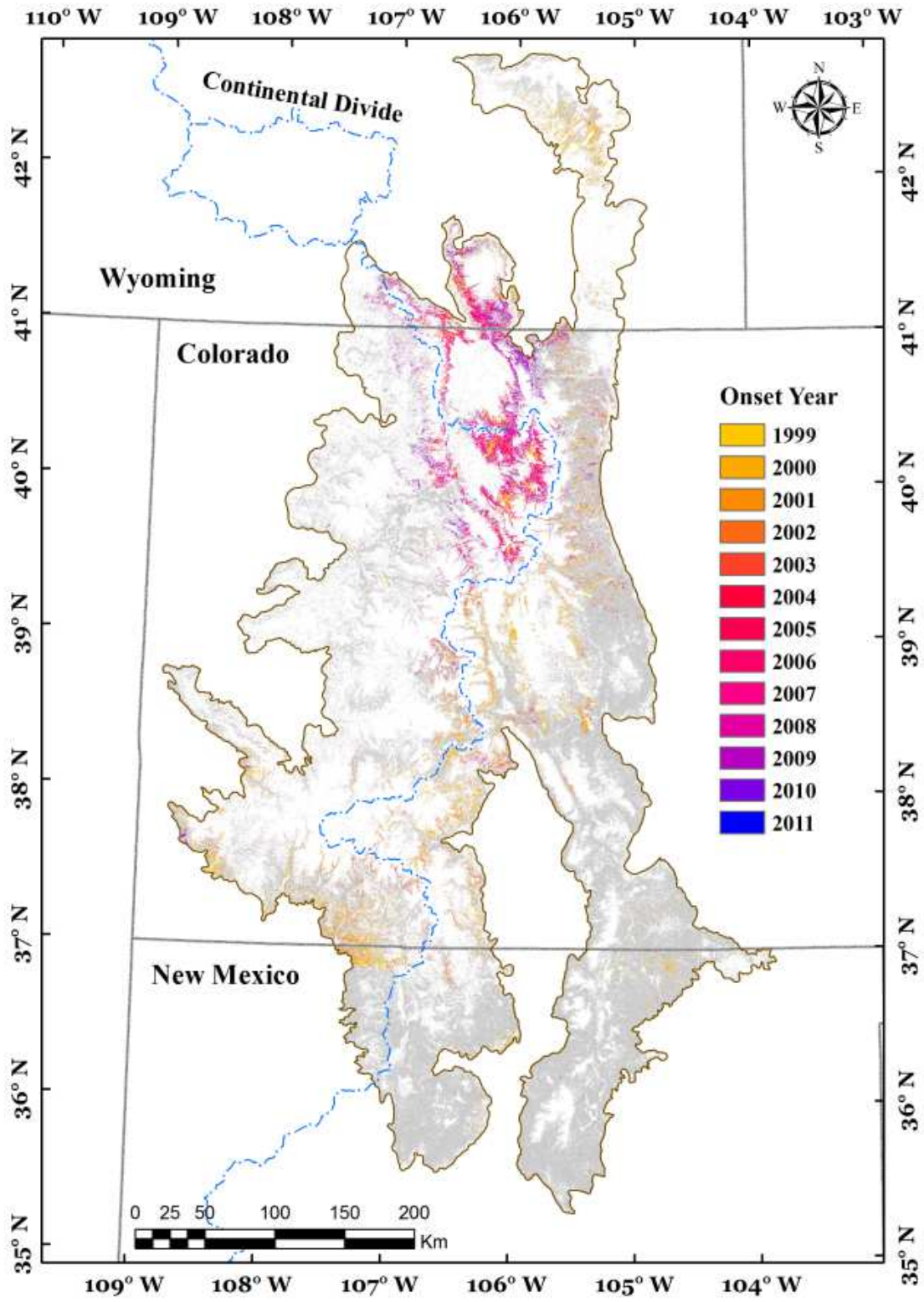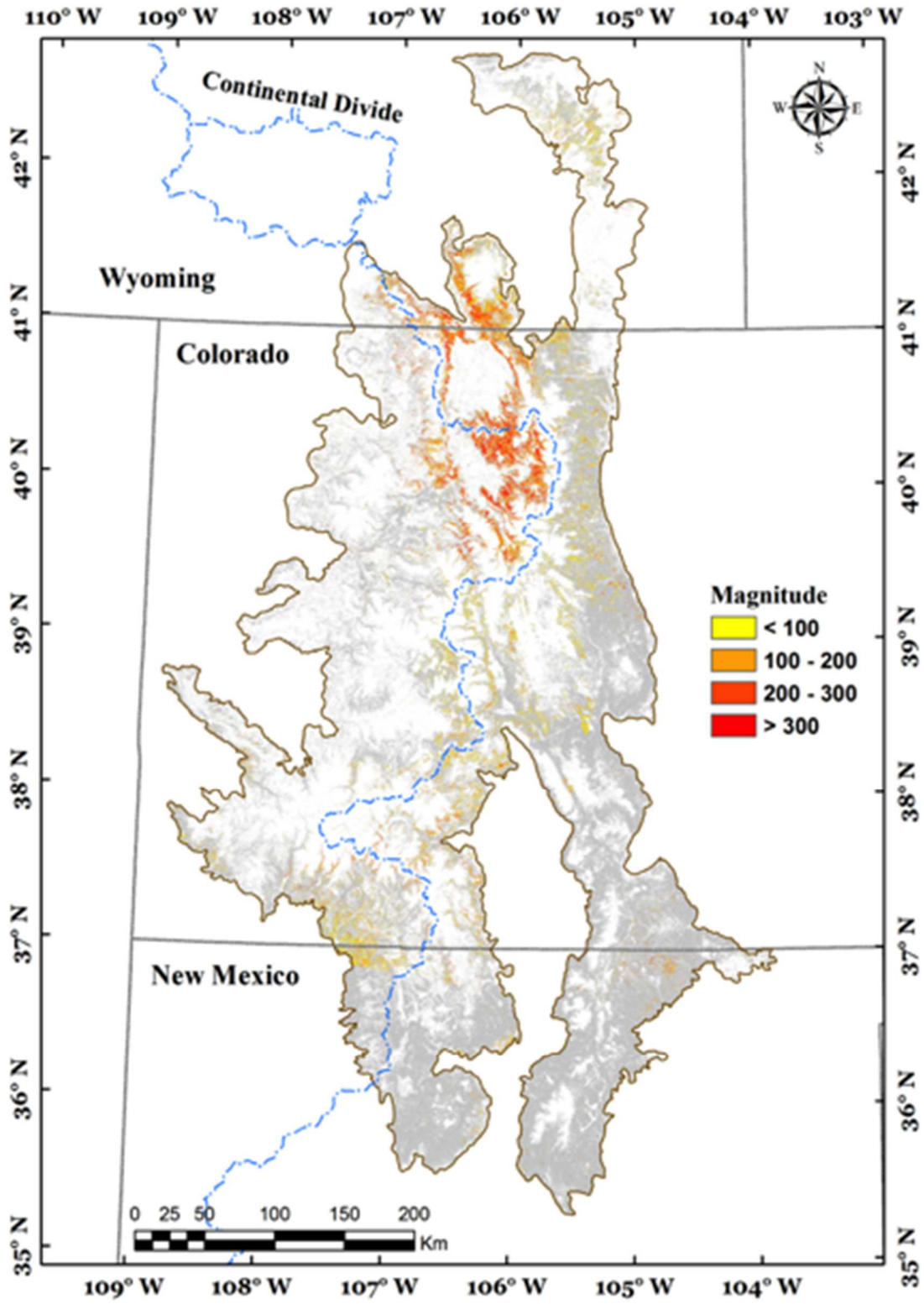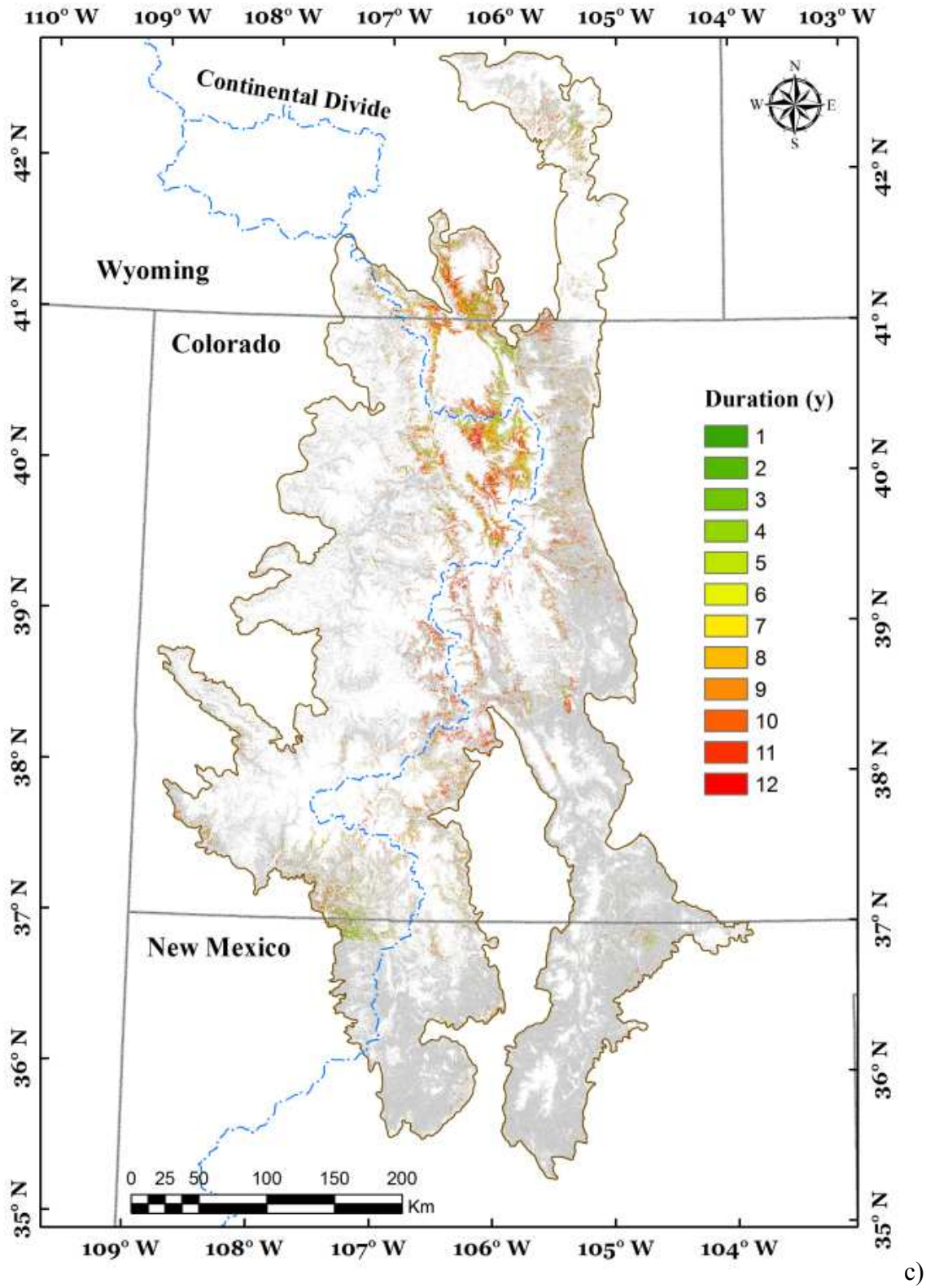
Figure 6. Spatial pattern of onset year (a), NBR change magnitude (b) and outbreak duration (c) for MPB disturbance.

Disturbance size: During the study period, fires, MPB mortality, and clearcuts together affected 10,504 km² of forest in this region (17.3% of the host forest area). Mountain pine beetle mortality contributed most to the forest loss (7,359 km²). The disturbance event affecting the second largest area was fire (2,467 km²). Clearcut events accounted for 678 km² of disturbed area. There were 2,539 km² area classified as forest recovering from disturbances (Figure 7).

Figure 7. Area of forests in mountain pine beetle (MPB) mortality, clearcut, fire and regrowth classes from 1999 to 2011 in Southern Rocky Mountain Ecoregion.

Onset time: Time series of the disturbed area revealed a constantly increasing trend of MPB caused tree mortality, and two apparent peak years were observed, sep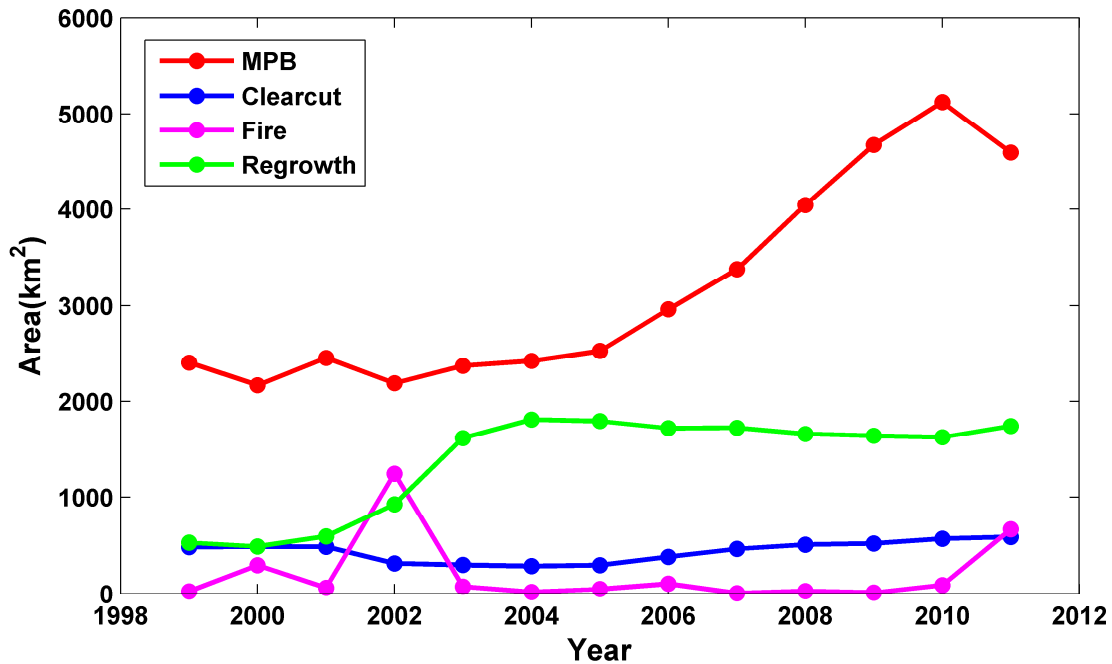arately 2001 and 2008 (Figure 8a). From 2005, the amount of area with new MPB mortality accelerated. Notable years with large burned areas (Figure 7) included 2000, 2002 and 2011, and the other years had a fairly small amount of burned forest area. Clearcut events (Figure 7) had a relative stable trend over the time span of this study. The amount of area classified as regrowth in the SRME was low in the first five years of the study, but after a sharp increase in 2003, the annual area in regrowth stabilized, but was almost twice as large as it was in the early part of our study.

Magnitude: We divided the disturbance magnitude into four levels according to the NBR changes, and defined them as low (ΔNBR:<100), low-middle (ΔNBR:100 to 200), middle (ΔNBR:200 to 300), and high severity (ΔNBR: >300). The magnitude of MPB outbreaks tended to increase from south to north (Figure 4). More than 30% of the MPB disturbed regions were characterized by low-severity beetle mortality (Figure 8b), which corresponds to 10.6% canopy cover change per site as inferred from the delta model in Kennedy et al. (2010). The most severe outbreaks were observed to happen in northern

Colorado and Southern Wyoming, where beetles' presence became more prevalent in the later years (Figure 6).

Duration: About 20% of beetle outbreaks in this region lasted for 3 years, which matched well with the time frame of the commonly acknowledged "green-red-gray" stages (Figure 8c). The spatial visualization of duration pattern also revealed that while the epicenters of MPB mortality harbored longer-lasting outbreaks (>3 years), their peripheral regions were characterized by shorter duration attacks.
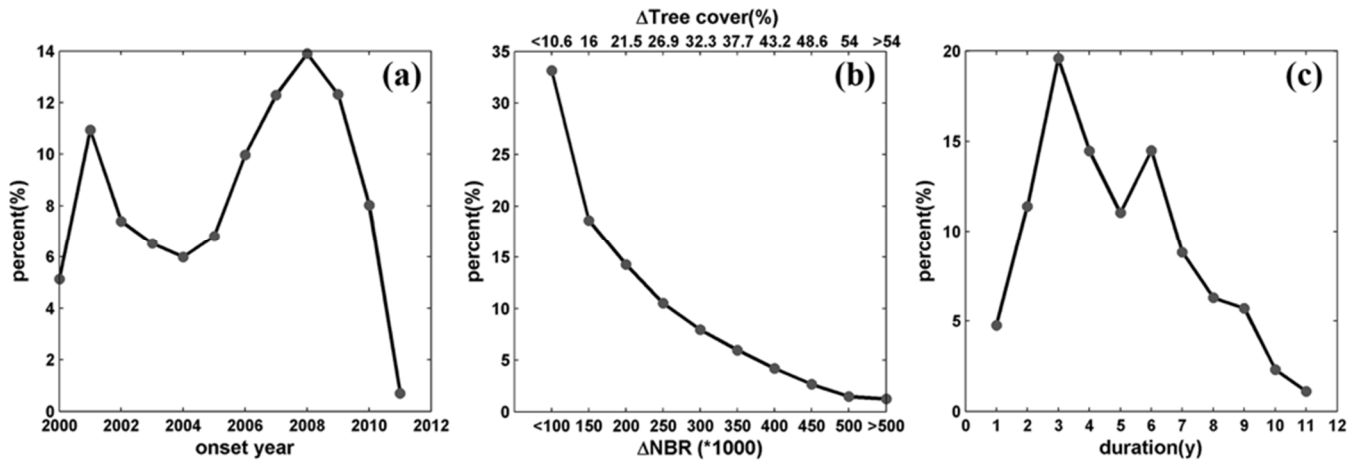
Figure 8. The percentage of mountain pine beetle mortality pixels for each (a) onset year, (b) normalized burn ratio (NBR) / tree cover percentage change interval, and (c) duration.

Table 1. Segment features and their definitions.

Category	#features	Definition
Vertex1_year	1	Year of the head vertex
Vertex1_NBR	1	NBR value of the head vertex
Vertex2_NBR	1	NBR value of the tail vertex
Dur	3	Duration of the segment: {pre_cur, cur_dur, post_dur}
Mag	3	Magnitude of change in NBR between the head and tail vertex: {pre_mag, cur_mag, post_mag}
Slope	3	Magnitude/duration: {pre_slope, cur_slope, post_slope}
max8slope	8	Max slopes over the duration of the focal segment for its eight spatially adjacent pixels: {$\max(S_{a1},S_{b1},\ldots,S_{n1})$, $\max(S_{a2},S_{b2},\ldots,S_{n2})$,…, $\max(S_{a8},S_{b8},\ldots,S_{n8})$}
avg_max8slope	1	Mean of Max8slope: mean {$\max(S_{a1},S_{b1},\ldots,S_{n1})$, $\max(S_{a2},S_{b2},\ldots,S_{n2})$,…, $\max(S_{a8},S_{b8},\ldots,S_{n8})$}
std_max8slope	1	Standard deviation of max8slope: Std {$\max(S_{a1},S_{b1},\ldots,S_{n1})$, $\max(S_{a2},S_{b2},\ldots,S_{n2})$,…, $\max(S_{a8},S_{b8},\ldots,S_{n8})$}
max8fit	8	Maximum fitted NBR value over the duration of the focal segment for its eight spatially adjacent pixels: {$\max(F_{a1},F_{b1},\ldots,F_{n1})$, $\max(F_{a2},F_{b2},\ldots,F_{n2})$,…, $\max(F_{a8},F_{b8},\ldots,F_{n8})$}
avg_max8fit	1	Mean of max8fit: avg{$\max(F_{a1},F_{b1},\ldots,F_{n1})$, $\max(F_{a2},F_{b2},\ldots,F_{n2})$,…, $\max(F_{a8},F_{b8},\ldots,F_{n8})$}
std_max8fit	1	Standard deviation of max8fit: Std {$\max(F_{a1},F_{b1},\ldots,F_{n1})$, $\max(F_{a2},F_{b2},\ldots,F_{n2})$,…, $\max(F_{a8},F_{b8},\ldots,F_{n8})$}
min8fit	8	Minimum fitted NBR value over the duration of the focal segment for its eight spatially adjacent pixels: {$\min(F_{a1},F_{b1},\ldots,F_{n1})$, $\min(F_{a2},F_{b2},\ldots,F_{n2})$,…, $\min(F_{a8},F_{b8},\ldots,F_{n8})$}
avg_min8fit	1	Mean of min8fit: avg{$\min(F_{a1},F_{b1},\ldots,F_{n1})$, $\min(F_{a2},F_{b2},\ldots,F_{n2})$,…, $\min(F_{a8},F_{b8},\ldots,F_{n8})$}
std_min8fit	1	Standard deviation of min8fit: Std {$\min(F_{a1},F_{b1},\ldots,F_{n1})$, $\min(F_{a2},F_{b2},\ldots,F_{n2})$,…, $\min(F_{a8},F_{b8},\ldots,F_{n8})$}

Note: all the notations used in sets follow the definition in figure 4.

4.3 Disturbance interactions and successional pathways

Despite the fact that the SRME experienced a diverse range of disturbances, we did not observe a significant amount of secondary disturbance happening after a primary disturbance within the decade-long time period of this study. Only 2.3% of the areas burned by fires had subsequent MPB outbreaks. And the percentages were even smaller for fires and clearcuts in MPB infested forests, which were 1.7% and 0.8% of the area affected by MPB mortality, respectively. Although the probability of disturbance interactions was low in this region, their combined impact could potentially be different than the impacts of individual disturbances. As revealed from the ANOVA test, there was a significant difference in the magnitude of MPB and fire events between the fire+MPB target and population groups, but no significant difference was found between the MPB+fire target and population groups with regard to both events. Their comparison also revealed that stands experiencing fire+MPB interaction were attributed with higher fire magnitude but lower beetle outbreak magnitude than those without (Figure 9).
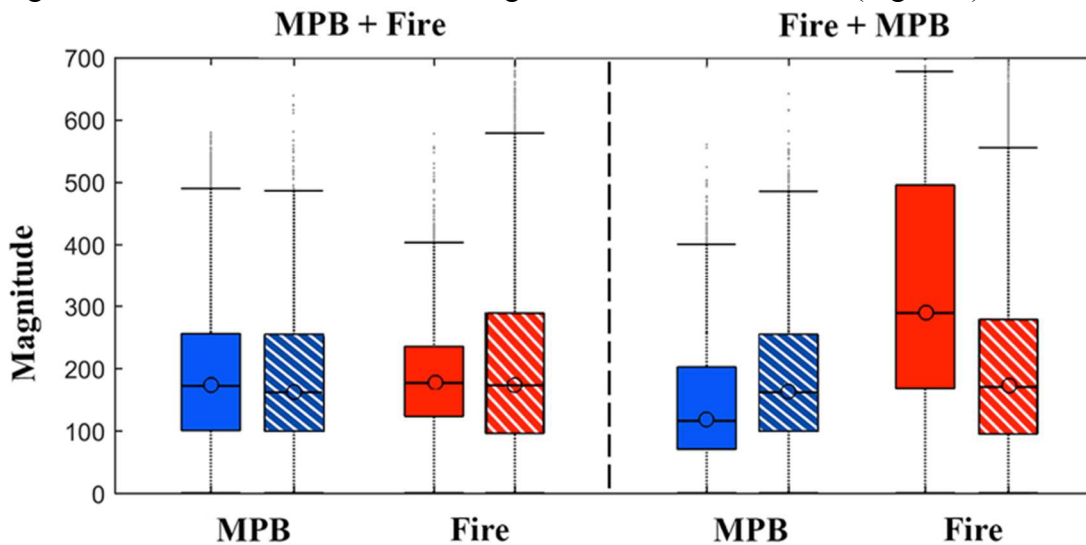
Figure 9. Differences in the magnitude of individual disturbances for areas with multiple disturbances. The boxes with solid color represent the target group, and the boxes with dash lines represent the random samples selected from the whole population besides the target group. The bottom and top of the box are the first and third quartiles, and the band inside the box is the median. The whiskers represent the 1.5 interquartile range of the lower and upper quartile.

We outlined the major successional pathways in SRME (Figure 10). During the 13-year period of this study, the forest area recovering from all kinds of disturbances was 2,539 km^2, which accounted for 24.2% of the total disturbed area. To understand what was happening in the disturbed regions showing no sign of recovery till year 2011, we summed the area for each specific event according to their onset years (Figure 11), and found that most of those regions just experienced very recent disturbances. For instance, 64.6% of the disturbances with no regrowth were happened within 5 years (Figure 11). This implies that the recovery rate may be higher than 24.2% since most regions were still undergoing disturbances.
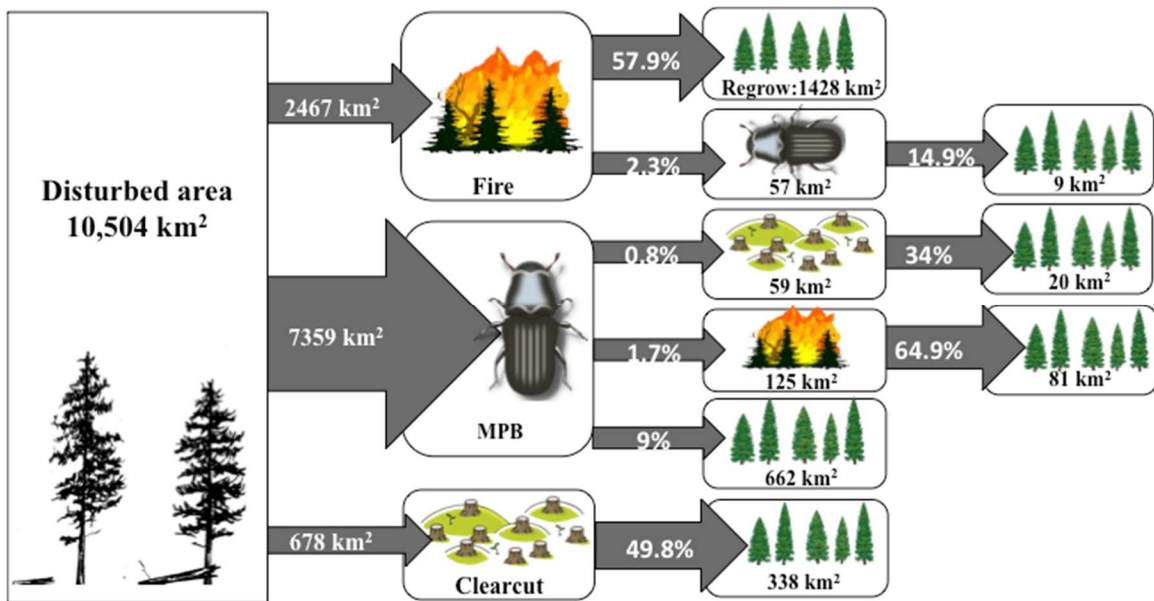
Figure 10. Disturbance and recovery pathways in South Rocky Mountain Ecoregion. Percentages in the arrow indicate the percentage of area in the left box to that in the right box.

For places that experienced a single disturbance, burned areas had the most regrowth, with a total area of 1,428 km^2. Sites with only standing-replacing clearcut disturbances had the second largest area in regrowth (338 km^2), which was 49.8% of the total clearcut area, and MPB disturbed forests had the least amount of area classified as recovering (662 km^2). The regeneration rate, which was defined here as the ratio of post-disturbance regrowth area to the disturbed area, was 57.9% for fire burned sites, and 49.8% for clearcut sites over the 13-year study. However, only 9% of the forest area was recovering within the MPB-induced mortality zones. In terms of multiple disturbances, their compounded effects on the subsequent recovery were evident. The results showed that the regeneration rate for fire+MPB was 14.9%, and MPB+fire produced the highest regeneration rate (64.9%) amongst all kinds of singular and compounded disturbances.
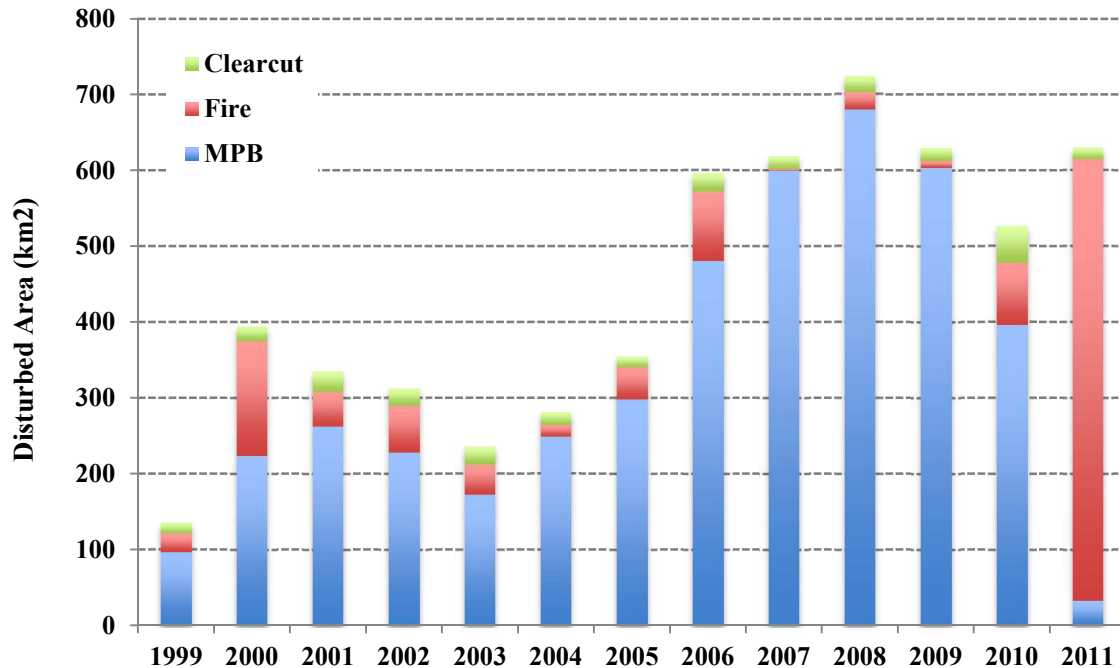
Figure 11. The summed disturbed area of mountain pine beetle (MPB), fire and clearcut in regions without regrowth according to their onset year.

5 Discussion

5.1 New classification framework and uncertainties

Mapping over a decade of forest DR history at the ecoregion scale using moderate spatial resolution satellite imagery presented challenges that led to our development of new methodological techniques. Considering the large-scale geographic coverage, high levels of landscape heterogeneity and the diversity of disturbance agents, the mean OA of 85.9% demonstrated the efficiency of this framework. This framework can also contribute to the remote sensing community from two perspectives. One is the SOA/NOA sampling strategy. Selecting samples in the overlapping areas between adjacent Landsat scenes, in particular between paths on the same row, can reduce the time required for image interpretation or on-site data collection. By further including NOA clusters sharing dissimilar spectral features with the SOA clusters, we increased the overall spectral variability spanned by the selected samples and consequently enhanced the sample representativeness that is of particular importance for parametric algorithms (Gong et al., 2013).

Another contribution exists in our usage of segments as the basic classification unit and the integration of spatio-temporal neighborhood features. Classification of segments can reduce predicted illogical annual changes since the labels are consistent over the course of the segment. The inclusion of an adequate number of spatio-temporal neighborhood features can improve the robustness of RF performance, but also minimize the "salt-and-pepper" effects from both spatial and temporal perspective.

Nevertheless, there are several limitations in our mapping procedure that might impact the subsequent ecological analysis. First, the temporal segmentation was run on a unified set of parameters that were calibrated with data from Grand County, Colorado (Liang et al., 2014a), where a high concentration of both lodgepole pines and MPB mortality are located. The differences in MPB populations and the type and density of host tree species might impact the segmentation outputs, and result in a certain amount of false positive errors in MPB mortality pixels. Second, segments showing slow and gradual declining trends do not necessarily correspond to MPB-induced mortality. Forests experiencing drought-induced tree die-off, disturbance from other insects or disease-causing pathogens and mistletoes, or undergoing thinning and partial harvest, could also present this kind of pattern, and therefore be incorrectly attributed to MPB-mortality. Restricting our analysis within the MPB host tree species can minimize but not entirely avoid this confusion.

5.2 Interactions between fire and MPB outbreaks

Although the area of post-MPB fires was almost double that of post-MPB clearcuts, its coverage was fairly small compared with the vast area affected by MPB mortality. Thus, it remains challenging to draw any solid conclusions about the role of MPB mortality in increasing the risks of fire hazards in SRME. There is a growing body of ecological research exploring the relationships between MPB and fire, and some have conflicting conclusions (Hicke et al., 2012; Schoennagel et al., 2012; Simard et al., 2011). Most of them were carried out by measuring the surface and canopy fuels in a time-since-beetle-outbreak chronosequence at a limited number of field sites to parameterize fire simulation models, and to predict future potential fire behavior. However, beetle-fire interactions could be nonlinear under different environments (Simard et al., 2011), and the small quantities of on-site data used in past studies may not fully capture the underlying heterogeneity and variation. Our satellite measures, although lacking the details of the site-level collections, are capable of providing information about where and when those events happened at the landscape level.

In SRME, burn severity was largely unrelated to pre-fire MPB outbreak severity. For fires that burned through beetle-impacted forests, their severity did not show any significant difference from fires that burned through forests that were not affected by beetles. Beetles can affect the forest ecosystem in a variety of ways. Wind penetration through stands may increase if the beetle killed trees started to fall, but we did not observe a large proportion of fallen trees in this region during field visits and on high-resolution images. The surface and canopy fuel would be altered after the mortality of individual trees, but not in a consistent way. Shortly after beetle mortality, canopy fuels are high due to the declining foliage moisture. Over several years, the fuel load in the canopy layer may be reduced because limbs and trees fall, whereas the surface fuel loads would increase because of the thicken fuel bed and accumulated fallen dead needles. Thus, it is hard to predict the compound effects on fire potential since their contrary characteristics may be counteracting each other and leading to the uncorrelated relationship that we observed. Besides, fuel is not the only factor and sometimes there are other less important factors that control the burn severity. Studies using either satellite or field measures of burn severity indicated that relative humidity, wind speed, topography and burning conditions are often more critical factors in determining burn severity than

pre-fire outbreak severity (Bigler et al., 2005; Collins et al., 2007; Harvey et al., 2013; Romme et al., 2006).

However, post-fire beetle severity has been shown to decrease with burn severity, which suggested that MPB usually cause less damage in forests in which there had been a prior fire event. Wildfire can impose immediate stress on trees. A prominent effect of fire injury is reflected in the low substrate quality, as the brood production declined with the degree of fire injury (Powell et al., 2012). Hence, heavily burned stands would harbor less density of beetles, and result in milder outbreaks. Moreover, fires consume a larger amount of biomass, and if the fire-affected stands did not recover back to their healthy status before the beetle attack, the decline in canopy cover will be less evident than when beetles attack more healthy stands.

5.3 Impacts of singular and compounded disturbance on forest resilience mechanisms

Our analysis found that more than half of the burned area was classified as regrowth. Lodgepole pines, which dominate our study area in the SRME, have serotinous cones, which need high temperatures to trigger their cones to open and release their seeds. This fire-dependent characteristic allows for post-fire tree regeneration soon after fires (Turner et al., 1997), although the abundance might vary with fire regimes and pre-fire seed density (Schoennagel et al., 2006). Lodgepole pine start seed production at an early age, approximately 5-10 years (Burns & Honkala, 1990), and thus it is not surprising to expect this high regeneration rate. Another question that many researchers and stakeholders are concerned with is how forest responds to post-MPB disturbances. Our results showed that a small portion of the MPB disturbed forests was on a trajectory to full recovery. The remaining areas were either under disturbance or were recovering at a slower rate. These observations may be related to dead trees dominating the spectral signal observed by Landsat, or to warmer and drier climate conditions that have been unfavorable for tree regeneration in recent years, as well as related to the size of disturbed patches being much larger than the short dispersal distances of tree species in the SRME (Bentz, 2010; Kurz et al., 2008; Sambaraju, 2012).

Interactions between disturbance processes can amplify or mute the overall effects of changes (Vose et al., 2012), and the outcome is largely determined by the magnitude and direction of effects they created, as well as the order of events. One interesting piece of evidence we found is that beetle outbreaks could alter ecosystem response to subsequent fire by increasing the post-fire regeneration rate of serotinous lodgepole pines in SRME. Despite the fact that beetles might reduce seed availability by killing large seed-producing trees (Bjorklund & lindgren, 2009), they can also help in redistributing the remaining viable cones and seeds, like what the wind blow or animal carrier do (Chambers & MacMahon, 1994), and promote the generation of a larger number of seedlings as aided by the following fire. However, this finding could only be valid in this particular ecosystem and under specific conditions, such as stand age, density and burn severity, because we found some contradictory conclusions in other studies. For instance, Harvey et al. (2014) suggested that there is no direct effect of outbreak severity on initial post-fire regeneration of lodgepole pine in Greater Yellowstone.

6 Conclusions

In this study, we documented the disturbance and recovery history in the lodgepole pine forests in the SRME using Landsat time series classification maps, which were generated from a novel SOA/NOA sampling strategy, the integration of Landtrendr with an RF classifier to attribute disturbance type, and the inclusion of spatio-temporal neighbor features. By tracking the spatial and temporal of patterns of MPB mortality and burned areas, we found that the linkage, strength, and direction of interactions between bark beetle mortality and fire to be related to their sequence of occurrence. The severity of fire was unlinked to pre-fire outbreak severity, and no evidence was found towards the role of MPB in increasing the risks of fire hazard. However, post-fire beetle severity tended to decrease in more severe fire injured stands. Most recovery events happened immediately after stand-replacing disturbances, whereas chronic beetle disturbance that contributed most to the forest loss, showed an extremely low regeneration establishment rate. Although the occurrence probability of multiple disturbance events is low in this region, their compound effects on the resilience mechanism of serotinous lodgepole pine forests can be of great ecological value. The most evident impact is the increased regeneration rate after the combination of pre-fire beetle outbreaks and subsequent fire. As bark beetle outbreaks and wildfire occurrence are both predicted to increase with continued climate warming in North America (Kurz et al., 2008; Westerling et al. 2011), the maps and findings presented in this study could serve as baseline information for assessing landscape-scale effects of disturbance and recovery on forest ecosystems, and help inform effective management options.

Acknowledgements

Chapter 4 Projecting future potential patterns of beetle outbreaks in the Southern Rocky Mountains

Abstract

The recent widespread mountain pine beetle (MPB) outbreak in the Southern Rocky Mountains presents an opportunity to investigate the relative influence of anthropogenic, biologic, and physical drivers that have shaped the spatiotemporal patterns of the outbreak. The aim of this study was to quantify the landscape-level drivers that explained the dynamic patterns of MPB mortality, and simulate areas with future potential MPB mortality under projected climate-change scenarios in Grand County, Colorado, USA. The outbreak patterns of MPB were characterized by analysis of a decade-long Landsat time-series stack, aided by automatic attribution of change detected by the Landsat-based Detection of Trends in Disturbance and Recovery algorithm (LandTrendr). The annual area of new MPB mortality was then related to a suite of anthropogenic, biologic, and physical predictor variables under a general linear model (GLM) framework. Data from years 2001–2005 were used to train the model and data from years 2006–2011 were retained for validation. After stepwise removal of non-significant predictors, the remaining predictors in the GLM indicated that neighborhood mortality, winter mean temperature anomaly, and residential housing density were positively associated with MPB mortality, whereas summer precipitation was negatively related. The final model had an average area under the curve (AUC) of a receiver operating characteristic plot value of 0.72 in predicting the annual area of new mortality for the independent validation years, and the mean deviation from the base maps in the MPB mortality areal estimates was around 5%. The extent of MPB mortality will likely expand under two climate-change scenarios (RCP 4.5 and 8.5) in Grand County, which implies that the impacts of MPB outbreaks on vegetation composition and structure, and ecosystem functioning are likely to increase in the future.

1 Introduction

As a native species, mountain pine beetle (*Dendroctonus ponderosae*; MPB) populations have existed at endemic levels and periodically have grown to epidemic levels in the pine forests of western North America for centuries (Amman, 1977, Baker & Veblen, 1990; Raffa et al., 2008). By infesting and killing older and stressed trees with larger diameters, MPB plays a critical role in shaping forest composition and structure, accelerating the movement of nutrients in biogeochemical cycles, and affecting forest productivity (Collins et al., 2011; Edburg et al., 2012). In recent decades this historical balance has

been disrupted, and the area affected by MPB has been vastly extended, exceeding the extent and impacts of outbreaks documented in the past 125 years (Raffa et al., 2008). The current MPB outbreak has impacted large expanses of lodgepole and ponderosa pine forests, reduced their ability to act as carbon sinks (Caldwell et al., 2013, Kurz et al., 2008; Running, 2008), altered wildfire hazards (Hicke et al., 2012a, Jenkins et al., 2008, Parker et al., 2006; Schoennagel et al., 2012), modified local surface energy balance (Boon, 2009), threatened water quality (Mikkelson et al., 2013), and changed regional climate (Maness et al., 2013).

The population dynamics of bark beetles are governed by a variety of biotic and abiotic factors and their interactions (Raffa et al., 2008). Forest characteristics, including homogenous even-aged, high-density, and large-diameter stands, are favorable for MPB mass attack (Raffa & Berryman, 1983). Long-term drought or other events causing stress can exert either positive or negative effects on tree susceptibility to beetle attack, and the overall impact remains controversial. While the primary defense mechanism of trees will be weakened by drought stress because of reduced resin quantities (Creeden et al., 2014, Preisler et al., 2012; Raffa et al., 2008), beetle brood production can also be reduced since the tree's phloem thickness is attenuated (Amman & Cole, 1983). Thermal regimes, typically represented by minimum winter temperature or year-round temperature, impact beetles' developmental timing, cold-induced mortality, and the associated fungal community (Bentz et al., 2010; Preisler et al., 2012). Meanwhile, factors like elevation, direct solar radiation, and beetle mortality in adjacent areas have also been indicated as important predictors of outbreaks (Coops et al., 2006b, Simard et al., 2012, Walter & Platt, 2013; Wulder et al., 2006b). Most previous studies have focused on the effects of one or several factors. In this study, we took a comprehensive approach and considered a large set of relevant factors to improve our understanding of the spatiotemporal patterns of MPB outbreaks and investigate their drivers.

For this study, we were also concerned about the identification of forested areas with high risk for future MPB mortality. There have been a number of prior efforts to predict patterns of MPB mortality. Through an integrated seasonality and cold tolerance model, Bentz et al. (2010) suggested that rising temperatures could increase MPB population growth rates, and their range would expand along latitude and elevation gradients. Aided by an ecological niche model, Evangelista et al. (2011) predicted that new areas of forest susceptible to MPB mortality would emerge over time but the existing area of susceptible forests to MPB mortality would also shrink, leading to an overall decrease in the amount of suitable habitat area for MPB in the future. Using a process-based model, Hicke et al. (2006) found that projected warming in the western United States will result in substantial reductions in the overall area of adaptive seasonality (the synchronous emergence of adults that allows MPB to overwhelm tree defenses). Unlike population models, which can improve the mechanistic understandings of biological responses to environmental variability, but may consider a limited number of explanatory variables because of model complexity, statistical approaches are capable of incorporating a large number of explanatory variables and quantifying their relative roles. This is a crucial preliminary step before adopting and improving process-based mechanistic models.

Understanding the factors driving patterns of MPB outbreaks and predicting future outbreaks has been challenging given the types of data available that depict the spatial and temporal extents of outbreaks. The quality of response variables could affect the performance of predictive models. In general, locations of MPB mortality are collected in the field or extracted from remotely sensed imagery. Although in-situ surveys can provide accurate data, they often have restricted geographic and temporal coverage. State and federal agencies have conducted Forest Health Monitoring Aerial Detection Surveys (ADS) to identify forest disturbances since the mid-twentieth century (Man, 2010). These publicly available datasets have been used extensively in many fields, but errors introduced via observer fatigue, observer-to-observer variation, misregistration and the scale of observation (Meigs et al., 2011) are rarely estimated and could introduce an unknown amount of uncertainty.

Remote sensing of forest disturbances offers an alternative to the ADS data for monitoring tree mortality caused by insect outbreaks (Coops et al., 2006a; White et al., 2004). Landsat data are especially popular for this application because they are freely available, and have multispectral data, a broad spatial extent, and temporal continuity. For these reasons, Landsat time series stacks (LTSS) have been used in large-scale efforts to detect forest disturbances (Masek et al., 2013) using the Vegetation Change Tracker algorithm (VCT; Huang et al., 2010). Remotely sensed disturbance maps produced by VCT and similar change-detection algorithms like the Landsat-based Detection of Trends in Disturbance and Recovery algorithm (LandTrendr; Kennedy et al., 2010) currently lack information about the cause of the disturbance, and that limits their utility for use in our study. Notwithstanding, several studies have demonstrated the usefulness of Landsat in capturing the patterns of MPB-caused tree mortality at various geographic scales (e.g. Masek et al., 2013; Meddens et al., 2013). Considering the uncertainties in the ADS data, and limitations of existing VCT and LandTrendr change-detection products, we utilized data from an automated procedure that labeled disturbance types (especially MPB mortality) detected by LandTrendr in an LTSS to generate spatially explicit annual maps of MPB occurrences over a decade-long time span (Liang et al., 2014a).

In this paper, we integrated remote sensing techniques and statistical models to evaluate the effects of a set of factors affecting the dynamic pattern of MPB mortality, and projected future MPB mortality in response to climate change. Our aim was to address the following questions: What drivers promote the extensive development and progressive MPB outbreak in an area situated in the Southern Rocky Mountains ecoregion? How accurately can we predict MPB disturbance with this set of response and explanatory variables? And what will future outbreak trends be?

2 Study area

Grand County is located in north central Colorado, covering approximately 4830 square kilometers of the Southern Rocky Mountains ecoregion (Figure 1). The elevation ranges from 2225 m along the Colorado River to 4131 m at the summit of the Continental Divide (Grand County Department of Natural Resources, 2006). Its climate is characterized by year-round sunny days (around 244 days/year on average), with average

summer temperatures of 26.6 °C, and the average rainfall of approximately 30.48 cm (Grand County Department of Natural Resources, 2006). The diversity of elevation, soil, climate, as well as strong topographic-moisture gradients leads to a variety of vegetation composition within the county, among which sagebrush shrub and steppe is the most dominant ecosystem. Lodgepole pine forests occupy a quarter of the landmass, followed by spruce-fir forests and aspen forests (Grand County Department of Natural Resources, 2006). In recent decades, MPB infestation, wildfire, and timber harvesting are recognized as the three major disturbance agents in Grand County. Wildfire occurrence has been low, but the widespread MPB outbreak affected approximately 68% of privately owned land and 70% of federally owned land (Witcosky, 2007).
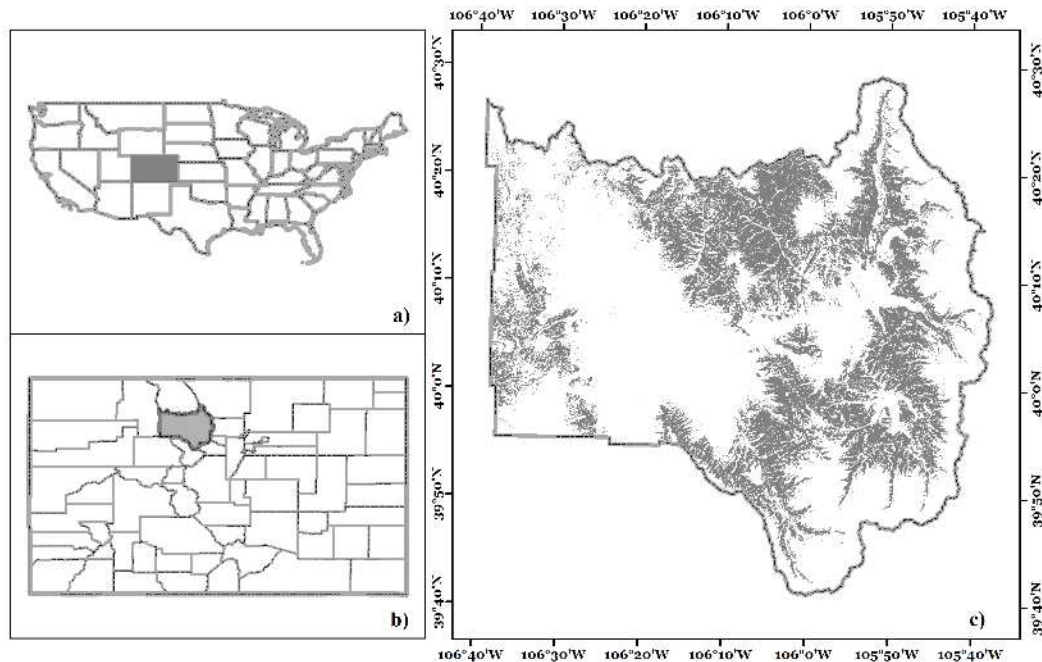
Figure 1. Spatial location of (a) the State of Colorado within the United States of America, (b) Grand County within Colorado, and (c) areas of lodgepole pine forest (derived from the LANDFIRE existing vegetation type data layer) within Grand County, Colorado.

3 Methods

3.1 Change detection analysis in detecting long-term MPB outbreaks

Maps of MPB mortality in Grand County were generated by automatic attribution of LandTrendr segmentation outputs applied to a time series of 17 Landsat images spanning 2000–2011 (path 34, row 32; Liang et al., 2014a). This approach integrated a temporal segmentation technique to identify areas with change (Kennedy et al., 2010) and a decision tree modeling procedure to attribute the changes to specific disturbance types (Liang et al., 2014a). The steps in this approach were to enhance the signal-to-noise ratio of the time series curve via linear regressions, and decompose it into a sequence of straight-line segments, whose event attributes were identified based on the segment

characteristics (duration, magnitude and vertex value) using calibrated decision tree rules (Figure 2). The temporal trajectories were constructed using the Normalized Burn Ratio (Key & Benson, 2006). Key parameters that were used to calibrate both temporal segmentation and decision tree components were trained using ground-truth data from 106 sample locations, visually selected and interpreted from 1-m resolution U.S. Department of Agriculture (USDA) National Agricultural Imagery Program (NAIP) imagery (available in 2005, 2009, and 2011 from USDA Geospatial Data Gateway). Technical details can be found in Liang et al. (2014a). The trend analysis outputs included a series of disturbance maps that depict healthy forest, forest with MPB mortality, and clearcut areas at an annual time step. The disturbance maps were validated with a set of randomly placed NAIP test samples in Liang et al. (2014a).
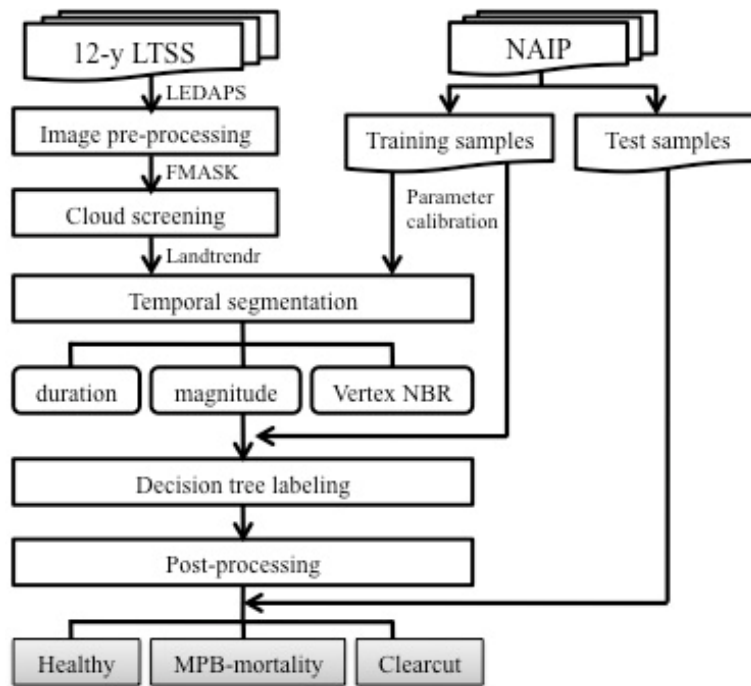
Figure 2. Processing steps in the change-detection analysis. LTSS: Landsat time-series stacks; NAIP: National Agricultural Imagery Program; LEDAPS: Landsat Ecosystem Disturbance Adaptive Processing System; FMASK: Function of Mask; LandTrendr: Landsat-based Detection of Trends in Disturbance and Recovery algorithm; NBR: Normalized Burn Ratio; MPB: mountain pine beetle

3.2 Model development

3.2.1 Response variable

We were interested in simulating the spread of MPB mortality into new regions over time, instead of modeling their suitable habitats. Thus, we set the response variable in our models to be the annual presence (case) of new MPB mortality and absence (control) of MPB mortality, where presence refers to the new mortality in a pixel which was healthy in the previous year. The time-series of disturbance maps were used as the base for sample selection. First, we made a random sample of newly emerged areas of MPB

mortality stratified by each year from 2001 to 2011. A stratum containing persistently (2001–2011) healthy forest pixels was also constructed for control sample selection. Second, since the sample size in each stratum determines the distance between observations, and thus affects the potential for spatial autocorrelation to influence model interpretation, we initially selected 300 sample units from each stratum, and successively decreased the sample size with decrements of 10. For each sample size, a general linear model (GLM) was fit and Moran's *I* was calculated to test for spatial autocorrelation in the model residuals (Moran, 1950). We ultimately selected the largest sample size that had insignificant spatial autocorrelation in the model residuals, that is, we selected a sample with enough spacing between points so that spatial autocorrelation effects were avoided.

A set of training samples was extracted using observations from 2001 to 2005, and the model with forward predictions was validated with observations from 2006 to 2011. Year 2000 was not included in modeling because we could not infer its prior information for certain predictors, such as distance to nearest cell with MPB mortality in the previous year. Validation data collected after 2008, when spread of the MPB outbreak was reduced, were used to determine whether or not the model over predicted MPB mortality.

3.2.2 Explanatory variables

Thirty-four biotic and abiotic variables that fell into seven categories were used to develop a number of GLMs (Table 1). All datasets, except for the two climate variables, were in raster format with the same spatial resolution as our disturbance maps (30 m). The values from all the rasters were extracted at the locations of the training or validation sample points.

Anthropogenic variables included residential housing density and distance to nearest road. Both of them are proxies for the intensity of human activities, whose impacts have rarely been investigated in prior MPB associated studies. The biggest human impact on forest ecosystems is likely to be habitat fragmentation since silvicultural treatments, such as thinning or logging, are still the most common management strategy in mitigating MPB outbreaks (Coops et al., 2008). How human intervention affects MPB host selection remains unknown, however. To quantify the magnitude of this potential effect, we used residential housing density data from the 2010 U.S. Census Bureau block-level housing-density data (Radeloff et al., 2010), and distance to nearest road from the National Overview Road Metric Euclidean Distance dataset (Watts et al., 2007). Both continuous variables were log + 1 transformed prior to use because they had skewed distributions.

Lodgepole pine forests exist along a topographic-moisture gradient that controls vegetation growth as a function of soil water holding capacity, evapotranspiration and surface runoff. Six topographic variables derived from the Shuttle Radar Topography Mission Digital Elevation Model were used to represent this gradient (USGS, 2004). Aspect was recalculated in a way that the first 45° from true north to east was recorded as 1, and increased by 1 as the aspect increased every 45° clockwise. Southwestness is a cosine-transformation of aspect that ranges from −1 to 1 (Franklin et al., 2000). Topographic wetness index (TWI) is the steady-state humidity index (Beven & Kirkby,

1979). Higher TWI values indicate greater soil moisture, and we expected TWI and the distance to stream channel networks to be negatively correlated with MPB mortality.

We used tree cover prior to the MPB outbreak as a proxy for the pre-disturbance health and abundance of MPB host species. The Landsat vegetation continuous fields tree cover layer for circa-2000 provides estimates of the aboveground woody vegetation percentage in each 30 m pixel (Sexton et al., 2013). Under most circumstances, canopy cover is positively and significantly correlated with diameter at breast height (Gill et al., 2000), and thus high canopy cover usually represents large-diameter trees, which are more likely to be attacked by MPB (Amman, 1977; Klutsch et al., 2009).

Spatial proximity to areas previously affected by MPB can be a critical facilitator in driving local outbreaks because MPB is a relatively poor disperser (Simard et al., 2012), and we included two types of dispersal-related variables to represent it. Distance to nearest mortality is computed as the Euclidean distance from one cell to its closest cell with MPB mortality in the previous year. Shorter distance between sites enhances their connectivity, and thus increases the probability of beetle dispersal to adjacent healthy sites.

Neighborhood mortality is the amount of adjacent pixels with MPB mortality in the previous year. Because spatial synchrony is prevalent among beetle populations during epidemic years (Aukema et al., 2006), more beetle presence in the immediate neighborhood increases the likelihood of a mass attack on adjacent healthy forest. The scale of neighborhood depends on the beetles' dispersal pattern, which has been summarized into two modes: short-distance and long-distance dispersal. Short-distance dispersal happens within stands (Safranyik et al., 1989), and long-distance dispersal usually occurs when beetles are transported above the forest canopy by wind (de la Giroday et al., 2011; Jackson et al., 2008; Robertson et al., 2007; Robertson et al., 2009). The common distances in the short-distance range dispersal are 30–50 m (Robertson et al., 2007, Safranyik et al., 1989; Safranyik et al., 1992), whereas the long-distance flight dispersal that depends on the wind speed, preflight weight, flight duration, and lipid content (Evenden et al., 2014) can be more variable, ranging from several to tens of kilometers. In field observations, 2–3 km were commonly found to be the maximum distance beetles can disperse by entering a new stand from surrounding areas (Robertson et al., 2008; Robertson et al., 2009), whereas laboratory flight mill bioassay showed that the mean MPB flight distance ranged between 2.12 and 5.95 km (Evenden et al., 2014). Since there is no consensus about which mode is more important in driving the beetle expansion, we defined a number of neighborhood distances: 30 m, 100 m, 250 m, 500 m, 1 km, 1.5 km, 2 km and 3 km. Those distances were used as the radius of a circular window, and all pixels with MPB mortality in the previous year covered by this window would then be counted to be the neighborhood mortality value for the center cell.

Table 1. Predictor variables selected for use in the general linear models (GLMs).

Category	Variables	Abbreviation	Resolution	Unit
1. Anthropogenic	Distance to the nearest road	road	30 m	m
	Residential housing density	house	30 m	m
2. Topography	Elevation	dem	30 m	m
	Aspect	aspect		degree
	Slope	slope		degree
	Southwestness	sw		no unit
	Topographic Wetness Index	twi		no unit
	Distance to channel network	dis2chan		m
3. Vegetation condition	Tree cover	tc	30 m	percentage
4. Spatial proximity	Distance to closest mortality in the previous year	dis2prev	30 m	m
5.Neighborhood mortality	Number of pixels in an 8-pixel neighborhood with MPB mortality in the previous year	Nm_30m		no unit
	Number of pixels in a 100 m circular neighborhood with MPB mortality in the previous year	nm_100m		no unit
	Same as above, but in a 250 m circular neighborhood	nm_250m		no unit
	Same as above, but in a 500 m circular neighborhood	nm_500m		no unit

	Same as above, but in a 1 km circular neighborhood	nm_1km		no unit
	Same as above, but in a 1500 m circular neighborhood	nm_1500m		no unit
	Same as above, but in a 2 km circular neighborhood	nm_2km		no unit
	Same as above, but in a 3 km circular neighborhood	nm_3km		no unit
6. Climate	Summer mean temperature*	tmean_summer	4 km	℃
	Winter mean temperature*	tmean_winter		℃
	Summer mean precipitation	ppt_summer_cur		℃
	Warmest temperature	Tmax_cur		℃
	Coldest temperature from October to May	Tmin_cur		℃
	Mean annual temperature of previous year	tmean_last		℃
	Mean annual precipitation of previous year	ppt_mean_last		mm
	Mean summer precipitation of previous year	ppt_summer_last		mm
7. Climate anomalies	Mean summer precipitation anomaly	ppt_summer_cur2normal	4 km	mm
	Mean winter temperature anomaly	tmean_winter2normal		℃

Warmest temperature anomaly	tmax_cur2normal	℃
Coldest temperature anomaly	tmin_cur2normal	℃
Mean annual precipitation anomaly of previous year	ppt_mean_last2normal	mm
Mean annual temperature anomaly of previous year	tmean_last2normal	℃
Mean summer temperature anomaly of previous year	tmean_summer2normal	℃
Mean summer precipitation anomaly of previous year	ppt_summer_last2normal	mm

* Summer is from June through August, and winter is from December through February.

We used climate datasets generated by the Parameter-evaluation Regressions on Independent Slopes Model (PRISM Climate Group, 2010) in which monthly and annual weather data are available at a resolution of approximately 4 km (Daly et al., 2002). Besides annual mean temperature and precipitation information in the PRISM data, we derived six additional variables that are controlling factors in the beetles' life cycle (Kaufmann et al., 2008): summer mean temperature, winter mean temperature, summer mean precipitation, warmest summer temperature, coldest winter temperature, and summer mean precipitation in the previous year. Additionally, we computed eight climate anomalies by taking the differences between each climate variable and their 30-year averages from 1981 to 2010, since climate change has been indicated to have both direct and indirect impact on MPB outbreaks (Kurz et al., 2008).

3.2.3 Modeling approach

We used general linear models (GLM) with a logit link and binary response to identify which variables explained recent patterns of MPB mortality and assess potential new areas of MPB mortality. We first applied univariate GLMs to each of the 28 predictor variables to assess their individual relationship with MPB mortality. These models were evaluated by their coefficient estimates and associated significance tests. Their spatial autocorrelation effects were examined using Moran's *I* on the model residuals. Variables with *p*-values greater than 0.05 on the spatial autocorrelation tests were excluded from further analyses, to avoid violation of the assumption of independently and identically distributed errors in GLMs (Dormann et al., 2007). We then fit a full model starting with all predictor variables that were not removed because of spatial autocorrelation in the univariate models. We retained statistically significant predictor variables in the full model based on the Bayesian Information Criterion (BIC) in a multiple backward stepwise selection algorithm implemented in R (R Core Team, 2013). We chose BIC because of the large number of predictor variables and BIC penalizes the number of parameters more strongly than commonly used Akaike Information Criterion.

Predictive maps of MPB mortality were generated using the final GLM after backward stepwise selection with the equation:

$$P = 1/(1 + exp(-(\beta_0 + \beta_1 X_1 + \beta_2 X_2 + \cdots + \beta_i X_i + C)))$$

where P is the probability of MPB mortality, β_0 is the intercept, X_i is a predictor variable, and β_i is the regression coefficient estimate for the associated predictor variable X_i. The correction factor (C) was used to account for model bias introduced because of different ratios of case and control observations in the sample and in the population (Manly et al., 2002):

$$C = \log\left(\frac{\#\,sample.\,control\,/\,\#\,pop.\,control}{\#\,sample.\,case\,/\,\#\,pop.\,case}\right)$$

where # sample.control and # pop.control are the number of healthy (no MPB mortality) occurrences in the sample and the population, respectively; # sample.case and # pop.case are the number of observations with MPB mortality in the sample and the population, respectively.

3.3 Model performance evaluation

Model performance was evaluated in three ways. (1) The new presence of MPB mortality each year predicted by our GLM was visually compared with observed MPB mortality in the Landsat classifications. This provided an immediate and intuitive way to perform the evaluation. (2) The areal estimates of MPB mortality derived from remote sensing and GLM were compared and their accuracy was evaluated against the criteria: the peak of tree mortality should occur around 2005 and 2008 (Klutsch et al., 2009), and the rate of change should be the greatest at the beginning and then reduced until reaching a stable level. (3) A quantitative accuracy assessment was also conducted. First, 10-fold cross-validation was applied to test the model performance in the training phases to avoid problems like overfitting. Second, to determine the model's predictive capacity, predicted MPB mortality was compared with an independent dataset extracted from the base maps from 2006 to 2011 in two ways. A set of 3000 points were randomly picked for areas of healthy forest and MPB mortality from the base image of each year, in order to provide an overall evaluation of landscape-level patterns. Another set of 3000 points were selected from areas of persistent healthy forest and new MPB mortality each year, to access the prediction ability for the occurrence of new MPB mortality. Both evaluations were judged by the area under curve (AUC) of the receiver operating characteristics (ROC) curve, as well as overall accuracy (OA; Fielding & Bell, 1997; Hanley & McNeil, 1982). Overall accuracy was generated from the confusion matrix of the binary maps, where the probability of MPB mortality was separated from healthy forest with an optimal threshold calculated according to a criterion that maximizes the sum of sensitivity and specificity (Freeman & Moisen, 2008).

3.4 Projections under future climate scenarios

Future MPB mortality was projected using future climate conditions from the Coupled Model Intercomparison Project 5 (CMIP5). We used results from 14 global climate models (GCMs) downscaled to 4-km resolution by the Multivariate Adaptive Constructed Analogs (MACA) method, which was designed for wildfire applications in the western USA (Abatzoglou & Brown, 2012; Table 2). Projections under two future Representative Concentration Pathways, RCP4.5 and RCP8.5, have been adapted by MACA for downscaling. They represent a high pathway for which relative radiative forcing reaches >8.5 W/m^2 by 2100, and an intermediate pathway where radiative forcing is stabilized at 4.5 W/m^2 after 2100, separately. We made projections for each GCM and RCP, generated spatially-explicit maps, and calculated mean, 25th quartile, 75th quartile, lowest and highest probability of all GCM projections for each year and each RCP. Because data incorporating the climate change effects on the future forest extent and residential housing density at the spatial resolution of our model are not currently available, our projections assumed no changes in the distributions of forest and housing densities, as well as other controlling factors, such as the supply of nutritionally optimal host trees (Raffa et al., 2008).

Table 2. The 14 global climate models (GCMs) from which downscaled climate projections were used in this paper and the modeling groups developing them.

Model Name	Modeling Group

BCC-CSM1.1	Beijing Climate Center, China Meteorological Administration
BNU-ESM	College of Global Change and Earth System Science, Beijing Normal University
CanESM2	Canadian Centre for Climate Modelling and Analysis
CNRM-CM5	Centre National de Recherches Météorologiques / Centre Européen de Recherche et Formation Avancée en Calcul Scientifique
CSIRO-Mk3.6.0	Commonwealth Scientific and Industrial Research Organization in collaboration with Queensland Climate Change Centre of Excellence
GFDL-ESM2G GFDL-ESM2M	National Oceanic and Atmospheric Administration Geophysical Fluid Dynamics Laboratory
HadGEM2-ES HadGEM2-CC	Met Office Hadley Centre (additional HadGEM2-ES realizations contributed by Instituto Nacional de Pesquisas Espaciais)
INM-CM4	Institute for Numerical Mathematics
MIROC5	Atmosphere and Ocean Research Institute (The University of Tokyo), National Institute for Environmental Studies, and Japan Agency for Marine-Earth Science and Technology
MIROC-ESM MIROC-ESM-CHEM	Japan Agency for Marine-Earth Science and Technology, Atmosphere and Ocean Research Institute (The University of Tokyo), and National Institute for Environmental Studies
MRI-CGCM3	Meteorological Research Institute

4 Results

In Liang et al. (2014a), we reported that our Landsat-based change-detection analysis for mapping disturbances resulted in an overall accuracy (OA) ranging from 87% to 94%, which was 20–30% higher than single-scene classifications performed by a maximum likelihood classifier and an ensemble random forest classifier. Because of Landsat's medium resolution, the percentage of dead trees in one pixel can be variable. We visually interpreted the dead tree cover percentage on NAIP imagery within the 30 m pixel window of the test samples, and found that 90% of the MPB-mortality pixels had more than 50% dead tree cover, while 58% of them have more than 80% dead tree cover. Since the Landsat-derived MPB mortality data were used as observations when constructing our models, our results should be interpreted as explaining and predicting the spatiotemporal patterns of moderate to severe MPB mortality (>50% dead tree cover).

Sixteen out of 34 predictors had statistically significant coefficients at the 0.05 level as tested by univariate GLMs (Table 3), and none of the predictors produced models with spatially autocorrelated residuals except TWI. Residential housing density, all neighborhood mortality variables, mean temperature in the previous year, mean summer precipitation and maximum summer temperature, and winter mean temperature anomaly were positively related with MPB mortality. Negative relationships were found between MPB mortality and elevation, distance to MPB mortality in previous year, mean annual precipitation in the previous year, and mean summer precipitation.

Table 3. Predictor variable coefficients and significance levels, and Moran's I for univariate general linear models (GLMs), and predictor variable coefficients and significance levels, and standard errors for the full multivariate GLM and the final multivariate GLM after stepwise selection. See table 1 for explanations of the predictor variable abbreviations.

Variable abbreviation	Univariate GLMs		Multivariate GLM (full)		Multivariate GLM (final)	
	coef	Moran's I	coef	SE	coef	SE
road	0.126	-0.026	0.396**	0.143		
house	1.089*	-0.034	1.258	0.661	1.198*	0.477
dem	-0.003**	-0.042	0.002	0.002		
aspect	0.041	-0.017	0.038	0.078		
slope	-0.026	-0.024	-0.026	0.025		
Sw	0.136	-0.017	0.140	0.264		
Twi	-1.104***	0.132*				
dis2chan	0.001	-0.019	0.000	0.004		
tc	-0.020	-0.025	-0.009	0.016		
dis2prev	-0.211***	-0.062	-0.070**	0.063		
nm_30m	0.582***	-0.028	0.660	0.205	0.642***	0.097
nm_100m	0.085***	-0.045	0.026	0.047		
nm_250m	0.010***	-0.053	-0.006	0.010		
nm_500m	0.002***	-0.050	0.001	0.003		
nm_1km	0.001**	-0.046	0.000	0.001		
nm_1500m	0.000*	-0.041	0.000	0.001		

	coef	SE	coef	SE	coef	SE
nm_2km	0.000*	-0.039	0.002	0.002		
nm_3km	0.000*	-0.039	-0.003	0.003		
ppt_mean_last	-0.003**	-0.040	0.000	0.004		
tmean_last	0.405**	-0.046	11.880	7.005		
tmean_winter	0.132	-0.013	-5.131	3.280		
tmean_summer	0.246*	-0.031	-6.126*	3.619		
ppt_summer_cur	-0.014	-0.026	3.338*	36.820	-0.037**	0.014
ppt_summer_last	-0.011	-0.029	-3.395	36.820		
tmin_cur	-0.014	-0.021	0.048	0.786		
tmax_cur	0.155**	-0.026	-0.384	0.870		
ppt_mean_last2normal	0.000	-0.020	-0.018	0.010		
tmean_last2normal	-0.529	-0.012	-13.10	7.173		
tmean_winter2normal	0.030	-0.018	6.801	3.404	0.659**	0.205
tmean_summer2normal	-0.043	-0.021	8.662	3.800		
ppt_summer_cur2normal	0.002	-0.020	-3.388	36.820		
ppt_summer_last2normal	0.005	-0.019	3.459	36.820		
tmin_cur2normal	0.033	-0.017	-0.313	0.794		
tmax_cur2normal	-0.005	-0.020	-1.575	1.087		
(intercept)			15.330	19.340	0.460	0.652

Note: coef - coefficient estimate on the variable; SE - standard error; * denotes significance level of 0.05; ** denotes significance level of 0.01; and *** denotes significance level of 0.001.

Four predictor variables were retained in the full model after the backward stepwise selection (Table 3). Residential housing density, number of pixels in the nearest eight pixels that had MPB mortality in the previous year, and winter mean temperature anomaly were positively related to the likelihood of MPB mortality. Summer precipitation was also retained in the full model, but was negatively related to MPB mortality.

Besides quantifying the relative influence of the various drivers of MPB mortality, we were also curious about the predictive capacity of our GLM in a spatially explicit context. By assuming the satellite-derived disturbance maps were a true representation of landscape patterns of MPB mortality, we compared them against the GLM predictions for the validation years (Figure 3). We observed that the predicted areas of MPB mortality

generally matched well with the Landsat-based observations across the landscape. For instance, the northeast corner of Grand County is an area where the MPB outbreak progressively grew from 2006 to 2011. By carefully examining this zone, we found that the shrinking extent of healthy forests and the spread of MPB mortality as predicted by our model were basically in accordance with the satellite observed patterns. In the meantime, the areal estimates of MPB mortality predicted by the GLM for the whole county deviated little from the Landsat base maps, with 13% as the largest relative difference and the smallest relative difference was only 2%. Only year 2006 was under predicted and the remaining five independent validation years were over predicted. The annual predictions followed a pattern similar to that of the observed data (Figure 4): both showed a steady increase in the amount of area with MPB mortality, with a more rapid rate of increase before 2008 and slower rate of change after that. In terms of quantitative evaluations, the average AUC generated from 10-fold cross-validation was 0.97, with small variation among years. Overall accuracy ranged from 82 to 93% and the average was 88% (Table 4). When we assessed accuracy only in areas of new MPB mortality each year, our model achieved a mean AUC of 0.72, a mean OA of 0.66.
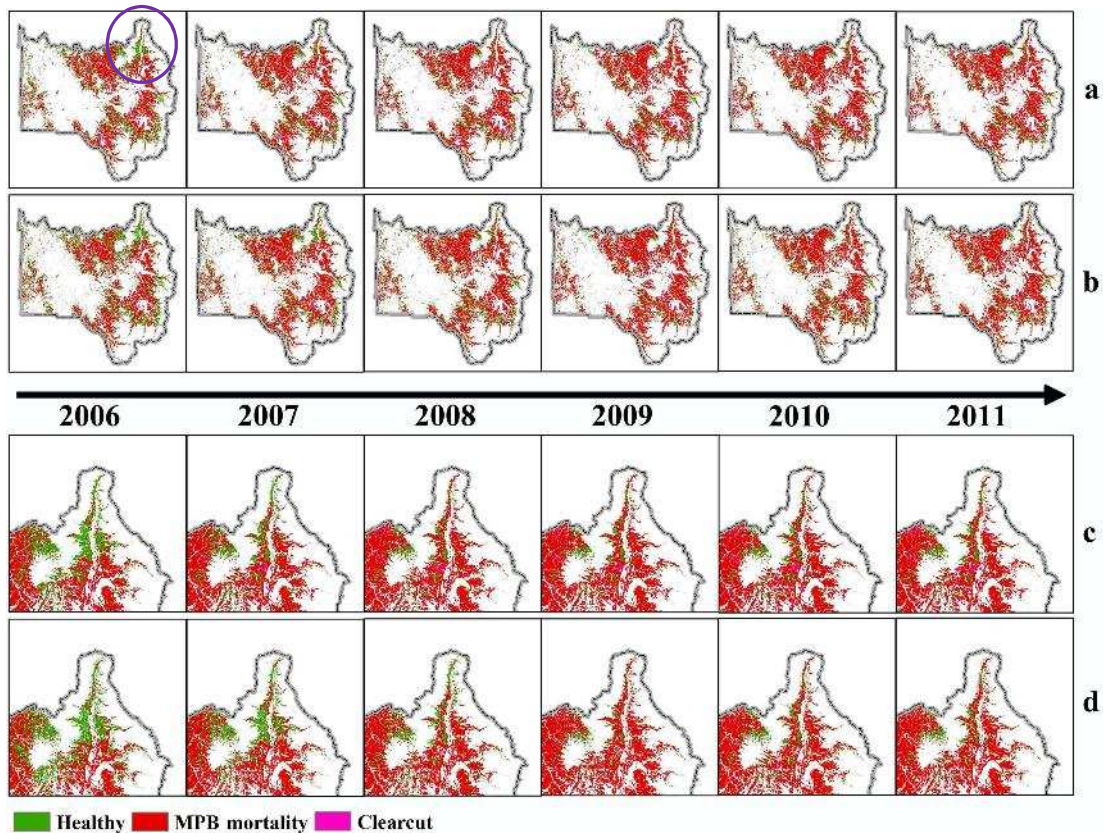
Figure 3. The comparison between observed disturbances in the change-detection analysis (panels a, c) and predictions of MPB mortality using the final GLM (panels b, d) in the independent validation years. Panels c and d show the detailed images from the northeast corner of the study area, the area of which is indicated by the circle in the leftmost panel a.
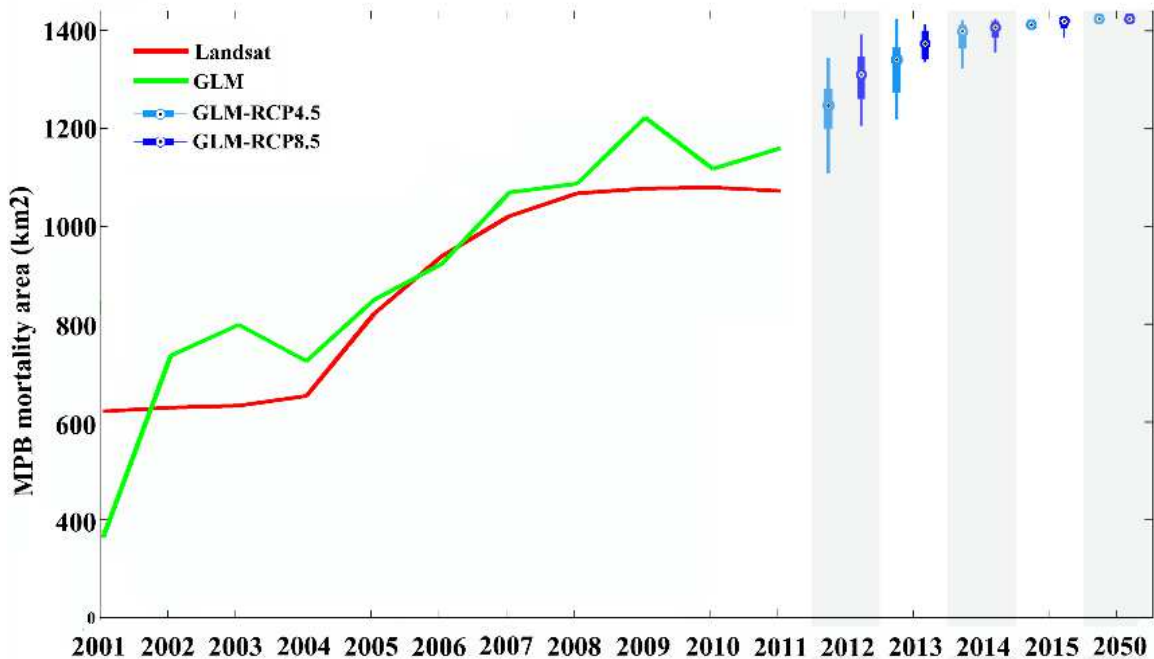
Figure 4. Accumulated area of mountain pine beetle (MPB) mortality detected by Landsat and predicted by our general linear model from 2001 to 2011, as well as forecasted MPB mortality to 2050.

Table 4. Comparison of the final general linear model (GLM) to Landsat observed disturbances.

| | | AA1 | | AA2 | | | | |
		AUC	OA	AUC	OA	Landsat (km²)	GLM (km²)	RD
Training period	2000-2005	0.98	0.87			833.23	861.62	0.03
	2006	0.94	0.89	0.67	0.63	950.03	934.55	-0.02
Validation years	2007	0.96	0.87	0.63	0.58	1031.18	1079.10	0.05
	2008	0.97	0.91	0.66	0.57	1077.13	1096.70	0.02
	2009	0.98	0.82	0.77	0.73	1087.08	1230.60	0.13
	2010	0.98	0.93	0.79	0.73	1088.95	1126.70	0.03
	2011	0.98	0.87	0.80	0.71	1082.05	1168.40	0.08

AA1: accuracy assessment on the predicted annual image (previous year's + new mortality area); AA2: accuracy assessment on the predicted newly emerged mortality areas. For training period, the accuracy is tested by the 10-fold cross-validation. AUC: area under the curve of a receiver operating characteristic plot. OA: overall accuracy.

Projections of future MPB mortality made with the GCM projections suggest that the MPB outbreak in Grand County would continue to spread until around year 2015 (Figure 3, Figure S1). The outbreak area predicted under the RCP8.5 scenario was consistently higher than that under RCP4.5. From 2015 to 2050, less variation existed in the projections among the GCMs and climate projections, as shown from the smaller difference between the upper and lower quartiles.

5 Discussion

Our Landsat-derived disturbance maps documented an evolving pattern where a severe MPB outbreak emerged in the early 2000s, spread throughout the decade with the population reaching epidemic levels and peak mortality around 2006. Based on that historical record of forest disturbance (Liang et al., 2014a), and the models developed in this study, our research provided a means of simulating the landscape-level outbreak pattern over time. The major controls on the observed patterns of MPB mortality during the time period of this study included residential housing density, density of adjacent MPB mortality in previous years, and climate predictors. The diversity of predictor variables indicated the complexity in predicting the incidence of MPB mortality, and we anticipate that landscape-level outbreak will become more extensive and severe.

5.1 Detecting spatiotemporal changes in MPB activity and associated uncertainties

During the course of this study, we experienced challenges in obtaining an ideal dataset that accurately depicted the dynamic extent of MPB mortality at a landscape scale because of the heterogenous nature of MPB outbreaks. Mortality is rarely complete within forest plots, stands, and/or pixel-level satellite observations. Healthy trees are often found next to attacked trees and attacked trees can be present in various stages of mortality (e.g., red, gray). In addition to those issues, data with high levels of omission and/or commission errors should be avoided for use in descriptive and predictive models as they may result in false inferences being made about the underlying mechanisms influencing patterns of MPB mortality and result in erroneous predictions. However, there are very few publicly available data describing the spatial and temporal patterns of MPB mortality, and most studies predicting patterns of beetle occurrence collected their response variables via field work, ADS, or image interpretation. Among these, ADS has been used more widely because of its availability and information richness, such as host species and type of disturbance agent (Hicke et al., 2013, Meddens et al., 2012, Preisler et al., 2012; Strohm et al., 2013), but the subjective nature and the limited spatiotemporal extent of the ADS data made their integration in our analysis problematic (Hicke et al., 2012a). Johnson & Ross (2008) suggested that the accuracy of ADS data is most acceptable for coarse-scale (>500 m) studies, and less suitable at intermediate scales (>50 m), and should be cautiously used at fine spatial scales. We also lacked enough time-series samples in the disturbed areas to conduct a quantitative evaluation of the ADS data. Nonetheless, our visual examination suggested that there are substantial duplications in areas of mortality sketch mapped among different years and that the fine-scale heterogeneous patterns of MPB outbreaks are not well characterized. Thus, future studies that utilize the ADS data should incorporate methods to assess their uncertainties and the impacts they have on analyses relying upon them.

Instead of relying on the ADS data, we implemented our own algorithm to track and identify forest disturbances with Landsat data (Liang et al., 2014a). Our method built upon the LandTrendr algorithm (Kennedy et al., 2010), but incorporated methods to automatically label changed areas identified by LandTrendr with the type of disturbance causing the change. The change detection analysis disturbance maps used in this study showed promising results, especially in their ability to produce long-term time series of insect mortality. Our next steps will pursue testing and application of the change detection analysis for disturbance mapping at greater spatial extents. There have been several efforts in providing the broad patterns of forest dynamics across the continent, e.g., the North American Forest Dynamics project (Masek et al., 2013), and a recent 30-m resolution global forest change product (Hansen et al., 2013), but the lack of information identifying specific disturbance types limits their usability in studies identifying the drivers behind the change. Meanwhile, errors from our mapping procedure may have affected the accuracy and applicability of the subsequent models. For instance, in the accuracy assessment, we found that although the overall accuracy was as high as 90%, the commission errors of MPB mortality were higher than omission errors by an average of 10%, and higher omission errors were found in the clearcut land cover type (Liang et al., 2014a). This might have resulted in sampling errors that were propagated in the GLM results.

5.2 Driving factors of the dynamic beetle infestation pattern

Residential housing density, beetle pressure and climate were key predictors in the final model after stepwise selection, which reflects the effects of human impacts, biological dispersal and physical environmental factors in MPB outbreaks. Except for housing density, the function of the other key variables in driving beetle outbreaks has already been highlighted in some previous studies. For instance, Preisler et al. (2012) found beetle pressure, minimum winter temperature, and two-year cumulative precipitation to be important predictors of MPB-caused tree mortality. The positive effect of residential housing density on MPB mortality indicated that anthropogenic influences provide a positive feedback to beetle outbreaks. We suspect that the positive association exists for two reasons. First, tree removal resulting from hazard mitigation, timber harvesting, and recreational facility construction such as ski resorts is common in Grand County. Increasing fragmentation of remaining forests, leaving them with higher edge-to-area ratios (Raffa et al., 2008) and drier conditions because of higher levels of solar radiation (Bone et al., 2013). Consequently, those forests are more likely to be exposed to mass attack by MPB. Second, modern urban environments have greatly altered soil physical and biochemical properties and heavier pollutant loads, all of which could hamper tree growth and make them more susceptible to insect attacks (Bone et al., 2013).

The importance of the number of adjacent pixels with MPB mortality in the previous year in predicting MPB mortality in our models is in agreement with the current understanding of MPB population dynamics (Aukema et al., 2008; Walter & Platt, 2013). Greater MPB densities allow for mass attack and increase the likelihood of tree mortality regardless of the vigor and defense system of host trees. Simard et al. (2012) demonstrated that the amount of beetle-killed forest in adjacent areas was a key predictor of subsequent mortality, and that beetle density is also a potentially factor limiting stand-scale outbreaks from developing into landscape-scale outbreaks (Raffa et al., 2008). Meanwhile, we

observed that among all the eight neighborhood mortality variables, only nm_30m was retained in the final GLM model, which indicated to us that short-distance dispersal was the dominant mode of expansion of the MPB outbreak in Grand County. Long-distance dispersal has been suggested to be crucial in the initiation and early stages of infestations, but short-distance dispersal dominates the stage when infestations intensify and populations reach epidemic levels (Chen & Walton, 2011). Our starting year was 2000, at which time MPB had already formed two outbreak clusters in the northern and southern corners of our study area. Because of the relatively important role of the short-distance dispersal, it is not surprising that we observed and predicted a continuously expanding pattern of MPB mortality in subsequent years instead of isolated MPB infestations.

Our study also identified a negative relationship with summer precipitation and a positive relationship with winter temperature and MPB mortality. These relationships have also been found by other studies; higher temperatures foster outbreaks whereas lower temperatures depress beetle populations (Bentz et al., 2010; Kaufmann et al., 2008; Raffa et al., 2008). A warmer climate will reduce the cold-induced mortality in the adult and larval stages, and will accelerate the developmental timing within one generation. The thermal changes can also determine the abundance of the fungal species vectored by MPB (Six & Bentz, 2007), which will ultimately affect the success of MPB populations. The association between precipitation and MPB mortality is less understood than the relationships with temperature. Preisler et al. (2012) found that precipitation in the previous year increased the odds of outbreak intensification, which could be related to the increased beetle brood production within thicker phloem. In contrast, longer drought periods may lead to increased host susceptibility and thus result in a higher probability of outbreak intensification. The negative effect of summer precipitation as indicated from our study supports the latter statement.
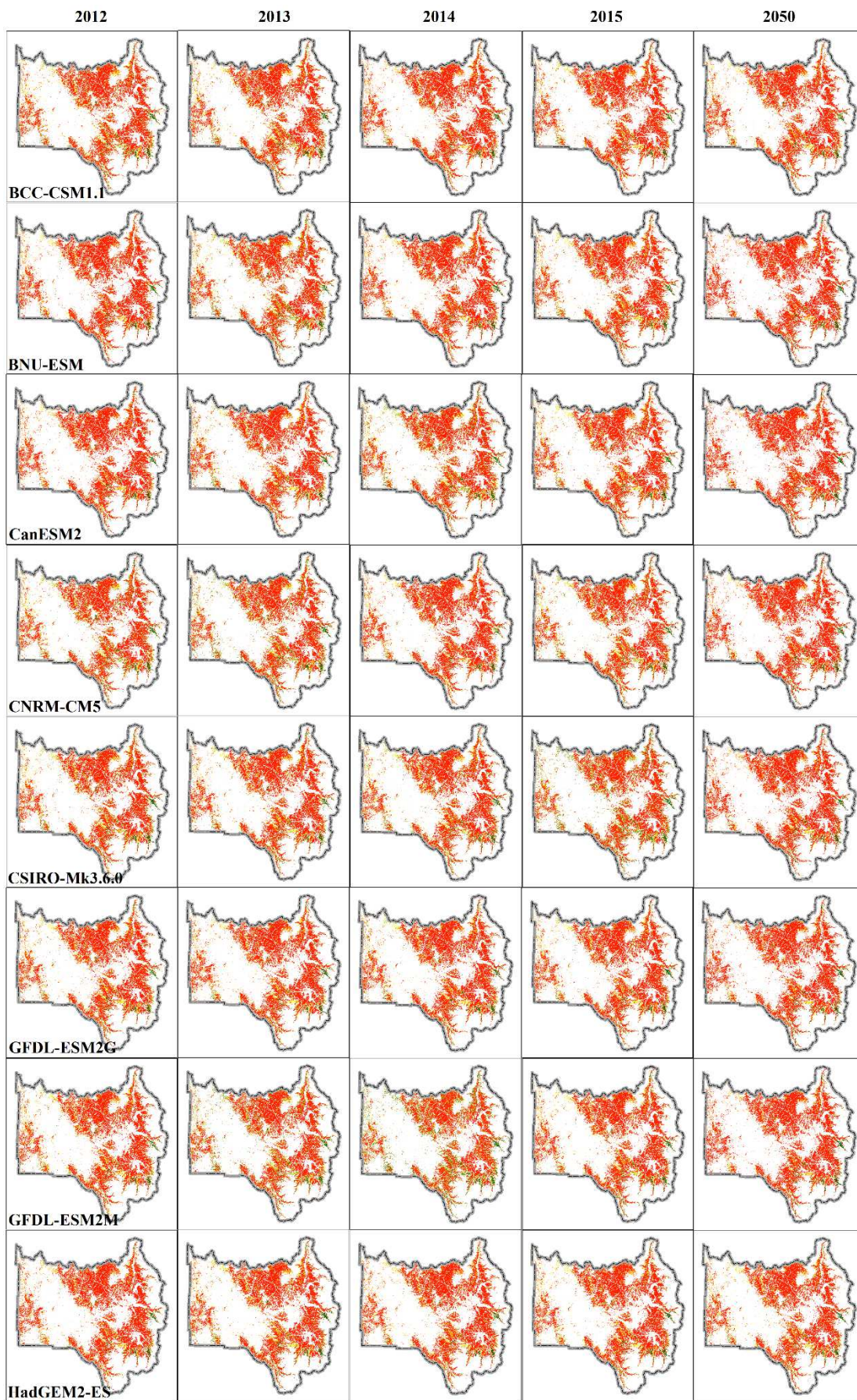
6 Conclusions

Evidence has been accumulating to document the contribution of climate change to recent increases in the frequency, duration, extent, and severity of insect disturbances (Kurz et al., 2008). Despite uncertainty in downscaled forecasts of future climate elements, both the RCP 4.5 and 8.5 climate-change scenarios indicated an expanding extent of MPB mortality, with the implication that future climate conditions in Grand County, Colorado will be more suitable for MPB survival. Little variation existed in the projected area of MPB mortality in Grand County between years 2015 and 2050, because a limited amount of healthy forest with MPB host species may remain at that point. Because of this, our projections for Grand County do not fully depict the situation in the Southern Rocky Mountains ecoregion, as there is a substantial amount of lodgepole and other species of pine forests that currently remain healthy outside of Grand County. Given that projected climate conditions within the ecoregion are likely to follow those within Grand County, we anticipate the area of forest with MPB mortality within the ecoregion will increase. The influence of climate and weather factors on the beetle-caused tree mortality varies among different locations (Creeden et al., 2014), and not all areas across western North America are expected to be more suitable to MPB survival as temperatures increase (Hicke et al., 2006). Thus, the models developed, and the conclusions drawn from this study might not be applicable to other areas. However, our overall approach is applicable

to other regions experiencing similar insect outbreaks and can aid in generating consistent and high-temporal frequency data on insect mortality and other disturbances impacting carbon cycling and other ecosystem services.

Acknowledgments

	2012	2013	2014	2015	2050

BCC-CSM1.1

BNU-ESM

CanESM2

CNRM-CM5

CSIRO-Mk3.6.0

GFDL-ESM2G

GFDL-ESM2M

HadGEM2-ES

Figure S1. The spatial explicit maps of predicted MPB mortality under the RCP8.5 scenario using the final general linear model and the fourteen global climate model outputs.

Chapter 5 Summary and broader impacts

In this dissertation, I incorporated multi-disciplinary knowledge and techniques, including remote sensing, geographic information science, forestry, ecology, geostatistics, statistics and climate science, to answer some critical questions with regard to the mountain pine beetle disturbance in the highly landscape heterogeneous Southern Rocky Mountain Ecoregion:

1) How can satellite images with moderate resolution be applied in monitoring the chronic mountain pine beetle disturbance over a decadal long period with high accuracy and efficiency?
2) What biotic and abiotic drivers promote the extensive development and progressive MPB outbreaks? And what is the future habitat of mountain pine beetle under climate change scenarios?
3) What are the characteristics of disturbance regime, their interactions and the successional pathway in this region?

To address the first question, I investigated the benefits of trajectory-based classification for time-series forest disturbance mapping at the Grand County, Colorado, where a high concentration of lodgepole pines and MPB mortality are located. Unlike using pixels as the basic unit in the traditional classifications, this method employed the temporal segment component derived from the image spectral trajectory. Several advantages were presented in this method. Firstly, it is suitable for applications of which images are not well radiometrically corrected, since it is designed to remove spikes and enhance the signal-to-noise ratio of the often noisy time series. Secondly, because one segment represents a same type of event happening over the duration, the illogical land cover changes can be minimized. Thirdly, a smaller amount of training samples was needed in order to achieve the same accuracy as the single-date classification. We further advanced this trajectory based procedure to ecoregion scale, and more efforts were put on improving the algorithm efficiency by replacing decision tree labeling procedure with an automatic random forest step. A set of segment features and their spatial-temporal neighborhood features were fed to the random forest classifier to enhance its discrimination ability of abrupt and chronic disturbance types. Another remarkable improvement is the application of an effective scene overlapping area sampling strategy, by which substantial time and labor efforts can be saved in selecting training data.

Based on the satellite measures of disturbance and recovery pattern, I was able to quantify the relative influence of various anthropogenic, biologic and physical drivers that have shaped the spatio-temporal patterns of the MPB outbreaks via an ecological niche modeling framework. After the removal of spatial autocorrelation effects and non-significant predictors, the final model suggested that beetle neighborhood mortality, winter mean temperature anomaly, and residential housing density were positively associated with MPB mortality, whereas summer precipitation was negatively correlated. The four variables reflected the effects of human impacts, biological dispersal and physical environmental factors separately in outbreaks. I further identified the forested area with high risk for future MPB mortality in Grand County to provide informative

future distribution information for management purposes. It was found that the extent of MPB would likely to expand under both two future climate change projections. Those findings imply that future climate conditions will be more suitable for MPB survival.

The highly spatially and temporal variable disturbance and recovery pattern as revealed from the remote sensing mapping results highlighted the importance of resolving the complex relationship between different disturbance events, and their compounded effects on the resilience mechanism of pine forest ecosystem. Besides bark beetle, fire is another major forest disturbance agent in this region whose occurrence is largely determined by the environmental conditions. Although it is presumed that beetle infestation could increase the risks of fire hazard, I found that fire severity was largely unrelated to pre-fire MPB outbreak severity at the landscape level. Beetles can affect the forest ecosystem in a variety of ways, and thus it is hard to predict the synergic effects on fire potential since the positive and negative impacts could counteract with each other. Fire severity, nevertheless, was found to be negatively correlated with the post-fire beetle severity, and can result in milder outbreaks. I further assessed the impacts of singular and multiple disturbances on the forest regeneration pattern. Stand-replacing events, including fire and clearcut, have a high seedling reestablishment rate, whereas only a small portion of the MPB disturbed forests was on a trajectory to full recovery. Interactions between processes can amplify or mute the overall effects of changes. In this ecoregion, beetle can synergistic with fire in increasing the post-fire regeneration rate of serotinous lodgepole pines, which suggests that the beetle disturbance created novel characteristics on the forest resilience response to fire.

This dissertation can be offered as a persuasive and informative case study that demonstrates and further expands the power of remote sensing application in monitoring and modeling landscape ecosystem changes. The outcomes of this dissertation, from the aspect of methodology, map product or ecological findings, could be applied to a broad range of scientific domains, such as biological conservation, carbon science, hydrology, soil science, and ecology. Below I listed two areas that can directly benefit from this research. Besides the scientific merits, the results can also provide meaningful and timely information to decision makers, which is especially beneficial for vulnerable zones that are facing dramatic environment transformations or climate changes.

Dynamic land cover mapping and phonological metrics. The automatic trajectory-based time-series classification working flow proposed in this dissertation could contribute to future fine resolution dynamic land cover mapping, which will involve various spatial scales and more diverse thematic classes, and thus higher complexity in classification. Dynamic land cover is essential in assessing whether a fluctuation caused by human intervention or climate change in the system is within the range of natural variation or not, and is also a critical land surface parameter in global earth system models. Numerous techniques of land cover change detection have been developed, but no single technique works well in all contexts, so does this algorithm as its limitations had been summarized previously. Besides conducting time-series mapping as a routine task, our trajectory-based classification framework is also capable of providing phonological metrics of all ecosystems exhibiting identifiable seasonal or annual phenology, such as the onset,

duration and magnitude of greenness increase and decrease, and biomass maximum and minimum. Those metrics are valuable in enhancing understanding the landscape dynamics over time and improving models of phonological responses to climate change.

More accurate estimation on carbon and biomass. Accurate depiction of forest disturbance and recovery over large extent and continuous time is essential in monitoring forest carbon fluxes and understanding the role of forest ecosystems in the global climate. Since terrestrial carbon fluxes cannot realistically be measured at a regional or global scale using modern techniques such as flux tower, remote sensing offers the most feasible way in providing such information. There have been successful cases that integrated maps of harvest disturbance history and age derived from Landsat time-series with ecosystem models (eg. Cohen et al., 1996; Masek & Collatz, 2006). However, unlike physical disturbances such as fire and windthrow, biotic agent caused mortality is never instantaneous under any pathogen and insect pathway, and this inherent feature makes the long-term growth reduction due to forest insects absent from ecosystem process models, which further lead to the systematic overestimation of carbon uptake and storage across wide regions. The present MPB mortality maps generated from this dissertation that are superior in the fine spatial resolution (30 m) and high temporal frequency (1 year), could be utilized as inputs to the processed-based forest productivity models or terrestrial ecosystem models, to provide greater realism to modeled impacts. Additionally, the potential range shifts of MPB associated with changing climate as estimated by the bioclimatic niche model I developed in Chapter four can also be fed into the ecosystem models to explore future trends of the impacts on carbon.

References

Abatzoglou, J.T. & Brown, T.J. (2012) A comparison of statistical downscaling methods suited for wildfire applications. *International Journal of Climatology*, 32, 772-780.

Abbott, B., Van Kooten, G. C. & Stennes, B. (2008) *An economic analysis of mountain pine beetle impacts in a global context*. Resource Economics & Policy Analysis Research Group, Department of Economics, University of Victoria.

Ainslie, B. & Jackson, P. L. (2011) Investigation into mountain pine beetle above-canopy dispersion using weather radar and an atmospheric dispersion model. *Aerobiologia*, *27*, 51-65.

Amman, G. D. (1977) *The role of mountain pine beetle in lodgepole ecosystems*, Impact on succession in: The Role of Arthropods in Forest Ecosystem, edited by: Mattson, W. J., Springer-Verlag, New York.

Amman, G.D. & Cole, W.E. (1983) *Mountain pine beetle dynamics in lodgepole pine forests*. Part II: Population dynamics. General Technical Report, Intermountain Forest and Range Experiment Station, USDA Forest Service.

Anees, A. & Aryal, J. (2014) A statistical framework for near-real time detection of beetle infestation in pine forests using MODIS data. *IEEE Geoscience and Remote Sensing Letters, 11*, 1717-1721.

Aukema, B.H., Carroll, A.L., Zhu, J., Raffa, K.F., Sickley, T.A. & Taylor, S.W. (2006) Landscape level analysis of mountain pine beetle in British Columbia, Canada: Spatiotemporal development and spatial synchrony within the present outbreak. *Ecography*, *29*, 427-441.

Aukema, B.H., Carroll, A.L., Zheng, Y., Zhu, J., Raffa, K.F., Dan Moore, R., Stahl, K. & Taylor, S.W. (2008) Movement of outbreak populations of mountain pine beetle: influences of spatiotemporal patterns and climate. *Ecography*, *31*, 348-358.

Backsen, J.C. & Howell, B. (2013) Comparing aerial detection and photo interpretation for conducting forest health surveys. *Western Journal of Applied Forestry*, *28*, 3-8.

Baker, W. (1995) Long-term response of disturbance landscapes to human intervention and global change. *Landscape Ecology, 10*, 143–159.

Baker, W.L. & Veblen, T.T. (1990) Spruce beetles and fires in the nineteenth-century subalpine forests of western Colorado, U.S.A. *Arctic and Alpine Research*, *22*, 65-80.

Bale, J.S., Masters, G.J., Hodkinson, I.D., Awmack, C., Bezemer, T.M., Brown, V.K., Butterfield, J., Buse, A., Coulson, J.C., Farrar, J., Good, J.E.G., Harrington, R., Hartley, S., Jones, T.H., Lindroth, R.L., Press, M.C., Symrnioudis, I., Watt, A.D. & Whittaker, J.B. (2002) Herbivory in global climate change research: direct effects of rising temperature on insect herbivores. *Global Change Biology*, *8*, 1-16.

Baldocchi, D. (2008) Breathing of the terrestrial biosphere: lessons learned from a global network of carbon dioxide flux measurement systems. *Australian Journal of Botany, 56*, 1-26.

Barbour, M.G. & Billings, W.D. (Eds.) (2000) *North American terrestrial vegetation*. Cambridge University Press.

Barnes, B.V., Zak, D.R., Denton, S.R. & Spurr, S. H. (1997) *Forest ecology* (No. Ed. 4). John Wiley and Sons.

Bater, C.W., Wulder, M.A., White, J.C. & Coops, N.C. (2010) Integration of lidar and digital aerial imagery for detailed estimates of lodgepole pine (*Pinus contorta*)

volume killed by mountain pine beetle (*Dendroctonus ponderosae*). *Journal of Forestry*, *108*, 111-119.

Battisti, A., Stastny, M., Buffo, E. & Larsson, S. (2006) A rapid altitudinal range expansion in the pine processionary moth produced by the 2003 climatic anomaly. *Global Change Biology*, *12*, 662-671.

Bentz, B.J., Logan, J.A. & Vandygriff, J.C. (2001) Latitudinal variation in Dendroctonus ponderosae (Coleoptera: Scolytidae) development time and adult size. *The Canadian Entomologist, 133*, 375-387.

Bentz, B.J. & Mullin, D.E. (1999) Ecology of mountain pine beetle (Coleoptera: Scolytidae) cold hardening in the Intermountain West. *Environmental Entomology, 28*, 577-587.

Bentz, B.J., Régnière, J., Fettig, C.J., Hansen, E.M., Hayes, J.L., Hicke, J.A., Kelsey, R.G., Negrón, J.F. & Seybold, S.J. (2010) Climate change and bark beetles of the western United States and Canada: direct and indirect effects. *BioScience*, *60*, 602-613.

Beven, K. & Kirkby, M.J. (1979) A physically based, variable contributing area model of basin hydrology. *Hydrological Sciences Journal*, *24*, 43-69.

Bigler, C., Kulakowski, D. & Veblen, T.T. (2005) Multiple disturbance interactions and drought influence fire severity in Rocky Mountain subalpine forests. Ecology,86(11) ,3018-3029.

Birdsey, R.A. (1992) *Carbon storage and accumulation in United States forest ecosystems*. Gen. Tech. Rep. WO-59. Washington D.C. U.S. Department of Agriculture, Forest Service, Washington Office. 51p.

Birdsey, R.A. & Heath L.S. (1995) *Carbon changes in U.S. forests*. In: Joyce, L.A., ed. Productivity of America's Forests and Climate Change. Gen. Tech. Rep. RM-GTR-271. Fort Collins, CO: U.S. Department of Agriculture, Forest Service, Rocky Mountain Forest and Experiment Station: 56-70.

Björklund, N. & Lindgren, B.S. (2009) Diameter of lodgepole pine and mortality caused by the mountain pine beetle: factors that influence their relationship and applicability for susceptibility rating. *Canadian Journal of Forest Research*, 39(5), 908-916.

Bonan, G.B. (2008) Forests and climate change: forcings, feedbacks, and the climate benefits of forests. *Science, 320*, 1444-1449.

Bond, M.L., Lee, D.E., Bradley, C.M. & Hanson, C.T. (2009) Influence of pre-fire tree mortality on fire severity in conifer forests of the San Bernardino Mountains, California. *Open Forest Science Journal*, 2, 41-47.

Bone, C., White, J.C., Wulder, M.A., Robertson, C. & Nelson, T.A. (2013) Impact of forest fragmentation on patterns of mountain pine beetle-caused tree mortality. *Forests*, *4*, 279-295.

Boon, S. (2009) Snow ablation energy balance in a dead forest stand. *Hydrological Processes*, *23*, 2600-2610.

Borden, J.H. (1982) *Aggregation pheromones*. Pages 74-139 in J.B. Mitton and K.B. Sturgeon, eds. Bark beetles in North American conifers: a system for the study of evolutionary biology. University of Texas Press, Austin, TX. 527 p.

Breiman, L. (2001) Random forests. *Machine Learning*, *45*, 5-32.

Bright, B.C., Hicke, J.A. & Hudak, A.T. (2012) Landscape-scale analysis of aboveground tree carbon stocks affected by mountain pine beetles in Idaho. *Environmental Research Letters*, *7*, 045702.

Bright, B.C., Hudak, A.T, Kennedy, R.E. & Meddens, A.J.H. (2014) A landsat time series and lidar as predictors of live and dead basal area across five bark beetle-affected forests. *IEEE Journal of Selected Topics in Applied Earth Observations and Remote Sensing, 7,* 3440-3452.

Bright, B.C., Hudak, A.T., McGaughey, R., Andersen, H.E. & Negrón, J. (2013) Predicting live and dead tree basal area of bark beetle affected forests from discrete-return lidar. *Canadian Journal of Remote Sensing*, *39*, S99-S111.

British Columbia Ministry of Forests, Forest Practices Branch & Canadian Forest Service, Forest Health Network for the Resources Inventory Committee. (2000) *Forest Health Aerial Overview Survey Standards for British Columbia*. The B.C. Ministry of Forests adaptation of the Canadian Forest Service's FHN Report 97-1 "Overview Aerial Survey Standards for British Columbia and the Yukon".

Buma, B., Pugh, E.T. & Wessman, C.A. (2013) Effect of the current major insect outbreaks on decadal phenological and LAI trends in southern Rocky Mountain forests. *International Journal of Remote Sensing, 34,* 7249-7274.

Buma, B. & Wessman, C.A. (2011) Disturbance interactions can impact resilience mechanisms of forests. *Ecosphere, 2*, art64.

Bunting, P. & Lucas, R. (2006) The delineation of tree crowns in Australian mixed species forests using hyperspectral Compact Airborne Spectrographic Imager (CASI) data. *Remote Sensing of Environment, 101*, 230-248.

Byrne, G., Crapper, P. & Mayo, K. (1980) Monitoring land cover change by principle component analysis of multi-temporal Landsat data. *Remote Sensing of Environment*, 10, 175-184.

Caldwell, M., Hawbaker, T., Briggs, J., Cigan, P. & Stitt, S. (2013) Simulated impacts of mountain pine beetle and wildfire disturbances on forest vegetation composition and carbon stocks in the Southern Rocky Mountains. *Biogeosciences*, *10*, 12919-12965.

Calkin, D.E., Gebert, K.M., Jones, J.G. & Neilson, R.P. (2005) Forest Service large fire area burned and suppression expenditure trends, 1970–2002. *Journal of Forestry*, 103(4), 179-183.

Campbell, J.B. (2002) *Introduction to Remote Sensing*; CRC Press: Boca Raton, FL, USA.

Carroll, A.L., Taylor, S.W., Régnière, J. & Safranyik, L. (2003) *Effect of climate change on range expansion by the mountain pine beetle in British Columbia*. In Pages 223-232 in TL Shore et al.(eds) Mountain Pine Beetle Symposium: Challenges and Solutions, Oct. 30-31, 2003. Kelowna BC. Natural Resources Canada, Infromation Report BC-X-399, Victoria.

CCSP (2007) *The First State of the Carbon Cycle Report (SOCCR): The North American Carbon Budget and Implications for the Global Carbon Cycle*. A Report by the U.S. Climate Change Science Program and the Subcommittee on Global Change Research, National Oceanic and Atmospheric Administration, National Climatic Data Center, Asheville, NC.

Chambers, J.C. & MacMahon, J.A. (1994) A day in the life of a seed: movements and fates of seeds and their implications for natural and managed systems. *Annual Review of Ecology and Systematics*, 263-292.

Chapman, J.W., Reynolds, D.R., Smith, A.D., Riley, J.R., Telfer, M.G. & Woiwod, I.P. (2005) Mass aerial migration in the carabid beetle Notiophilus biguttatus. *Ecological Entomology*, *30*, 264-272.

Chapman, T.B., Veblen, T.T. & Schoennagel, T. (2012) Spatiotemporal patterns of mountain pine beetle activity in the southern Rocky Mountains. *Ecology*, *93*, 2175-2185.

Chen, H.P. & Walton, A. (2011) Mountain pine beetle dispersal: spatiotemporal patterns and role in the spread and expansion of the present outbreak. *Ecosphere*, *2*, art66.

Chen, Y. & Gong, P. (2013) Clustering based on eigenspace transformation–CBEST for efficient classification. *ISPRS Journal of Photogrammetry and Remote Sensing*, *83*, 64-80.

Clow, D.W., Rhoades, C., Briggs, J., Caldwell, M. & Lewis Jr, W.M. (2011) Responses of soil and water chemistry to mountain pine beetle induced tree mortality in Grand County, Colorado, USA. *Applied Geochemistry*, *26*, S174-S178.

Coggins, S., Coops, N.C. & Wulder, M.A. (2008) Initialization of an insect infestation spread model using tree structure and spatial characteristics derived from high spatial resolution digital aerial imagery. *Canadian Journal of Remote Sensing, 34,* 485-502.

Cohen, W.B., Harmon, M.E., Wallin, D.O. & Fiorella, M. (1996) Two decades of carbon flux from forests of the Pacific Northwest. *BioScience*, 836-844.

Cohen, W.B., Maiersperger, T.K., Gower, S.T. & Turner, D.P. (2003) An improved strategy for regression of biophysical variables and Landsat ETM+ data. *Remote Sensing of Environment*, *84*, 561-571.

Cohen, W.B., Yang, Z. & Kennedy, R. (2010) Detecting trends in forest disturbance and recovery using yearly Landsat time series: 2. Timesync - Tools for calibration and validation. *Remote Sensing of Environment, 114*, 2911-2924.

Cole, W.E. (1981) Some risks and causes of mortality in mountain pine beetle populations: a long-term analysis. *Researches on Population Ecology, 23*, 116-144.

Collins, B.M., Kelly, M., van Wagtendonk, J.W. & Stephens, S.L. (2007) Spatial patterns of large natural fires in Sierra Nevada wilderness areas. *Landscape Ecology*, 22(4), 545-557.

Collins, B.J., Rhoades, C.C., Hubbard, R.M. & Battaglia, M.A. (2011) Tree regeneration and future stand development after bark beetle infestation and harvesting in Colorado lodgepole pine stands. *Forest Ecology and Management, 261*, 2168-2175.

Coops, N.C., Varhola, A., Bater, C.W., Teti, P., Boon, S., Goodwin, N. & Weiler, M. (2009) Assessing differences in tree and stand structure following beetle infestation using lidar data. *Canadian Journal of Remote Sensing*, *35*, 497-508.

Coops, N.C., Johnson, M., Wulder, M.A. & White, J.C. (2006a) Assessment of QuickBird high spatial resolution imagery to detect red attack damage due to mountain pine beetle infestation. *Remote Sensing of Environment*, *103*, 67-80.

Coops, N.C., Wulder, M.A. & White, J.C. (2006b) Integrating remotely sensed and ancillary data sources to characterize a mountain pine beetle infestation. *Remote Sensing of Environment*, *105*, 83-97.

Coops, N.C., Timko, J.A., Wulder, M.A., White, J.C. & Ortlepp, S.M. (2008) Investigating the effectiveness of mountain pine beetle mitigation strategies. *International Journal of Pest Management*, *54*, 151-165.

Coppin, P., Jonckheere, I., Nackaerts, K., Muys, B. & Lambin, E. (2004) Digital change detection methods in ecosystem monitoring: A review. *International Journal of Remote Sensing, 25,* 1565-1596.

Creeden, E.P., Hicke, J.A. & Buotte, P.C. (2014) Climate, weather, and recent mountain pine beetle outbreaks in the western United States. *Forest Ecology and Management*, *312*, 239-251.

Crist, E.P. & Cicone, R.C. (1984) A physically-based transformation of Thematic Mapper data - The TM tasseled cap. *IEEE Transactions on Geoscience and Remote Sensing. GE-22*, 256-263.

Dale, V.H., Joyce, L.A., McNulty, S., Neilson, R.P., Ayres, M.P., Flannigan, M.D., Hanson, P.J., Irland, L.C., Lugo, A.E., Peterson, C.J., Simberloff, D., Swanson, F.J., Stocks, B.J. & Wotton, B.M. (2001) Climate Change and Forest Disturbances: Climate change can affect forests by altering the frequency, intensity, duration, and timing of fire, drought, introduced species, insect and pathogen outbreaks, hurricanes, windstorms, ice storms, or landslides. *BioScience*, *51*, 723-734.

Daly, C., Gibson, W.P., Taylor, G.H., Johnson, G.L. & Pasteris, P. (2002) A knowledge-based approach to the statistical mapping of climate. *Climate Research*, *22*, 99-113.

de la Giroday, H.M.C., Carroll, A.L., Lindgren, B.S. & Aukema, B.H. (2011) Incoming! Association of landscape features with dispersing mountain pine beetle populations during a range expansion event in western Canada. *Landscape Ecology*, *26*, 1097-1110.

Dennison, P.E., Brunelle, A.R. & Carter, V.A. (2010) Assessing canopy mortality during a mountain pine beetle outbreak using GeoEye-1 high spatial resolution satellite data. *Remote Sensing of Environment*, *114*, 2431-2435.

Dietterich, T.G. (2000) An experimental comparison of three methods for constructing ensembles of decision trees: Bagging, boosting, and randomization. *Machine Learning*, *40*, 139-157.

Dormann, F.C., M McPherson, J., B Araújo, M., Bivand, R., Bolliger, J., Carl, G., G Davies, R., Hirzel, A., Jetz, W. & Daniel Kissling, W. (2007) Methods to account for spatial autocorrelation in the analysis of species distributional data: a review. *Ecography*, *30*, 609-628.

Edburg, S.L., Hicke, J.A., Brooks, P.D., Pendall, E.G., Ewers, B.E., Norton, U., Gochis, D., Gutmann, E.D. & Meddens, A.J. (2012) Cascading impacts of bark beetle-caused tree mortality on coupled biogeophysical and biogeochemical processes. *Frontiers in Ecology and the Environment*, *10*, 416-424.

Eidenshink, J., Schwind, B., Brewer, K., Zhu, Z.L., Quayle, B. & Howard, S. (2007) A project for monitoring trends in burn severity. *Fire Ecology*, *3*, 3-20.

Evangelista, P.H., Kumar, S., Stohlgren, T.J. & Young, N.E. (2011) Assessing forest vulnerability and the potential distribution of pine beetles under current and future climate scenarios in the Interior West of the US. *Forest Ecology and Management*, *262*, 307-316.

Evenden, M.L., Whitehouse, C.M. & Sykes, J. (2014) Factors influencing flight capacity of the mountain pine beetle (Coleoptera: Curculionidae: Scolytinae). *Environmental*

entomology, *43*, 187-196.

Fielding, A.H., and Bell, J.F. (1997) A review of methods for the assessment of prediction errors in conservation presence/absence models. *Environmental Conservation*, *24*, 38-49.

Foody, G.M. (2009) Sample size determination for image classification accuracy assessment and comparison. *International Journal of Remote Sensing*, *30*, 5273-5291.

Franklin, J., McCullough, P. & Gray, C. (2000) *Terrain variables used for predictive mapping of vegetation communities in Southern California.* Terrain analysis: principles and applications.

Franklin, J. F., Spies, T. A., Pelt, R. V., Carey, A. B., Thornburgh, D. A., Berg, D. R., Lindenmayer, D.B., Harmon, M.E., Keeton, W.S., Shaw, D.C., Bible, K. & Chen, J.Q. (2002) Disturbances and structural development of natural forest ecosystems with silvicultural implications, using Douglas-fir forests as an example. *Forest Ecology and Management, 155,* 399-423.

Franklin, S.E. & Wulder, M.A. (2002) Remote sensing methods in medium spatial resolution satellite data land cover classification of large areas. *Progress in Physical Geography, 26,* 173-205.

Franklin, S.E., Wulder, M.A., Skakun, R. & Carroll, A. (2003) Mountain pine beetle red-attack forest damage classification using stratified Landsat TM data in British Columbia, Canada. *Photogrammetric Engineering & Remote Sensing*, *69*, 283–288.

Freeman, E.A. & Moisen, G. (2008) PresenceAbsence: An R package for presence absence analysis. *Journal of Statistical Software*, *23*, 1-31.

Friedl, M.A. & Brodley, C.E. (1997) Decision tree classification of land cover from remotely sensed data. *Remote Sensing of Environment*, *61*, 399-409.

Gao, B.C. (1996) NDWI - A normalized difference water index for remote sensing of vegetation liquid water from space. *Remote Sensing of Environment*, *58*, 257-266.

Geiszler, D.R., Gara, R.I. & Littke, W.R. (1984) Bark beetle infestations of Lodgepole pine following a fire in South Central Oregon. *Zeitschrift für angewandte Entomologie*, 98(1-5), 389-394.

Ghimire, B., Rogan, J. & Miller, J. (2010) Contextual land-cover classification: Incorporating spatial dependence in land-cover classification models using random forests and the getis statistic. *Remote Sensing Letters*, *1*, 45-54.

Gibbs, H. K., Brown, S., Niles, J. O. & Foley, J. A. (2007) Monitoring and estimating tropical forest carbon stocks: making REDD a reality. *Environmental Research Letters, 2*, 045023.

Gibson, K.E., Skov, K., Kegley, S., Jorgensen, C., Smith, S. & Witcosky, J. (2008) *Mountain Pine Beetle Impacts in High-Elevation Five-Needle Pines: Current Trends and Challenges*; U.S. Department of Agriculture, Forest Service, Forest Health Protection: Washington, DC, USA.

Gill, S.J., Biging, G.S. & Murphy, E.C. (2000) Modeling conifer tree crown radius and estimating canpy cover. *Forest Ecology and Management*, *126*, 405-416.

Gong, P., Wang, J., Yu, L., Zhao, Y., Zhao, Y., Liang, L., Niu, Z., Huang, X., Fu, H., Liu, S., Li, C.C., Li, X.Y., Fu, W., Liu, C.X., Xu, Y., Wang, X.Y., Cheng, Q., Hu, L.Y., Yao, W.B., Zhang, H., Zhu, P., Zhao, Z.Y., Zhang, H.Y., Zheng, Y.M., Ji, L.Y., Zhang, Y.W., Chen, H., Yan, A., Guo, J.H., Yu, L., Wang, L., Liu, X.J., Shi, T.T.,

Zhu, M.H., Chen, Y.L., Yang, G.W., Tang, P., Xu, B., Ciri, C., Clinton, N., Zhu, Z.L., Chen, J. & Chen, J. (2013) Finer resolution observation and monitoring of global land cover: First mapping results with Landsat TM and ETM+ data. *International Journal of Remote Sensing*, *34*, 2607-2654.

Goodale, C.L., Apps, M.J., Birdsey, R.A., Field, C.B., Heath, L.S., Houghton, R.A., Jenkins, C.J., Kohlmaier, G.H., Kurz, W., Liu, S.R., Nabuurs, G.J., Nilsson, S. & Shvidenko, A.Z. (2002) Forest carbon sinks in the Northern Hemisphere. *Ecological Applications*, *12*, 891-899.

Goodwin, N.R., Coops, N.C., Wulder, M.A., Gillanders, S., Schroeder, T.A. & Nelson, T. (2008) Estimation of insect infestation dynamics using a temporal sequence of Landsat data. *Remote Sensing of Environment*, *112*, 3680-3689.

Goodwin, N.R., Magnussen, S., Coops, N.C. & Wulder, M.A. (2010) Curve fitting of time-series Landsat imagery for characterizing a mountain pine beetle infestation. *International Journal of Remote Sensing*, *31*, 3263-3271.

Gough, C.M., Vogel, C.S., Harrold, K. H., George, K. & Curtis, P.S. (2007) The legacy of harvest and fire on ecosystem carbon storage in a north temperate forest. *Global Change Biology, 13*, 1935-1949.

Grand County Department of Natural Resources. (2006) Grand County Community Wildfire Protection Plan.

Griffiths, P., Kuemmerle, T., Baumann, M., Radeloff, V.C., Abrudan, I.V., Lieskovsky, J., Munteanu, C., Ostapowicz, K. & Hostert, P. (2013) Forest disturbances, forest recovery, and changes in forest types across the Carpathian ecoregion from 1985 to 2010 based on Landsat image composites. *Remote Sensing of Environment*, *151*, 72-88.

Groffman, P.M., Baron, J.S., Blett, T., Gold, A.J., Goodman, I., Gunderson, L. H., Levinson, B.M., Palmer, M.A., Paerl, H.W., Peterson, G.D., Poff, N.L., Rejeski, D.W., Reynolds, J.F., Turner, M.G., Weathers, K.C. & Wiens, J. (2006) Ecological thresholds: the key to successful environmental management or an important concept with no practical application?. *Ecosystems*, 9(1), 1-13.

Haack, R.A. & Byler, J.W. (1993) Insects and pathogens: regulators of forest ecosystems. *Journal of Forestry*, *91*, 32-35.

Hanley, J.A. & McNeil, B.J. (1982) The meaning and use of the area under a receiver operating characteristic (ROC) curve. *Radiology*, *143*, 29-36.

Hansen, M.C. & Loveland, T.R. (2012) A review of large area monitoring of land cover change using Landsat data. *Remote Sensing of Environment*, *122*, 66-74.

Hansen, M., Potapov, P., Moore, R., Hancher, M., Turubanova, S., Tyukavina, A., Thau, D., Stehman, S., Goetz, S. & Loveland, T. (2013) High-resolution global maps of 21st-century forest cover change. *Science*, *342*, 850-853.

Harvey, B.J., Donato, D.C., Romme, W.H. & Turner, M.G. (2013) Influence of recent bark beetle outbreak on fire severity and postfire tree regeneration in montane Douglas-fir forests. *Ecology*, 94(11), 2475-2486.

Harvey, B.J., Donato, D.C. & Turner, M.G. (2014) Recent mountain pine beetle outbreaks, wildfire severity, and postfire tree regeneration in the US Northern Rockies. *Proceedings of the National Academy of Sciences*, 111(42), 15120-15125.

Hicke, J.A., Allen, C.D., Desai, A.R., Dietze, M.C., Hall, R.J., Kashian, D.M., Moore, D., Raffa, K.F., Sturrock, R.N. & Vogelmann, J. (2012a) Effects of biotic disturbances

on forest carbon cycling in the United States and Canada. *Global Change Biology*, *18*, 7-34.

Hicke, J.A., Johnson, M.C., Hayes, J.L. & Preisler, H.K. (2012b) Effects of bark beetle-caused tree mortality on wildfire. *Forest Ecology and Management*, *271*, 81-90.

Hicke, J.A. & Logan, J. (2009) Mapping whitebark pine mortality caused by a mountain pine beetle outbreak with high spatial resolution satellite imagery. *International Journal of Remote Sensing*, *30*, 4427-4441.

Hicke, J.A., Logan, J.A., Powell, J. & Ojima, D.S. (2006) Changing temperatures influence suitability of modeled mountain pine beetle (*Dendroctonus ponderosae*) outbreaks in the western United States. *Journal of Geophysical Research,111*, G02019, doi: 10.1029/2005JG000101.

Hicke, J.A., Meddens, A.J., Allen, C.D. & Kolden, C.A. (2013) Carbon stocks of trees killed by bark beetles and wildfire in the western United States. *Environmental Research Letters*, *8*, 035032.

Hilker, T., Coops, N.C., Coggins, S.B., Wulder, M.A., Brownc, M., Black, T.A., Nesic, Z. & Lessard, D. (2009). Detection of foliage conditions and disturbance from multi-angular high spectral resolution remote sensing. *Remote Sensing of Environment*, *113*, 421-434.

Hopkins, A.D. (1909) Practical information on the scolytid beetles of North American forests. USDA Bureau of Entomology Bulletin 83, U.S. Government Printing Office, Washington, D.C., USA.

Huang, C., Goward, S.N., Masek, J.G., Thomas, N., Zhu, Z. & Vogelmann, J.E. (2010) An automated approach for reconstructing recent forest disturbance history using dense Landsat time series stacks. *Remote Sensing of Environment*, *114*, 183-198.

Hudak, A.T., Crookston, N.L., Evans, J.S., Falkowski, M.J., Smith, A.M., Gessler, P.E. & Morgan, P. (2006) Regression modeling and mapping of coniferous forest basal area and tree density from discrete-return lidar and multispectral satellite data. *Canadian Journal of Remote Sensing*, *32*, 126-138.

Jenkins, M.J., Hebertson, E., Page, W. & Jorgensen, C.A. (2008) Bark beetles, fuels, fires and implications for forest management in the Intermountain West. *Forest Ecology and Management*, *254*, 16-34.

Jensen, J.R. (1996) *Introductory Digital Image Processing: A Remote Sensing Perspective*; Prentice-Hall Inc.: Upper Saddle River, NJ, USA.

Jackson, P.L., Straussfogel, D., Lindgren, B.S., Mitchell, S. & Murphy, B. (2008) Radar observation and aerial capture of mountain pine beetle, *Dendroctonus ponderosae* Hopk. (Coleoptera: Scolytidae) in flight above the forest canopy. *Canadian Journal of Forest Research*, *38*, 2313-2327.

Jewett, J.T., Lawrence, R.L., Marshall, L.A., Gessler, P.E., Powell, S.L. & Savage, S.L. (2011) Spatiotemporal relationships between climate and whitebark pine mortality in the Greater Yellowstone Ecosystem. *Forest Science*, *57*, 320-335.

Johnson E.W. & Ross J. (2005) *USDA Forest Service Rocky Mountain Region Forest Health Aerial Survey Accuracy Assessment 2005 Report*; Technical Report R2-06-08; USDA Forest Service: Lakewood, Colorado, USA.

Johnson, E.W. & Ross, J. (2008) Quantifying error in aerial survey data. *Australian Forestry*, *71*, 216-222.

Johnstone, J.F., Hollingsworth T.N., Chapin F.S. & Mack, M.C. (2010) Changes in fire regime break the legacy lock on successional trajectories in Alaskan boreal forest. *Global Change Biology,* 16:1281–1295.

Justice, C.O., Giglio, L., Korontzi, S., Owens, J., Morisette, J. T., Roy, D., Descloitres, J., Alleaume, S., Petitcolin, F. & Kaufman, Y. (2002) The MODIS fire products. *Remote Sensing of Environment, 83,* 244-262.

Kaufmann, M.R., Aplet, G.H., Babler, M.G., Baker, W.L., Bentz, B., Harrington, M., Hawkes, B., Huckaby, L.S., Jenkins, M.J., Kashian, D.M., Keane, R.E., Kulakowski, D., McCaughey, W., McHugh, C., Negron, J., Popp, J., Romme, W.H., Shepperd, W. Smith, F.W., Sutherland, E.K., Tinker, D. & Veblen, T.T. (2008) *The Status of Our Scientific Understanding of Lodgepole Pine and Mountain Pine Beetles: A Focus on Forest Ecology and Fire Behavior*. Arlington, VA: Nature Conservancy.

Kautz, M. (2014) On correcting the time-lag bias in aerial-surveyed bark beetle infestation data. *Forest Ecology and Management, 326*, 157-162.

Kennedy, R.E., Yang, Z. & Cohen, W.B. (2010) Detecting trends in forest disturbance and recovery using yearly Landsat time series: 1. LandTrendr—Temporal segmentation algorithms. *Remote Sensing of Environment, 114*, 2897-2910.

Kennedy, R.E., Yang, Z., Cohen, W. B., Pfaff, E., Braaten, J. & Nelson, P. (2012) Spatial and temporal patterns of forest disturbance and regrowth within the area of the Northwest Forest Plan. *Remote Sensing of Environment, 122*, 117-133.

Key, C.H. & Benson, N.C. (2006) Landscape assessment (LA). FIREMON: Fire effects monitoring and inventory system. Gen. Tech. Rep. RMRS-GTR-164-CD, Fort Collins, CO: US Department of Agriculture, Forest Service, Rocky Mountain Research Station.

Klutsch, J.G., Negron, J.F., Costello, S.L., Rhoades, C.C., West, D.R., Popp, J. & Caissie, R. (2009) Stand characteristics and downed woody debris accumulations associated with a mountain pine beetle (*Dendroctonus ponderosae* Hopkins) outbreak in Colorado. *Forest Ecology and Management, 258*, 641-649.

Kuemmerle, T., Chaskovskyy, O., Knorn, J., Radeloff, V.C., Kruhlov, I., Keeton, W.S. & Hostert, P. (2009) Forest cover change and illegal logging in the Ukrainian Carpathians in the transition period from 1988 to 2007. *Remote Sensing of Environment, 113*, 1194-1207.

Kurz, W.A., Dymond, C., Stinson, G., Rampley, G., Neilson, E., Carroll, A., Ebata, T. & Safranyik, L. (2008) Mountain pine beetle and forest carbon feedback to climate change. *Nature*, 452, 987-990.

Lester, J.D. & Irwin, J.T. (2012) Metabolism and cold tolerance of overwintering adult mountain pine beetles (*Dendroctonus ponderosae*): Evidence of facultative diapause?. *Journal of insect physiology, 58*, 808-815.

Li, C.C., Wang, J., Wang, L., Hu, L.Y. & Gong, P. (2013) Comparison of classification algorithms and training sample sizes in urban land classification with Landsat Thematic Mapper imagery. *Remote Sensing*, doi:10.3390/rs6020964.

Liang, L., Chen, Y., Hawbaker, T.J., Zhu, Z.L. & Gong, P. (2014a) Mapping Mountain Pine Beetle Mortality through Growth Trend Analysis of Time-Series Landsat Data. *Remote Sensing, 6*, 5696-5716.

Liang. L., Hawbaker, T., Chen, Y.L., Zhu, Z.L. & Gong, P. (2014b) Characterizing recent and projecting future potential patterns of mountain pine beetle outbreaks in the

Southern Rocky Mountains. *Applied Geography.* DOI: 10.1016/j.apgeog.2014.09.012

Liang, L. & Gong, P. (2010) An assessment of MODIS Collection 5 global land cover product for biological conservation studies. *Geoinformatics, 2010 18th International Conference on* IEEE, 1-6.

Liu, D. & Cai, S. (2012) A spatial-temporal modeling approach to reconstructing land-cover change trajectories from multi-temporal satellite imagery. *Annals of the Association of American Geographers*, *102*, 1329-1347.

Logan, J.A., Bolstad, P.V., Bentz, B.J. & Perkins, D.L. (1995) *Assessing the effects of changing climate on mountain pine beetle dynamics*. Pages 92-105 in R.W. Tinus, ed. Proceedings of the Interior west global change workshop, April 25-27, 1995, Fort Collins, Colorado, USDA Forest Service, Rocky Mountain Forest and Range Experiment Station, General Technical Report RM-GTR-262.

Lunetta, R.S., Knight, J.F., Ediriwickrema, J., Lyon, J.G. & Worthy, L.D. (2006) Land-cover change detection using multi-temporal MODIS NDVI data. *Remote Sensing of Environment, 105*, 142-154.

Man, G. (2010) *Major forest insect and disease conditions in the United States: 2009 update*. US Department of Agriculture, Forest Service, Forest Health Protection, Washington.

Maness, H., Kushner, P. & Fung, I. (2013) Summertime climate response to mountain pine beetle disturbance in British Columbia. *Nature Geoscience*, *6*, 65-70.

Manly, B., McDonald, L., Thomas, D., McDonald, T. & Erickson, W. (2002) *Resource selection by animals: statistical analysis and design for field studies*. Nordrecht, The Netherlands: Kluwer.

Martin, K., Norris, A. & Drever, M. (2006) Effects of bark beetle outbreaks on avian biodiversity in the British Columbia interior: Implications for critical habitat management. *Journal of Ecosystems and Management*, *7*, 10-24.

Masek, J.G. & Collatz, G.J. (2006) Estimating forest carbon fluxes in a disturbed southeastern landscape: Integration of remote sensing, forest inventory, and biogeochemical modeling. J*ournal of Geophysical Research: Biogeosciences* (2005–2012), 111(G1).

Masek, J.G., Goward, S.N., Kennedy, R.E., Cohen, W.B., Moisen, G.G., Schleweiss, K. & Huang, C.Q. (2013) United States forest disturbance trends observed with Landsat time series. *Ecosystems*, *16*, 1087-1104.

Masek, J.G., Vermote, E.F., Saleous, N.E., Wolfe, R., Hall, F.G., Huemmrich, K.F., Gao, F., Kutler, J. & Lim, T.-K. (2006) A Landsat surface reflectance dataset for North America, 1990–2000. *IEEE Geoscience and Remote Sensing Letters*, *3*, 68-72.

Mathur, A. & Foody, G.M. (2008) Crop classification by support vector machine with intelligently selected training data for an operational application. *International Journal of Remote Sensing*, *29*, 2227–2240.

McCambridge, W.F. (1971) Temperature limits of flight of the mountain pine beetle, Dendroctonus ponderosae. *Annals of the Entomological Society of America, 64,* 534-535.

McConnell T.J., Johnson E.W. & Burns, B. (2000) *A guide to conducting aerial sketchmapping surveys*. U.S. Department of Agriculture Forest Service.

McCullough, D.G., Werner, R.A. & Neumann, D. (1998) Fire and insects in northern and boreal forest ecosystems of North America 1. *Annual review of entomology*, 43(1), 107-127.

Meddens, A.J., Hicke, J.A. & Vierling, L.A. (2011) Evaluating the potential of multispectral imagery to map multiple stages of tree mortality. *Remote Sensing of Environment, 115*, 1632-1642.

Meddens, A.J., Hicke, J.A. & Ferguson, C.A. (2012) Spatiotemporal patterns of observed bark beetle-caused tree mortality in British Columbia and the western United States. *Ecological Applications, 22*, 1876-1891.

Meddens, A.J., Hicke, J.A., Vierling, L.A. & Hudak, A.T. (2013) Evaluating methods to detect bark beetle-caused tree mortality using single-date and multi-date Landsat imagery. *Remote Sens. Environment, 132*, 49-58.

Meigs, G.W., Kennedy, R.E. & Cohen, W.B. (2011) A Landsat time series approach to characterize bark beetle and defoliator impacts on tree mortality and surface fuels in conifer forests. *Remote Sensing of Environment, 115*, 3707-3718.

Mikkelson, K.M., Bearup, L.A., Maxwell, R.M., Stednick, J.D., McCray, J.E. & Sharp, J.O. (2013) Bark beetle infestation impacts on nutrient cycling, water quality and interdependent hydrological effects. *Biogeochemistry, 115*, 1-21.

Mildrexler, D.J., Zhao, M. & Running, S.W. (2009) Testing a MODIS global disturbance index across North America. *Remote Sensing of Environment, 113*, 2103-2117.

Mitton, J.B. & Ferrenberg, S.M. (2012) Mountain pine beetle develops an unprecedented summer generation in response to climate warming. *The American Naturalist, 179*, E163-E171.

Moran, P.A.P. (1950) Notes on continuous stochastic phenomena. *Biometrika, 37*, 17-23.

Myneni, R.B., Keeling, C.D., Tucker, C.J., Asrar, G. & Nemani, R.R. (1997) Increased plant growth in the northern high latitudes from 1981 to 1991. *Nature, 386*, 698-702.

National c2001 Assessment. Available online: http://www.landfire.gov/dp_quality_assessment.php (accessed on 12 June 2014).

Nealis, V. & Peter, B. (2009) *Risk Assessment of the Threat of Mountain Pine Beetle to Canada's Boreal and Eastern Pine Forests*. Natural Resources Canada, Canadian Forest Service. Information Report BC-X-417.

Neigh, C.S., Bolton, D.K., Diabate, M., Williams, J.J. & Carvalhais, N. (2014) An Automated Approach to Map the History of Forest Disturbance from Insect Mortality and Harvest with Landsat Time-Series Data. *Remote Sensing, 6*, 2782-2808.

Nelson, K.J., Connot, J., Peterson, B. & Martin, C. (2013) The landfire refresh strategy: Updating the national dataset. *Fire Ecology, 9*, 80-101.

Nieminen, M., Leskinen, M. & Helenius, J. (2000) Doppler radar detection of exceptional mass-migration of aphids into Finland. *International journal of biometeorology, 44*, 172-181.

Pal, M. & Mather, P.M. (2003) An assessment of the effectiveness of decision tree methods for land cover classification. *Remote Sensing of Environment, 86*, 554–565.

Pal, M. (2005) Random forest classifier for remote sensing classification. *International Journal of Remote Sensing, 26*, 217-222.

Parker, T.J., Clancy, K.M. & Mathiasen, R.L. (2006) Interactions among fire, insects and pathogens in coniferous forests of the interior western United States and Canada.

Agricultural and Forest Entomology, *8*, 167-189.

Pflugmacher, D., Cohen, W.B., Kennedy, R.E. & Yang, Z. (2014) Using Landsat-derived disturbance and recovery history and lidar to map forest biomass dynamics. *Remote Sensing of Environment*, *151*, 124-137.

Potter, C., Klooster, S., Huete, A. & Genovese, V. (2007) Terrestrial carbon sinks for the United States predicted from MODIS satellite data and ecosystem modeling. *Earth Interactions*, *11*, 1-21.

Powell, E.N., Townsend, P.A. & Raffa, K.F. (2012) Wildfire provides refuge from local extinction but is an unlikely driver of outbreaks by mountain pine beetle. *Ecological Monographs*, 82(1), 69-84.

Preisler, H.K., Hicke, J.A., Ager, A.A. & Hayes, J.L. (2012) Climate and weather influences on spatial temporal patterns of mountain pine beetle populations in Washington and Oregon. *Ecology*, *93*, 2421-2434.

Prestemon, J.P., Abt, K.L., Potter, K.M. & Koch, F.H. (2013) An economic assessment of mountain pine beetle timber salvage in the west. *Western Journal of Applied Forestry*, *28*, 143-153.

PRISM Climate Group. (2010) *Gridded climate data for the contiguous USA.* http://prism.oregonstate.edu.

Quintero, I. & Wiens, J.J. (2013) Rates of projected climate change dramatically exceed past rates of climatic niche evolution among vertebrate species. *Ecology letters*, *16*, 1095-1103.

R Core Team (2013) *R: A language and environment for statistical computing*. R foundation for Statistical Computing.

Radeloff, V.C., Stewart, S.I., Hawbaker, T.J., Gimmi, U., Pidgeon, A.M., Flather, C.H., Hammer, R.B. & Helmers, D.P. (2010) Housing growth in and near United States protected areas limits their conservation value. *Proceedings of the National Academy of Sciences*, *107*, 940-945.

Raffa, K.F. & Berryman, A.A. (1983) The role of host plant resistance in the colonization behavior and ecology of bark beetles (Coleoptera: Scolytidae). *Ecological Monographs, 53*, 27-49.

Raffa, K.F., Aukema, B.H., Bentz, B.J., Carroll, A.L., Hicke, J.A., Turner, M.G. & Romme, W.H. (2008) Cross-scale drivers of natural disturbances prone to anthropogenic amplification: the dynamics of bark beetle eruptions. *Bioscience*, *58*, 501-517.

Reid, R.W. & Gates, H. (1970) Effect of temperature and resin on hatch of eggs of the mountain pine beetle (*Dendroctonus ponderosae*). *The Canadian Entomologist, 102*, 617-622.

Robertson, C., Nelson, T.A. & Boots, B. (2007) Mountain pine beetle dispersal: the spatial-temporal interaction of infestations. *Forest science*, *53*, 395-405.

Robertson, C., Wulder, M.A., Nelson, T.A. & White, J.C. (2008) Risk rating for mountain pine beetle infestation of lodgepole pine forests over large areas with ordinal regression modelling. *Forest Ecology and Management*, *256*, 900-912.

Robertson, C., Nelson, T.A., Jelinski, D.E., Wulder, M.A. & Boots, B. (2009) Spatial–temporal analysis of species range expansion: the case of the mountain pine beetle, Dendroctonus ponderosae. *Journal of Biogeography*, *36*, 1446-1458.

Rock, B., Vogelmann, J., Williams, D., Vogelmann, A. & Hoshizaki, T. (1986) Remote detection of forest damage. *BioScience*, *36*, 439–445.

Rodriguez-Galiano, V. F., Chica-Olmo, M., Abarca-Hernandez, F., Atkinson, P. M. & Jeganathan, C. (2012) Random Forest classification of Mediterranean land cover using multi-seasonal imagery and multi-seasonal texture. *Remote Sensing of Environment, 121*, 93-107.

Rodriguez-Galiano, V.F., Ghimire, B., Rogan, J., Chica-Olmo, M. & Rigol-Sanchez, J. (2012) An assessment of the effectiveness of a random forest classifier for land-cover classification. *ISPRS Journal of Photogrammetry and Remote Sensing*, *67*, 93-104.

Romme, W.H., Clement, J., Hicke, J., Kulakowski, D., MacDonald, L.H., Schoennagel, T.L. & Veblen, T.T. (2006) Recent forest insect outbreaks and fire risk in Colorado forests: a brief synthesis of relevant research. Fort Collins, Colorado, USA: Colorado Forest Restoration Institute.

Running, S.W. (2008) Ecosystem disturbance, carbon, and climate. *Science*, 321, 652-653.

Safranyik, L. (1978) Effects of climate and weather on mountain pine beetle populations. *Theory and practice of mountain pine beetle management in lodgepole pine forests. Symposium Proceedings*, University of Idaho, Moscow, ID, 77-84.

Safranyik, L., Carroll, A.L. & Wilson, B. (2007) The biology and epidemiology of the mountain pine beetle in lodgepole pine forests. *The mountain pine beetle: a synthesis of biology, management and impacts on lodgepole pine*, 3-66.

Sambaraju, K.R., Carroll, A.L., Zhu, J., Stahl, K., Moore, R.D. & Aukema, B.H. (2012) Climate change could alter the distribution of mountain pine beetle outbreaks in western Canada. *Ecography*, *35*, 211-223.

Safranyik, L., Linton, D.A, Silversides, R. & McMullen, L.H. (1992) Dispersal of released mountain pine beetles under the canopy of a mature lodgepole pine stand. *Journal of Applied Entomology, 113*, 441-450.

Safranyik, L., Shrimpton, D.M. & Whitney, H.S. (1974) *Management of lodgepole pine to reduce losses from the mountain pine beetle*. Canadian Forest Service Technical Report. 1, 24pp.

Safranyik, L., Silversides, R., McMullen, L.H. & Linton, D.A. (1989) An empirical approach to modeling the local dispersal of the mountain pine beetle (*Dendroctonus ponderosae* Hopk.) (Col., Scolytidae) in relation to sources of attraction, wind direction and speed. *Journal of Applied Entomology*, *108*, 498-511.

Schmid, J.M. & Amman, G.D. (1992) Dendroctonus beetles and old-growth forests in the Rockies. Pages 51–59 in Kaufmann, M.R., Moir, W.H. and Bassett, R.L. editors. Old growth forests in the Southwest and Rocky Mountain regions. Proceedings of a workshop. USDA Forest Service, Rocky Mountain Forest and Range Experiment Station, General Technical Report RM-213, Fort Collins, Colorado, USA.

Schoennagel, T., Turner, M.G., Kashian, D.M. & Fall, A. (2006) Influence of fire regimes on lodgepole pine stand age and density across the Yellowstone National Park (USA) landscape. *Landscape ecology*, 21(8), 1281-1296.

Schoennagel, T., Veblen, T.T., Negron, J.F. & Smith, J.M. (2012) Effects of mountain pine beetle on fuels and expected fire behavior in lodgepole pine forests, Colorado, USA. *PloS one*, 7(1), e30002.

Sexton, J.O., Song, X.-P., Feng, M., Noojipady, P., Anand, A., Huang, C., Kim, D.-H., Collins, K.M., Channan, S. & DiMiceli, C. (2013) Global, 30-m resolution continuous fields of tree cover: Landsat-based rescaling of MODIS vegetation continuous fields with lidar-based estimates of error. *International Journal of Digital Earth*, 6, 427-448.

Schroeder, T.A., Healey, S.P., Moisen, G.G., Frescino, T.S., Cohen, W.B., Huang, C., Kennedy, R.E. & Yang, Z. (2014) Improving estimates of forest disturbance by combining observations from Landsat time series with US Forest Service Forest Inventory and Analysis data. *Remote Sensing of Environment, 154*, 61-73.

Simard, M., Powell, E.N., Raffa, K.F. & Turner, M.G. (2012) What explains landscape patterns of tree mortality caused by bark beetle outbreaks in Greater Yellowstone? *Global Ecology and Biogeography*, *21*, 556-567.

Simard, M., Romme, W.H., Griffin, J.M. & Turner, M.G. (2011) Do mountain pine beetle outbreaks change the probability of active crown fire in lodgepole pine forests?. *Ecological Monographs, 81*, 3-24.

Simon, M., Plummer, S., Fierens, F., Hoelzemann, J.J. & Arino, O. (2004) Burnt area detection at global scale using ATSR-2: The GLOBSCAR products and their qualification. *Journal of Geophysical Research: Atmospheres* (1984–2012), 109(D14).

Six, D. & Bentz, B. (2007) Temperature determines symbiont abundance in a multipartite bark beetle-fungus ectosymbiosis. *Microbial Ecology*, *54,* 112-118.

Skakun, R.S., Wulder, M.A. & Franklin, S.E. (2003) Sensitivity of the Thematic Mapper Enhanced Wetness Difference Index (EWDI) to detect mountain pine needle red attack damage. *Remote Sensing of Environment, 86,* 433–443.

Skole, D. & Tucker, C. (1993) Tropical deforestation and habitat fragmentation in the Amazon. Satellite data from 1978 to 1988. *Science, 260*, 1905-1910.

Spruce, J. P., Sader, S., Ryan, R. E., Smoot, J., Kuper, P., Ross, K., Prados, D., Russell, J., Gasser, G., McKellip, R. & Hargrove, W. (2011) Assessment of MODIS NDVI time series data products for detecting forest defoliation by gypsy moth outbreaks. *Remote Sensing of Environment*, *115*, 427-437.

Stephens, S.L. (2005) Forest fire causes and extent on United States Forest Service lands. *International Journal of Wildland Fire*, 14(3), 213-222.

Strohm, S., Tyson, R. & Powell, J. (2013) Pattern formation in a model for mountain pine beetle dispersal: linking model predictions to data. *Bulletin of Mathematical Biology*, *75*, 1778-1797.

Stroppiana, D., Pinnock, S. & Gregoire, J.M. (2000) The Global Fire Product: Daily fire occurrence from April 1992 to December 1993 derived from NOAA AVHRR data. *International Journal of Remote Sensing, 21*, 1279-1288.

Sulla-Menashe, D., Kennedy, R.E., Yang, Z., Braaten, J., Krankina, O.N. & Friedl, M.A. (2013) Detecting forest disturbance in the Pacific Northwest from MODIS time series using temporal segmentation. *Remote Sensing of Environment*, doi:10.1016/j.rse.2013.07.042.

Trần, J.K., Ylioja, T., Billings, R.F., Régnière, J. & Ayres, M.P. (2007) Impact of minimum winter temperatures on the population dynamics of Dendroctonus frontalis. *Ecological Applications*, *17*, 882-899.

Tucker, C.J. (1979) Red and photographic infrared linear combinations for monitoring vegetation. *Remote Sensing of Environment*, *8*, 127–150.

Turner, M.G., Romme, W.H., Gardner, R.H. & Hargrove, W.W. (1997) Effects of fire size and pattern on early succession in Yellowstone National Park. *Ecological Monographs*, 67(4), 411-433.

Turner, M.G. (1998) Factors influencing succession: Lessons from large, infrequent natural disturbances. *Ecosystems, 1*, 511–523.

Turner, M.G. (2010) Disturbance and landscape dynamics in a changing world. *Ecology*, *91*, 2833–2849.

Turner, M.G., Romme, W.H., Gardner, R.H. & Hargrove, W.W. (1997) Effects of fire size and pattern on early succession in Yellowstone National Park. *Ecological Monographs*, 67(4), 411-433.

USGS. (2004) *Shuttle Radar Topography Mission, 1 Arc Second scene SRTM_u03_n008e004, Unfilled Unfinished 2.0.* Global Land Cover Facility, University of Maryland, College Park, Maryland, February 2000.

U.S. Environmental Protection Agency, 2013, Level III ecoregions of the continental United States: Corvallis, Oregon, U.S. EPA – National Health and Environmental Effects Research Laboratory, map scale 1:7,500,000, http://www.epa.gov/wed/pages/ecoregions/level_iii_iv.htm.

Veblen, T.T., Hadley, K.S., Nel, E.M., Kitzberger, T., Reid, M. & Villalba, R. (1994) Disturbance regime and disturbance interactions in a Rocky Mountain subalpine forest. *Journal of Ecology*, 125-135.

Vogelmann, J.E., Kost, J.R., Tolk, B., Howard, S., Short, K., Chen, X., Huang, C., Pabst, K. & Rollins, M.G. (2011) Monitoring landscape change for landfire using multi-temporal satellite imagery and ancillary data. *IEEE Journal of Selected Topics in Applied Earth Observations and Remote Sensing*, *4*, 252–264.

Vose, J.M., Peterson, D.L. & Patel-Weynand, T. (2012) *Effects of climatic variability and change on forest ecosystems: a comprehensive science synthesis for the US forest sector*. Portland, OR: US Department of Agriculture, Forest Service, Pacific Northwest Research Station.

Walter, J.A. & Platt, R.V. (2013) Multi-temporal analysis reveals that predictors of mountain pine beetle infestation change during outbreak cycles. *Forest Ecology and Management*, *302*, 308-318.

Wang, J., Zhao, Y., Li, C., Yu, L., Liu, D. & Gong, P. (2014) Mapping global land cover in 2001 and 2010 with spatial-temporal consistency at 250m resolution. *ISPRS Journal of Photogrammetry and Remote Sensing*. DOI: 10.1016/j.isprsjprs.2014.03.007.

Wang, W., Peng, C., Kneeshaw, D.D., Larocque, G.R. & Luo, Z. (2012) Drought-induced tree mortality: Ecological consequences, causes, and modeling. *Environmental Reviews*, *20*, 109-121.

Watts, R.D., Compton, R.W., McCammon, J.H., Rich, C.L., Wright, S.M., Owens, T. & Ouren, D.S. (2007) Roadless space of the conterminous United States. *Science*, *316*, 736-738.

Westerling, A.L., Turner, M.G., Smithwick, E.A., Romme, W.H. & Ryan, M.G. (2011) Continued warming could transform Greater Yellowstone fire regimes by mid-21st century. *Proceedings of the National Academy of Sciences*, 108(32), 13165-13170.

White, J.C., Coops, N.C., Hilker, T., Wulder, M.A. & Carroll, A.L. (2007) Detecting mountain pine beetle red attack damage with EO-1 Hyperion moisture indices. *International Journal of Remote Sensing*, *28*, 2111-2121.

White, J.C., Wulder, M.A., Brooks, D., Reich, R. & Wheate, R.D. (2004) Mapping mountain pine beetle infestation with high spatial resolution satellite imagery. *The Forestry Chronicle*, 80, 743-745.

White, J.C., Wulder, M.A., Brooks, D., Reich, R. & Wheate, R.D. (2005) Detection of red attack stage mountain pine beetle infestation with high spatial resolution satellite imagery. *Remote Sensing of Environment*, *96*, 340-351.

White, P.S. & Pickett, S.T. (1985) *Natural disturbance and patch dynamics: an introduction*. In The ecology of natural disturbance and patch dynamics. Edited by S.T.A. Pickett and P.S.White. Academic Press, Orlando. Pp.3-16.

Williams, A.P., Allen, C.D., Millar, C.I., Swetnam, T.W., Michaelsen, J., Still, C.J. & Leavitt, S.W. (2010) Forest responses to increasing aridity and warmth in the southwestern United States. *Proceedings of National Academy of Science*, *107*, 21289-21294.

Wilson, E.H. & Sader, S.A. (2002) Detection of forest harvest type using multiple dates of Landsat TM imagery. *Remote Sensing of Environment*, *80*, 385–396.

Witcosky, J. (2007) *Status of mountain pine beetle populations in lodgepole pine stands in northern Colorado and southern Wyoming*. USDA Forest Service, Rocky Mountain Region, Forest Health Management, Lakewood Service Center, LSC-07-06.

Wulder, M.A., Dymond, C.C., White, J.C., Leckie, D.G. & Carroll, A.L. (2006a) Surveying mountain pine beetle damage of forests: A review of remote sensing opportunities. *Forest Ecology and Management*, *221*, 27–41.

Wulder, M.A., White, J., Bentz, B., Alvarez, M. & Coops, N. (2006b) Estimating the probability of mountain pine beetle red-attack damage. *Remote Sensing of Environment*, 101, 150-166.

Wulder, M.A., Dymond, C.C., White, J.C. & Erickson, B. (2006c) Detection, mapping, and monitoring of the mountain pine beetle. *The mountain pine beetle: A synthesis of biology, management, and impacts on lodgepole pine. Natural Resources Canada, Canadian Forest Service, Pacific Forestry Centre, Victoria, BC*, 123-154.

Wulder, M.A., White, J.C., Coggins, S., Ortlepp, S.M., Coops, N.C., Heath, J. & Mora, B. (2012) Digital high spatial resolution aerial imagery to support forest health monitoring: the mountain pine beetle context. *Journal of Applied Remote Sensing*, *6*, 062527-1.

Zhou, D., Liu, S., Oeding, J. & Zhao, S. (2013) Forest cutting and impacts on carbon in the eastern United States. *Scientific reports, 3*.

Zhu, Z. & Woodcock, C.E. (2012) Object-based cloud and cloud shadow detection in Landsat imagery. *Remote Sensing of Environment*, *118*, 83-94.

Zhu, Z.L., ed., Bergamaschi, B., Bernknopf, R., Clow, D., Dye, D., Faulkner, S., Forney, W., Gleason, R., Hawbaker, T., Liu, J.X., Liu, S.G., Prisley, S., Reed, B., Reeves, M., Rollins, M., Sleeter, B., Sohl, T., Stackpoole, S., Stehman, S., Striegl, R., Wein, A. & Zhu, Z.L. (2010) A method for assessing carbon stocks, carbon sequestration, and greenhouse-gas fluxes in ecosystems of the United States under present conditions

and future scenarios: U.S. Geological Survey Open-File Report 2010–1144, 195 p., available online at http://pubs.usgs.gov/of/2010/1144/.